2009

Geoelectrical response of surfactant solutions in a quartzitic sand analog aquifer

Meghan Therese Magill
University of Nevada Las Vegas

GEOELECTRICAL RESPONSE OF SURFACTANT SOLUTIONS IN A QUARTZITIC SAND ANALOG AQUIFER

by

Meghan Therese Magill

Bachelor of Science
University of Oklahoma
2006

A thesis submitted in partial fulfillment of
the requirements for the

Master of Science in Geoscience
Department of Geoscience
College of Science

Graduate College
University of Nevada, Las Vegas
December 2009

UNIVERSITY OF NEVADA LAS VEGAS

THE GRADUATE COLLEGE

We recommend that the thesis prepared under our supervision by

Meghan Therese Magill

entitled

Geoelectrical Response of Surfactant Solutions in a Quartzitic Sand Analog Aquifer

be accepted in partial fulfillment of the requirements for the degree of

Master of Science
Geoscience

Dave Kreamer, Committee Chair

Dale Werkema, Committee Member

Michael Nicholl, Committee Member

Barbara Luke, Graduate Faculty Representative

Ronald Smith, Ph. D., Vice President for Research and Graduate Studies
and Dean of the Graduate College

December 2009

ABSTRACT

Geoelectrical Response of Surfactant Solutions in a Quartzitic Sand Analog Aquifer

by

Meghan Therese Magill

Dr. David Kreamer, Examination Committee Chair
Professor of Hydrology
University of Nevada, Las Vegas

In this project, the resistivity and phase shift of ten surfactant aqueous solutions in a sand matrix were measured using spectral induced polarization (SIP). In addition, specific conductivity, pH, dissolved oxygen, and dielectric constant measurements of the solutions were also evaluated. The frequency range assessed was 0.091-12000Hz. The surfactants, which are typically used in the remediation of tetrachloroethylene, were Aerosol MA 80-I, Dowfax 8390, and Steol CS-330. The surfactants were mixed into solutions of both deionized and tap water at varying concentrations and injected into a closed system of silica sand. The surfactant treatments altered resistivity, specific conductivity, and pH to varying degrees. Increased real and specific conductivities associated with surfactant presence support the work of Werkema (2008), and the correlation between real and specific conductivities indicates that the primary electrical conduction mechanism in quartz sand-water environment. A decrease in the pH response associated with high concentration surfactant solutions could impact subsurface organisms, potentially affecting bioremediation. Phase, dissolved oxygen, and dielectric constant response to surfactant showed little change from the control. The positive results suggest that geoelectrical changes may be an applicable property to map and

monitor surfactant floods in the subsurface. In order to better understand how the geoelectrical response of surfactant solutions would respond in a field situation, it will be necessary to increase the complexity of the experimental set-up. Increasing the heterogeneity of both the solid materials and pore fluid through the addition of clays and chlorinated solvents are potential avenues to follow.

TABLE OF CONTENTS

ACKNOWLEDGEMENTS

This thesis was not completed in a vacuum. There are many people to whom I owe many thanks, which I can only begin to list. First and foremost, I would like to thank my advisors, Drs. Dave Kreamer and Dale Werkema for keeping me on track and helping me develop a project that I came to truly enjoy.

I am very appreciative to UNLV and the U.S. EPA for funding and support, particularly John Zimmerman at EPA for his invaluable help and wisdom in the lab. Thanks to Lisa Hancock, Ryan Joyce, Alan Williams, and Danney Glaser for logistical help in the laboratory, whether teaching me how to use a drill press or helping me find tubing after moving lab space 3 times. I would like to give particular acknowledgement to Maria, Liz, Kathryn, Rainee, and Joy in the Geoscience Department office and Marion in the EPA QAL office. Thanks for helping me with all the things I didn't realize I didn't know how to do.

I would like to extend my thanks to Anthony Endres and Alle van Calker for their insight into time domain reflectometry and dielectric constants, as well as to Tino Radic for developing the SIPLabII instrument and helping me over the associated bumps in the road.

Finally, I would like to thank my family and friends for putting up with me throughout this process. I promise I'll be back to normal soon. Thank you to Aaron Bell for his unbelievably helpful insight on life in general and the ability to keep things in perspective, and special thanks to my mom and dad for being supportive of my educational choices while still listening to me complain about them.

CHAPTER 1

INTRODUCTION

Groundwater contamination is a growing concern both domestically and internationally. Dense non-aqueous phase liquid (DNAPLs) comprise one category of contaminants. DNAPLs are immiscible, denser-than-water fluids that include creosote, common metal degreasers, and solvents used as dry cleaning fluid. Once released to the environment, DNAPLs are difficult to remediate, but some methods have been used to varying degrees of success, including the use of surfactants floods. While seemingly effective in field studies, there are questions and concerns regarding surfactant-enhanced aquifer remediation that suggest the need for further research. These include potential problematic behavior in the subsurface and possible impacts on future remediation.

There is a potential to use geophysical methods, particularly geoelectrical, to monitor surfactants in the subsurface to better understand their behavior. Previous work has indicated that measurements of pH and specific conductivity that were taken in surfactant solutions of deionized water had a different response than control samples (Werkema, 2008). This chapter will introduce the concepts fundamental to this thesis, with further details to follow in subsequent chapters.

Surfactants are amphiphilic monomers composed of a head and tail, generally a functional group and carbon chain, respectively. They are potential groundwater remediators of non-aqueous phase liquid (NAPL) through multiple mechanisms (e.g., U.S. EPA, 1996; Dwarakanath *et al.*, 1999; Londergan *et al.*, 2001). Their amphiphilic nature can both increase a contaminant's solubility through micellar solubilization as well as decrease the interfacial tension between the non-aqueous and aqueous phases.

Surfactant-enhanced aquifer remediation (SEAR) is a promising technology that utilizes water and surfactant solution floods to remove residual DNAPL from an aquifer (Brown et al., 1999; Dwarakanath et al., 1999; Londergan et al., 2001; U.S.EPA, 1996). This technique appears to be a viable method but has not experienced widespread acceptance. There are several criticisms of SEAR which require further research to resolve. Understanding of surfactant behavior in the subsurface is limited, and many surfactants are known to produce uneven wetting surfaces. In addition, the use of surfactants to decrease the interfacial tension between a contaminant and pore fluid may result in unwanted downward migration of the contaminant (Longino and Kueper, 1995). Finally, the current inability to monitor surfactants' behavior in the subsurface makes it difficult to determine whether surfactants are reaching the DNAPL-contaminated areas (Conrad et al., 2002), potentially resulting in less efficient use of surfactants.

Geoelectrical methods including direct current (DC) resistivity, induced polarization (IP), spectral induced polarization (SIP), and ground penetrating radar (GPR) have been used to successfully map DNAPL in the subsurface (Adepelumi et al., 2006; Brewster et al., 1995; Brewster and Annan, 1994; Grimm et al., 2005; Sogade et al., 2006). To address the possibility of monitoring subsurface surfactant floods with non-invasive geophysical techniques, Werkema (2008) tested several physicochemical parameters of various surfactant aqueous solutions, without considering the contributions of solid materials to these responses. This work found that solutions with surfactants showed an increase in specific conductivity over solutions containing no surfactant. Dissolved oxygen (DO), pH, temperature, and density were also tested, with dissolved oxygen, pH, and specific conductivity showing the most predictable response. Because of the positive

response of conductivity to surfactant presence, this research focuses on geoelectrical methods and the parameters that affect them.

In an effort to further previous research, the inclusion of solid materials in the experimental design added more complexity to the conditions, as well as introducing a more realistic situation, closer to what would be encountered in a field application of SEAR. The working hypothesis of the research is that the addition of surfactants will result in a measurable geoelectrical response in analog aquifer materials that can be directly or indirectly detected with SIP and time domain reflectometry (TDR). This anticipated response may enable the use of non-invasive geoelectrical methods to map the subsurface distribution of a surfactant flood. The ability to detect the surfactants or the impact of those surfactants used in SEAR could reduce monitoring uncertainty and increase the technique's use, resulting in more effective clean-up of groundwater.

The hypothesis was tested through a series of 30 experiments. Resistance, phase, pH, DO, specific conductivity, and dielectric constant measurements were made and analyzed. The measured parameters and reasoning for including them are found in Chapter 2, Background Information. A simplistic analog aquifer was created using quartz sand saturated with ten testable surfactant solutions packed into an 18cm long column, 3.5cm in diameter. In this research, the term "analog aquifer" refers to a simulated aquifer environment made with clean quartz sand acting as aquifer solid material and the experimental solutions acting as pore fluid. The construction and further details of the analog aquifer are described in Chapter 3.

The research presented in this paper investigates the SIP response of surfactants in a quartz sand-water matrix, in addition to select water quality measurements and dielectric

constant, measured through time domain reflectometry (TDR). The overall objective of the research was to gain additional insight into the geophysical and physico-chemical responses that could occur during the use of surfactants in groundwater remediation in order to determine the feasibility of using geophysical methods, particularly geoelectrical, to monitor those surfactants in the subsurface. In addition, water quality parameters can indicate changes in physicochemical conditions that may affect geophysical responses of the subsurface or impact remediation efforts.

The ultimate goal of efforts in this field of research is to non-invasively monitor and map surfactants in the subsurface that have been introduced as part of a field application of SEAR. Eventually, it may also be possible to determine the effectiveness of SEAR remediation at a particular site by monitoring where the surfactants are located in the subsurface and whether the DNAPL contaminants are being effectively remediated.

In order to realize these goals, the geoelectrical response to surfactants must be characterized in a laboratory setting to isolate the response of the surfactant from the responses to conditions that will be encountered in the field. Performing small-scale experiments in the lab allows conditions to be adjusted and monitored in order to isolate and scale the experimental response. To enable proper scaling of response, complexity must be incrementally added to the system until it is well understood.

The research described in this thesis represents an early stage of characterizing the geoelectrical and water quality responses of surfactants used in SEAR. Previous work has not included a solid matrix in experiments to represent the solid materials in the subsurface. This research has implemented a simple matrix of 20-30 sieve-size silica sand. The absence of clay in the matrix material was purposeful as clays introduce an

additional level of complexity to the system beyond simple quartzitic sand. Clays have a complex geoelectrical signature, in addition to reacting with surfactants in the subsurface.

The near-uniform grain size and mineral composition limits the heterogeneity and any anomalous response associated with changing environmental conditions. In short, changes in geoelectrical and water quality response should indicate changes in the pore fluid, as opposed to changes in packing method and mineral composition.

The experiment plan was designed with the help of Design Expert 7.0 (Stat-Ease, 2007), an experimental design statistical software used mainly in manufacturing and industrial engineering to optimize performance through combinations of factors (Anderson and Whitcomb, 2000). The design utilized in this project is a General Factorial, more specifically a two factor interaction (2FI). As the name implies, this project utilizes two categorical factors, surfactant and water type, with five measured responses: resistivity, phase, specific conductivity, dissolved oxygen, and dielectric constant. Three repetitions of each surfactant and water treatment were performed, resulting in 30 experiments. Further description of experimental design is found in Chapters 2 and 3. One of the goals of this project is to develop a statistical model for each of the tested responses (i.e., the dependent variables) of real and imaginary conductivity, pH, dissolved oxygen, specific conductivity, and dielectric constant due to the experimental factors. The independent variables in this research are the surfactant treatment and water type.

Investigating the anticipated geophysical response using SIP may enable the use of non-invasive or partially invasive geoelectrical methods to map the subsurface distribution of a surfactant flood. The ability to detect the surfactants or the impact of

those surfactants used in SEAR could reduce monitoring uncertainty and increase its use, resulting in more effective clean-up of groundwater. This research addresses this issue by investigating the geophysical response to select surfactants in a saturated quartzitic sand matrix.

CHAPTER 2

BACKGROUND INFORMATION

The goal of this chapter is to provide the reader with background information relevant to this thesis. Topics covered include dense non-aqueous phase liquids, surfactants and groundwater remediation techniques utilizing them, and geophysical methods. Information on relevant water quality measurements, as well as the experimental design and statistics used in analysis, are also located in this chapter.

Dense Non-Aqueous Phase Liquids

Dense non-aqueous phase liquids are chemical compounds that are generally immiscible, only slightly soluble in water, and have specific gravities greater than one g/cm^3. Common DNAPLs include chlorinated solvents like tetrachloroethylene (PCE), as well as polychlorinated biphenyls (PCBs), coal tar, and creosote (e.g., Brewster et al., 1995; Reynolds and Kueper, 2000). Many DNAPLs are carcinogens and possible teratogens. As such, they are a threat to human health when released to the environment (U.S.EPA, 1991).

Transport of DNAPL in the subsurface is complex and primarily driven by gravity and capillary forces (Figure 1). A typical DNAPL contaminant plume will flow through the vadose zone to the transition zone and associated capillary fringe, where the capillary forces of the pore fluids can inhibit its further downward movement into finer-grained materials. In this situation, the contaminant will flow horizontally or build vertically until its fluid pressure overcomes the capillary pressure in the pore spaces (Zhong et al., 2001).

Upon penetration of the saturated zone, DNAPL will continue to move downward, displacing groundwater until it reaches an impermeable barrier or a fining textural interface. Textural interfaces include changes in pore size, permeability, wettability, and capillary pressures (Bradford et al., 1998).

The dense nature of DNAPL can result in its pooling at low spots in the aquifer base and migration against the groundwater gradient, resulting in up-gradient contamination beyond expected diffusion. In addition, any heterogeneities of the aquifer, including changes in porosity, permeability, capillary pressure, or groundwater flow will alter the migration of the contaminant (National Research Council of the National Academies, 2005).

Traditional pump-and-treat remediation methods do not appear to be completely effective in removing DNAPL from the subsurface due to complex migration and the DNAPL physical characteristics (Kueper et al., 1993; Londergan et al., 2001; Mackay and Cherry, 1989; Mercer and Cohen, 1990; Qin et al., 2007; Zhong et al., 2001). Sinking DNAPL displaces fluids from the pore spaces. After the bulk of the DNAPL volume has moved through an area, the in-situ pore fluid reinvades and fragments the DNAPL into free-phase pools and disconnected ganglia (Zhong et al., 2001). The disconnected DNAPL is referred to as residual, which implies that the DNAPL is trapped in the pore spaces as a result of high interfacial tensions and pore size. Residual DNAPL is a problem because it can be a source of long-term contamination.

An interface is the boundary between two phases that are immiscible or have low miscibility. Interfacial tension is defined as the amount of work required to expand an interface between two phases by a unit area (e.g., Rosen, 2004). If one of the two phases

is a gas, this is generally referred to as surface tension. If both phases are liquid, it is simply termed interfacial tension. This term can also be used to describe the dissimilarity between the two phases. In general, two similar phases have lower interfacial tensions than two less similar phases (e.g., Rosen, 2004).

High interfacial tension inhibits the DNAPL from easily transitioning into the aqueous phase. The interfacial tension between groundwater and DNAPL has been measured at 20-50 dynes/cm (e.g., Mercer and Cohen, 1990), although interfacial tension of coal tar has been measured at 0.6 dynes/cm above a pH environment of 9.1 (Barranco and Dawson, 1999). While free or dissolved phase contaminant may be removed using traditional pump-and-treat techniques, the removal of residual contaminant requires impracticably high hydraulic gradients to overcome the capillary pressure of the aqueous pore fluids (Zhong et al., 2001).

Although residual DNAPL has proven to be resistant to non-traditional groundwater remediation methods, there are alternanative treatments. Potentially effective non-traditional methods of removing DNAPL include enhanced bioremediation, air sparging, in-situ chemical oxidation, and steam enhanced extraction, and surfactant-enhanced aquifer remediation (SEAR). The work presented here builds on earlier studies (Werkema, 2008) directed at evaluating the potential of SEAR for DNAPL remediation.

Surfactants and SEAR

A surfactant is a surface active agent, a chemical compound that acts at the interface between aqueous and non-aqueous fluids (Figure 2). Surfactants are amphiphilic monomers composed of a hydrophilic head and a hydrophobic tail. The hydrophilic

group is ionic or highly polar and determines the classification of the surfactant into anionic, ionic, nonionic, or zwitterionic. The hydrophobic group is generally composed of a carbon chain (Figure 3). As a result, surfactants are soluble in both water and organic solvents (Lowe et al., 1999; Mercer and Cohen, 1990; Sabatini and Knox, 1992; West and Harwell, 1992).

Surfactants have the potential to be successful DNAPL remediation agents because of their ability to interact with a NAPL contaminant in two ways. First, surfactants can decrease the interfacial tension between the aqueous and nonaqueous phases (e.g., Adamson and Gast, 1997), thus lowering the force required for the DNAPL to displace water from a saturated pore (National Research Council of the National Academies, 2005), resulting in increased contaminant mobility. Second, surfactants can also increase the solubility of nonaqueous contaminants through the formation of micelles (Adamson and Gast, 1997; Harwell, 1992; Londergan et al., 2001; Lowe et al., 1999; U.S.EPA, 1996). The addition of surfactants to a system above the critical micelle concentration (CMC) may result in the growth of surfactant monomers into micelles through aggradation. A micelle is a grouping of monomers of surface active agents (e.g., Rosen, 2004). Fifty to two hundred of these monomers may cluster together to form structures with hydrophobic interiors and hydrophilic exteriors (Harwell, 1992). NAPL contaminant molecules can collect in the micelle interiors, while the micelle itself is soluble in the aqueous phase (Figure 4). This process effectively increases the solubility of the contaminant by creating a macroemulsion that can be extracted from the subsurface (Lowe et al., 1999). An emulsion is a suspension of molecules of a liquid that lies within a second, immiscible liquid in the presence of an emulsifying agent. A

macroemulsion refers to the relatively large size of the particles in the suspension, which must be greater than 400 nm (e.g., Rosen, 2004).

Surfactant-enhanced aquifer remediation (Figure 5), is a promising technology that utilizes water and surfactant solution floods to remove residual DNAPL from an aquifer, although it is not yet widely used (Brown et al., 1999; Dwarakanath et al., 1999; Londergan et al., 2001; Qin et al., 2007; Robert et al., 2006; U.S.EPA, 1996). A typical surfactant-enhanced pump-and-treat remediation effort begins after the majority of free-phase DNAPL has been removed from the target area. This removal of free-phase DNAPL can be achieved through well skimming, vacuum-enhanced recovery (bioslurping), or water flooding (Lowe et al., 1999). Water flooding is often the most practical option in preparation of SEAR, as the same equipment can be utilized for the surfactant floods. It is important to note, however, that every site must be evaluated to determine the best method of remediation. After the free-phase contaminant has been removed, surfactant solutions are injected into the subsurface so that they will sweep through the target area. The surfactant floods increase contaminant solubility as they sweep through the subsurface. After surfactants have had time to equilibrate, water floods typically follow in order to flush the system of solubilized DNAPL and surfactant solution. Multiple pore volumes of surfactant solutions and flood cycles may be necessary depending on the swept volume (Lowe et al., 1999).

The length of time required to successfully complete a SEAR application will depend largely on the target zone permeability and heterogeneity, the number of pore volumes required to treat the area, and spacing between the delivery and recovery wells. While a full scale operation could take over a year to reach completion, it is believed that the

amount of contaminant removed using SEAR is larger than can be removed using another enhanced pump-and-treat or natural attenuation in the same amount of time (Harwell, 1992; Lowe et al., 1999).

Design of the SEAR process requires identifying the chemical make-up of the contamination, as well as determining subsurface geology and hydrogeology. Understanding the chemical system aids in the selection of the surfactant(s), while understanding the subsurface will help in understanding and predicting behavior of the surfactant floods (Harwell, 1992; Lowe et al., 1999).

There are several criticisms of SEAR which have limited its use thus far. As with most pump-and-treat remediation methods, the efficacy of treatment is a function of the hydraulic conductivity at the site (Fountain et al., 1996). Because of this, sites with low or heterogeneous hydraulic conductivity will continue to be difficult to remediate, although some laboratory experiments suggest that the addition of polymer to the surfactant solution can diminish these problems (Dwarakanath et al., 1999; Martel et al., 1998; Robert et al., 2006). Most surfactants display uneven wetting surfaces or fronts in the subsurface. These preferential flow paths, along with the present inability to monitor surfactant behavior in the subsurface, make it difficult to determine whether surfactants are reaching the DNAPL-contaminated areas. In addition, most field studies have treated relatively low amounts of contaminant at a small scale (Londergan et al., 2001), leaving uncertainties about the effectiveness of using surfactants at larger-scale sites. In addition, some surfactants can act as bactericides, inhibiting microbial activity and biodegradation in the subsurface (Bramwell and Laha, 2000; Willumsen et al., 1998). This may affect ongoing and future bioremediation at a site remediated with surfactants.

One of the principal criticisms is related to a surfactant's ability to decrease interfacial tension. In order to mobilize a contaminant, the interfacial tension between the aqueous and non-aqueous phases must be lowered to a high degree. This decrease could result in downward migration of the contaminant through low permeability barriers, fractures, or faults which had previously not acted as DNAPL conduits due to the high interfacial tension (Longino and Kueper, 1995). Research in this area has suggested that surfactant choice and mixture can decrease this problem. In general, a surfactant that is engineered to increase contaminant solubility will not necessarily result in a large decrease in surface tension (Harwell, 1992; Pope and Wade, 1995).

Some controlled field studies have experienced significant successes with SEAR, reporting over 85% reduction in NAPL mass (Fountain et al., 1996; Martel et al., 1998), and up to 98.5% (Brown et al., 1999; Londergan et al., 2001). There is some indication that SEAR is not as effective with increasing complexity of a mixed NAPL contaminant, although evidence for this statement is sparse (Jawitz et al., 1998).

Geophysical Methods

All materials have inherent geophysical and compositional properties which can be measured with proper instrumentation. These properties include, but are not limited to, density, electrical and magnetic fields, temperature, and chemical make-up. A wide range of geophysical methods and techniques for measuring some of these properties have been developed for application throughout the various branches of geoscience. Gravity, corresponding to density, and magnetic surveys can be used to locate large or small-scale anomalies in the subsurface due to density or magnetic property contrasts.

Seismic surveys, which utilize acoustic wave properties, can be used to identify subsurface structure (Lowrie, 2003; Telford et al., 1990).

Scientists have taken advantage of the electrical properties of many groundwater and soil contaminants in order to monitor the location and behavior of contaminant plumes. DNAPL plumes have been identified through GPR, IP, and resistivity surveys (Brewster et al., 1995; Brewster and Annan, 1994; Grimm et al., 2005; Hwang et al., 2008; Sogade et al., 2006). In particular, geoelectrical methods have been found useful as many contaminated areas show altered electrical conductivity relative to uncontaminated areas after the introduction of some pollutants.

Additionally, previous work (Werkema, 2008) indicated that the measured geoelectrical parameter of specific conductivity showed a larger response to surfactant presence, while density failed to respond substantially.

Aside from the Werkema 2008 EPA report, there is little in current peer-reviewed literature that indicates that the geophysical responses of surfactants used in SEAR have been or are being investigated. There is some indication of research within the petroleum industry, however. Specifically, the use of high resolution resistivity has been used to monitor surfactant floods, among other things, in deep formations (Black et al., 2007).

Geoelectrical Methods

Conductivity

All materials have inherent electrical properties including electrical conductivity or resistivity. Conductivity and resistivity are material properties that are independent of a material's thickness or geometry. Conductivity is the ability of a material to allow current to flow through it. Resistivity is its inverse, a relationship defined in Equation 1:

$$\sigma = \frac{1}{\Omega} \tag{1}$$

σ is conductivity and Ω is resistivity. Both parameters are measured in per unit length.

Conductance is an object property, as opposed to a material property. It is also termed the thickness-conductivity product (Telford et al., 1990) and is the conductivity of a material that has been corrected for the size and geometry of the object.

Electrical conduction is a broad category that encompasses several types of mechanisms. Common electrical mechanisms include ionic or electrolytic, surface, and electronic conduction.

Electrolytic, or ionic, conduction refers to electrical current flow via the pore fluid of a material and is the most common form of conduction in low-clay, uncontaminated, water-saturated environments (Figure 6).

Surface conduction refers to the transfer of electricity along the fluid-grain interface and the electrical double layer (if present), and is a function of surface charge density, grain surface area, and ion mobility (Endres and Knight, 1993; Lesmes and Frye, 2001; Marshall and Madden, 1959; Revil and Glover, 1998; Schwarz, 1962; Vinegar and Waxman, 1984). The surface conduction mechanism moves current through the electrical double layer (EDL), a small region adjacent to the grain surface (Figure 7). The EDL is often associated with clay materials and can also develop in the presence of biodegradation (Aal et al., 2004; Atekwana et al., 2004). The double layer is composed of two layers: a single fixed layer of ions adhered to a grain's surface and a diffuse layer of ions that exists adjacent to the grain's surface. Ions can move across the diffuse layer

in a process called surface conduction, which tends to be a slower mechanism than ionic conduction.

Clays and other phyllosilicates, unlike quartzitic sand, are not electrically inert. They are capable of cation exchange due to their sheetlike mineral structure (Schoen, 1996), and have the potential to impact geoelectrical response. Because of this structure, there is typically water trapped between the sheets, affecting conductivity. In addition, clays typically have a negative surface charge, which enables them to adsorb ions at their surfaces. Depending on the charge balance of the clay and the ions available for adsorption, the clay may form an electrical double layer instead (Schoen, 1996).

Biodegradation has several mechanisms by which surface conduction can be increased. These include excess charge build up in the fluid-grain interface and the potential for the microbes themselves to become polarized. Additionally, the increased in microbial colonies may result in a build-up of organic acid in the subsurface. The organic acid can increase etching of the grains, likely resulting in an increase in surface area, which is a partial control on surface conduction (Aal et al., 2004; Atekwana et al., 2004). It should be noted that the phenomenon of microbial-enhanced surface conduction is not well understood at this point in time.

Electronic, or ohmic, conduction can occur in the presence of metallic ions as a result of vibrations in the lattice (Howarth and Sondheimer, 1953). The free electrons in metals, and sometimes crystals, acquire a common drift velocity when an electrical field is applied. This slows and directs the electrons in the direction of the field. Resistivity by this mechanism is determined by the free time between collisions of the electrons into

the metal atoms. More frequent collisions means that resistivity is higher, while fewer collisions result in lower resistivity (Lowrie, 2003).

In the absence of clays, DC resistivity measurements can be related to the geoelectrical response of pore fluids to that of the matrix through Archie's Law (Eq. 2):

$$\rho_e = a * \rho_w * \phi^{-m} \quad (2)$$

ρ_e is bulk resistivity, ρ_w is resistivity of the pore fluid, ϕ is the porosity of the matrix, and a and m are empirical parameters relating to cementation (Archie, 1942).

In this context, the matrix refers to the solid materials in an aquifer, as well as the chemical and physical properties due to the solids. These properties include porosity, grain size, shape, composition, and sorting. While Archie's Law appears to be valid when conduction is primarily through pore fluids, it does not describe the role of surface conduction in bulk resistivity.

Archie's Law can be rearranged (Eq 3) to create a formation factor, FF, which is the portion of bulk resistivity that incorporates the matrix.

$$FF = \frac{\rho_e}{\rho_w} = \frac{a}{\phi^{-m}} \quad (3)$$

As stated previously, Archie's Law assumes conduction is through the pore fluid alone, known as electrolytic conduction. However, surface and electronic conduction are also common methods of conduction and capacitance (i.e. charge storage). Archie's Law is often modified to include a surface conduction term because of these additional conduction mechanisms, as well as the presence of clays in many aquifer materials (Waxman and Smits, 1968).

Alternating current conductivity (complex conductivity) is a complex parameter (Eq. 4), with real and imaginary components, as it consists of both a magnitude and a direction. The direction is referred to as phase (e.g., Zonge et al., 2005).

$$\sigma^* = \sigma' + i\sigma'' \quad (4)$$

This equation describes the relationship between complex conductivity and the real and imaginary components, σ* is the complex conductivity, σ' is the real component, and σ'' is the imaginary component of conductivity. Real conductivity is, in essence, the total or bulk conductivity of the system. It takes into account electrolytic conduction, surface conduction, and any electronic conduction. Imaginary conductivity is the component of the measured bulk conductivity that results from polarization of ions at the fluid-grain interface. When a current is applied to some materials, polarization at the fluid-grain interface occurs, separating the anions from the cations (Figure 8). When the current is turned off, the ions re-equilibrate along the interface. In the time domain, this polarization and re-equilibration appears as a decay curve over time. In the frequency domain, the polarization appears as a frequency-dependent phase shift, or change in angle, of the received sine wave relative to the transmitted signal (e.g., Zonge et al., 2005).

Spectral Induced Polarization

During spectral induced polarization (SIP), current is induced in the subsurface or experimental sample over a range of frequencies. SIP measures the resistivity magnitude and phase as functions of frequency, which can then be used to calculate real and imaginary conductivities (Eq. 5 and 6).

The calculations for real and imaginary conductivities utilize a phase shift term. The phase shift is the difference between the phase of the transmitted sine wave signal and the phase of the received sine wave signal. A large phase shift, suggests that some of the transmitted current was attenuated during conduction. A delayed current could indicate a change in conduction mechanism from electrolytic conduction to surface conduction or polarization because of their slow speeds relative to electrolytic conduction. It could also correlate to a change in chemistry or materials encountered during testing (e.g., Zonge et al., 2005). SIP assesses the frequency dependence of this response, which may be indicative of a specific material or set of conditions in the subsurface (e.g., Zonge et al., 2005).

$$\sigma' = |\sigma| \cos\phi \tag{5}$$

Equation 5 (e.g., Zonge et al., 2005) shows the calculation of real conductivity from the conductivity magnitude and phase shift from a SIP reading. σ' is the real conductivity component and ϕ is the phase shift in degrees.

$$\sigma'' = |\sigma| \sin\phi \tag{6}$$

Equation 6 (e.g., Zonge et al., 2005) shows the calculation of imaginary conductivity from the resistivity magnitude and phase shift of a SIP reading. σ'' is the imaginary conductivity component and ϕ is the phase shift in radians.

Spectral induced polarization has been used to successfully map DNAPLs in the subsurface (Brewster and Annan, 1994). If subsurface surfactant floods could also be monitored with SIP, it could be possible to develop models that aid in the SEAR process and allow for a single survey to monitor both types of substances.

Dielectric Constant and Time Domain Reflectometry

Electrical permittivity is a dimensionless term that describes an ion's ability to transmit charge or polarize due to an applied electric field in a particular medium (e.g., Lowrie, 2003). At some frequencies of alternating current, polarization occurs, resulting in a modification of effective conductivity (Lowrie, 2003). Normally, electrons are distributed symmetrically around an atom's nucleus. When an electrical field is applied, the electrons are displaced in an opposite direction to the field, while the nucleus shifts in the same direction as the field (Lowrie, 2003). As a result, the permittivity of the material is different from that of free space.

Dielectric constant, often referred to interchangeably with relative permittivity, is a dimensionless term that describes the relationship between electrical permittivity of free space and electrical permittivity of a medium (Lowrie, 2003) (Eq. 7).

$$\varepsilon = K * \varepsilon_0 \tag{7}$$

ε is the permittivity of a medium other than free space, ε_0 is the permittivity of free space, and K is the dielectric constant. Alternately, K can be represented by ε_r, indicating the relative permittivity. Equation 7 is then rearranged and substituting ε_r for K yields the ratio between permittivity of free space versus permittivity of another medium (Eq. 8) (Lowrie, 2003)

$$\frac{\varepsilon}{\varepsilon_0} = \varepsilon_r \tag{8}$$

The relative permittivity, or dielectric constant, can be represented by the complex parameter K*, which, as in complex conductivity, consists of real and imaginary components. The real component, K' describes energy storage, while the imaginary, K'' describes energy loss. K* has been shown to be frequency dependent in some

environments (Kelleners et al., 2005), as described in Eq. 9 (Topp et al., 1980). This frequency dependence also modifies the effective conductivity through the following relationship:

$$K^* = K' + i\left[K'' + \left(\frac{\sigma_{dc}}{2\pi f \varepsilon_0}\right)\right] \quad (9)$$

K* is the complex dielectric constant, K' is the real component of the dielectric constant, K'' represents the loss due to frequency-related relaxation mechanics, σ_{dc} is the zero-frequency conductivity, and f is frequency.

In direct current and low frequency environments, dielectric effects are considered negligible. In an environment with an alternating electrical field however, polarization changes with frequency, thus resulting in fluctuating polarization and effective conductivity.

Time domain reflectometry (TDR) is a method used to measure the apparent dielectric constant (or electrical permittivity) of a medium by sending a pulse of electromagnetic energy at 746 kHz through a transmission line embedded in the medium. During travel, the beam reflects off of discontinuities in the host material. When the pulse reaches the end of the line, it reflects most of the remaining energy (Dalton et al., 1984; Soilmoisture Equipment Corporation, 2005; Topp et al., 1980). The travel, or transit, time is recorded and used to determine the apparent dielectric constant in Equation 10 (Soilmoisture Equipment Corporation, 2005).

$$K_a = \left(\frac{t * c}{2L}\right)^2 \quad (10)$$

K_a is the apparent dielectric constant, t is the transit time, c is the speed of light, L is the length of the transmission line.

The dielectric constant can be used to determine moisture content of the host material through the empirical Topp Equation, illustrated in Equation 11 (Topp et al., 1980).

$$K_a = 3.03 + 9.3\theta_v + 146.0\theta_v^2 - 76.7\theta_v^3 \quad (11)$$

K_a is the apparent dielectric constant and θ_v is the volumetric moisture content.

It is also a physical property that is a factor in ground penetrating radar (GPR) transmission, as is conductivity. Electromagnetic wave propagation velocity and reflection interfaces are strongly influenced by dielectric constant (Martinez and Byrnes, 2001). The relationship between the velocity of wave propagation and the dielectric constant is described in Equation 12 (Martinez and Byrnes, 2001).

$$V = \frac{c}{\varepsilon^{0.5}} \quad (12)$$

V is the velocity of wave propagation, c is the speed of light in a vacuum, and ε is the permittivity of the material.

Dielectric constant is a direct and indirect factor in numerous geophysical methods, including GPR, which has been used successfully to map DNAPL (Brewster and Annan, 1994).

Water Quality Measurements

Dissolved Oxygen

Dissolved oxygen (DO) refers to the amount of oxygen that is dissolved in water. The range of DO in natural water is between 0 to 10,200 µg/L (Borden et al., 1995;

Kreamer, D.K., personal communication, November 2009). DO concentrations in a system affect chemical and biological reactions that depend upon available oxygen. Changes in redox or other conditions may alter surface conduction, resulting in a geoelectrical response (Werkema, 2008). Identifying changing DO in conjunction with conductivity, resistivity, and phase shift measurements, will aid in determining its impact on the geoelectrical response.

Understanding the change in subsurface dissolved oxygen as a result of surfactant application is important for multi-pronged remediation efforts. If biodegradation is being considered as a remediation process to follow SEAR, understanding how oxygen content is changing is imperative.

pH

pH measures the activity of hydrogen ions in a system, and ranges between 0 and 14. pH is the cologarithm (i.e. colog) of the activity of dissolved hydrogen ions (Eq. 13).

$$pH = -\log\left[H^{+}\right] \tag{13}$$

Acidity increases with smaller numbers, and larger numbers are increasingly alkaline. A measurement of 7 is considered neutral. pH values of natural waters typically range between 6.2 and 8.0 (Hoyle, 1989; Kehew and Passero, 1990; Nicholson et al., 1983).

The pH of a system can affect chemical and biological behavior. Low pH, indicative of an acidic system, or high pH, indicative of alkalinity, can affect which microorganisms will be present in an environment, how much chemical weathering of solids will occur, and the behavior of a contaminant plume in the subsurface, as well as the complex conductivity response (Olhoeft, 1985).

Lower pH in the subsurface has been associated with a higher degree of etching on the solid materials and grain surfaces (Atekwana et al., 2004; Sauck, 2000), which could result in a change in conductivity mechanism. As discussed previously in the chapter, this could result in a change in measured real or imaginary conductivity.

Specific Conductivity

Specific conductivity electrolytic conduction, or conduction by movement of ions through pore fluid. Specific conductivity measures electrical conduction through a medium that is under the influence of an applied electrical field. The range of specific conductivity values of typical natural waters is between 40 and 400 µS/cm (Williams et al., 1993).

Specific conductivity is a component of real conductivity. As such, the ability to compare any changes in specific conductivity with changes in the resistivity measured with SIP is a powerful tool which can help us to understand the importance of the different conduction mechanisms taking place in the subsurface.

Statistics

When reporting experimental results, it is important to be able to communicate the relevant information in a meaningful way. Statistical methods are helpful in describing a data set's overall character, relationships among the points in a data set, and relationships to a predictive model for large data populations. Common statistical evaluations include a data set's mean, standard deviation, and R^2 value. The following section will describe some of the statistical tools used in this project.

Regression Analysis

Regression analysis is a method used to fit a mathematical model to a data set (Anderson and Whitcomb, 2000). It is a way to produce a statistical model describing the relationship between a dependent variable, or response, and one or more independent variables, or factors (Kleinbaum et al., 1998). Regression analysis is useful for characterizing relationships, finding a quantitative formula to predict the trend of a response, or evaluating interactive effects of multiple factors on a response.

Proper experimental design and data analysis can result in statistical models, which then require careful consideration due to the inherent noise in all data sets. Alternately, a deterministic model, such as the equation to find a falling object's velocity on Earth, lacks error. It is considered a perfect mathematical model because the response (velocity) varies exactly as predicted as the model is derived analytically rather than empirically (Kleinbaum et al., 1998).

Analysis of Variance

Analysis of variance, also referred to as ANOVA, is a statistical method that assesses the significance of experimental results through evaluation of a data set's variance. Variance is the measure of spread or variability in a data set (Anderson and Whitcomb, 2000). Many basic statistical parameters, including standard deviation (σ), coefficient of variance (C.V.), and the multiple correlation coefficient (R^2) values, are based on estimates of several components of variance. The calculations of these fundamental statistical variables are either derived directly from variance, or indirectly through parameters like the sum of squares (Kleinbaum et al., 1998).

The term “analysis of variance” is derived from the method of determining the ANOVA statistics. The total variability within a data set is partitioned into separate components, which are used to calculate useful parameters like the sum of squares (Montgomery, 1997). The sum of squares terms are included in the ANOVA. A sum of squares is the sum of the squared distances of each data point from the data set mean (Anderson and Whitcomb, 2000). It can be separated into several components, including the total sum of squares (SS_{TOT}), the sum of squares between treatments (SS_{TRT}), the sum of squares due to error within treatments (SS_E), and several others (Montgomery, 1997).

The R^2 value is the multiple correlation coefficient. It ranges between 0 and 1 and provides an estimate of the overall variation in the data set which is accounted for by a proposed statistical model (Anderson and Whitcomb, 2000). More successful predictive models will maximize the R^2 values. It is calculated using sum of squares in Equation 14 (Montgomery, 1997).

$$R^2 = \frac{SS_{TOT} - SS_E}{SS_{TOT}} \tag{14}$$

R^2 is the multiple correlation coefficient, SS_{TOT} is the total sum of squares, and SS_E is the sum of squares due to the error or residuals.

There are three important versions of the R^2 parameter which should all be examined to determine the relevancy of a variable to the data set and the proposed model. The first version is the simple R^2, discussed above. The adjusted R^2 and predicted R^2 values are described below. Ideally, all three of the different R^2 values discussed in this section would be maximized and in close agreement. Values that differ greatly could indicate a problem in the experimental design.

R^2 is affected by the number of independent variables, or terms, included in the statistical model, and has a tendency to increase with the number of variables regardless of whether all terms are significant (Kleinbaum et al., 1998). Because of this, models with large R^2 values may actually be poor predictors of a response (Montgomery, 1997).

The dependence of R^2 on the number of independent factors has resulted in the development of the adjusted R^2 (R^2_{adj}). This term is the multiple correlation coefficient which is corrected for the number of model terms and points in the design. In general, if irrelevant terms are added to a model, the R^2_{adj} value will decrease; the more R^2 and R^2_{adj} differ, the more likely it is that non-significant terms have been added (Montgomery, 1997).

A third version of the R^2 value is predicted R^2 (R^2_{pred}) (Eq. 15) (Montgomery, 1997). This parameter describes the amount of variation in the predicted data set that cannot be explained by the model, and makes use of the predicted residual sum of squares (PRESS). PRESS is a measure of how well a statistical model fits each point in the design and is determined by repeatedly fitting the model to each of the design points except for the one that is being predicted. The difference between the predicted and actual value of each point is squared and summed, resulting in the PRESS (Anderson and Whitcomb, 2000). In short, it is the sum of squares of the PRESS residuals (Montgomery, 1997).

$$R^2_{pred} = 1 - \frac{PRESS}{SS_Y} \tag{15}$$

PRESS is the predicted sum of squares and SS_Y is the sum of squares of the response.

Experimental Design

Considered a way to develop and perform more effective experimentation, DOE (design of experiments) has been used in manufacturing for several years. While in the past, users were required to set up experiments to maximize or minimize responses based on limiting factors, several software programs now exist that can be operated on ordinary personal computers. Most of this software is able to not only aid in the set up of experimental designs, but also to perform statistical analysis on the experimental data.

The experimental agenda for this project was designed with the help of Design Expert 7.0 (Stat-Ease, 2007), an experimental design statistical software used mainly in manufacturing and industrial engineering to optimize performance through combinations of factors (Anderson and Whitcomb, 2000). Experimental designers must be careful not to use this software as a type of "black box" utility, however. In order for the software to suggest a design that will maximize potential response, the experimenter must understand the components and styles of experimental design.

A factor is a variable, ideally assumed to be independent of any other testable factors, that is manipulated during an experiment to examine its effect on responses. A response is a measurable product or effect that is thought to be affected by the experimental factors (Anderson and Whitcomb, 2000). There are two common types of factors: categorical and numerical. A categorical factor is one which has conditions that represent discrete levels or options (Anderson and Whitcomb, 2000). For example in this experiment, water type is either tap or deionized, with no other steps or possibilities in between considered. A numerical factor is a quantitative variable that can be adjusted through a

continuous range (Anderson and Whitcomb, 2000). Temperature and surfactant concentration are examples of this type of factor.

There are several different styles of experiments, ranging from simple comparison to the more complex response surface methods. The simplest form, the F-test, compares two or more discrete levels of a single factor by evaluating the variance among the treatments and comparing it to the variance among the individual repetitions within each treatment. It is considered a one-factor design (Anderson and Whitcomb, 2000).

If the factor has little to no effect on a response, the F-ratio will be close to 1. The F-ratio, or F-value, is a ratio used in the ANOVA (discussed below) that is derived from the F-test. It is essentially the ratio of the difference in response between the treatments compared to the experimental noise. As a factor's influence on a response increases, the F-ratio will also increase, while decreasing the chance that the suggested correlation is due to chance or noise. The p-value, derived from the F-ratio, is a parameter that sets a quantitative value on the probability that the correlation is due to noise. A p-value less than 0.05 (5%) indicates there may be a significant relationship between the tested factor and response (Anderson and Whitcomb, 2000).

The factorial group of designs is more complex than simple comparisons. These designs allow experimentation on multiple factors at multiple levels. The simplest of the factorial group of designs is 2 factors with 2 discrete levels. One of the advantages of the factorial designs is that they can require fewer experimental runs to produce statistically valuable results than experimental designs that test only one factor at a time. As such, the more factors and levels involved, the more advantageous it is to utilize a factorial design (Anderson and Whitcomb, 2000).

The nature of the factors can affect which experimental design type to implement. As described above, factors can be categorical or numerical. An experimenter with only categorical factors may find it best to perform a general factorial design. In this style of design, all of the possible combinations of factors are run (Anderson and Whitcomb, 2000).

In addition to factor and response consideration, experimental designs must also consider the effects of environmental changes that cannot be easily controlled. These include slight temperature changes that will affect conductivity measurements, diurnal effects, and instrumental drift. These variables can be accounted for through the use of blocking. Blocking is a DOE technique that divides a suite of experiments into packages that can be performed in a single time period. If a specific block has higher or lower measured values, they can be adjusted for during statistical analysis (Anderson and Whitcomb, 2000).

The project described in this thesis utilized a 2FI, or a two-factor interaction design. This is a version of a general factorial. In this design, the two factors are surfactant treatment and water type. Both are categorical. Traditional experimental design does not identify or detect interactions between factors or that interaction's effects on the tested responses. The 2FI design allows to evaluate the interactions of two factors at various discrete levels and the responses associated with them (Anderson and Whitcomb, 2000). The experiments were divided into three separate blocks of 10 experiments each. Each block was performed over 2 days.

This chapter has detailed some of the relevant background information that will be helpful in understanding the methods used in the project, as well as some of the reasons

behind attempting this particular type of research. The overall objective of the research was to gain additional insight into the geophysical and physico-chemical responses in a quartz sand-water environment in the presence of surfactants and to form a simple predictive model for each response. Changes in the measured parameters could indicate the feasibility of using geophysical field methods to monitor surfactants used in groundwater remediation of DNAPLs. The following chapter will detail the methods and materials used in the research described in this paper.

CHAPTER 3

MATERIALS AND METHODOLOGY

This chapter provides an explanation of the techniques and materials used in the project documented in this thesis. The constituents and construction of the experimental column are described, in addition to the methods used for the spectral induced polarization (SIP), water quality, and time domain reflectometry measurements. The last section of the chapter details the statistical analyses performed on the collected data, including how the data was manipulated and evaluated for integrity.

Experimental Column

A simplistic analog of an aquifer environment was created using electrically inert solid materials and an electrolyte. In this research, the term "analog aquifer" refers to a simulated aquifer environment made with clean quartz sand acting as aquifer solid material and the experimental solutions acting as pore fluid. It is considered analog because it is not a true aquifer environment. The testing conditions in the proposed experiments are surfactant-saturated, quartz sand environments. All experiments were performed using Ottawa silica sand as the aquifer matrix material. According to U.S. Silica Company (1997), sieve testing places 99% of the sand at 20-30 sieve size (0.600-0.850mm diameter), and chemical analysis places the quartz content at SiO_2 99.8%. Of the remaining 0.2%, 0.1% includes 0.02% Fe_2O_3, 0.06% Al_2O_3, 0.01%TiO_2, and less than 0.01% each of CaO, MgO, Na_2O, and K_2O. The remaining 0.1% was lost on ignition through analysis (U.S.Silica Company, 1997). The sand conforms to American Society for Testing and Materials C778, a standard specification.

Surfactants were mixed into separate deionized and tap water solutions at concentrations commonly used in the field, resulting in 10 experimental solutions (Table 1). The surfactant formulas chosen for this project have been successfully used in field and laboratory studies (Londergan et al., 2001; Ramsburg and Pennell, 2001; Rothmel et al., 1998) and include Aerosol MA-80-I (AMA-80-I), Dowfax 8390, and Steol CS-330. All of these surfactants are non-ionic and displayed the highest, median, and lowest response, respectively, in Werkema (2008). These responses are shown in Table 2. A control with no surfactant was also tested for this thesis. Concentrations used were 8% AMA-80-I, 5% Dowfax 8390, 0.5% Dowfax 8390, 0.025% Steol CS-330, concentrations that have previously been used in field and lab-based studies (Londergan et al., 2001; Ramsburg and Pennell, 2001; Rothmel et al., 1998). SIP experiments were also conducted on DI solutions of 8% Dowfax 8390 and 8% Steol CS-330 in order to compare the surfactant responses to one another.

Tap water was sourced from a single spigot in the U.S. EPA POS building, Room 21 on the U.S. EPA's Las Vegas campus. The water measured a specific conductivity value of 1025 µS/cm at the time that solutions were mixed. Deionized water was sourced from the DI system located at the Quality Assurance Lab, also on the U.S. EPA's Las Vegas campus. The DI system is monitored on a weekly basis by U.S. EPA contractors and is rated to 18 MΩ. All solutions were mixed in a 1 L Ehrlenmeyer flask and stored in cubitainers. Surfactant was added to the flask first, followed by the water. The flask was capped and swirled to mix the components. In the case of the 5% and 8% solutions, water was added to the flask 300 to 400 mL at a time. Swirling followed each addition to more efficiently and uniformly mix the components.

Spectral Induced Polarization

For the SIP experiments, the analog aquifer was confined to a custom-made PVC pipe apparatus engineered to hold the aquifer material (Figure 9). It is similar in design to columns used by several other researchers (Slater and Glaser, 2003; Slater and Lesmes, 2002; Vanhala and Soininen, 1995). The column, built on site, is 18 cm in length, 3.5 cm in diameter, and uses 4 silver-silver chloride (Ag-AgCl) electrodes, 2 current and 2 potential, to make the SIP measurements. Ag-AgCl electrodes were chosen because they have been shown to produce minimal surface impedance and voltage drop over time (Vanhala and Soininen, 1995). High surface impedance can result in large phase shifts, masking the true response (Vanhala and Soininen, 1995). To coat electrodes, 14 gauge fine silver (99.9%) wires, were cut and shaped, then soaked in bleach (NaClO) overnight. Current electrodes were coiled into a disk shape of slightly less than 3.5 cm diameter, while potential electrodes were straight lengths of wire cut to 4.5 cm long (Figure 9).

The potential electrodes are housed outside of and at right angles to the main experimental column within 0.8 cm diameter PVC pipe, and isolated from the solid aquifer materials by a 150 micron nylon mesh. The purpose of the mesh is to allow the electrolyte to submerge the potential electrodes, without allowing contact with the solid materials in order to avoid polarization of the electrodes.

The PVC column was sealed with rubber stoppers (Figure 9). Two stoppers (3.5 cm in diameter) were fitted in both ends of the cylinder and sealed into place with electrical tape. Two smaller stoppers (0.8 cm in diameter) were inserted into the ports that were designed to house the potential electrodes. All four stoppers described above were configured with one electrode each. A stopcock was placed at each end of the

experimental column to enable saturation and flow. Stopcocks were inserted into pre-drilled holes in the large stoppers and glued into place. In order to inhibit movement of aquifer material out of the column, a piece of 150 micron nylon mesh was glued over the internal portion the stopcock pipe.

Prior to a SIP measurement, the column was prepared for measurements. The empty column was weighed, followed by a zeroing of the balance. 286 g (±2.5 g) of Ottawa silica sand was added to the column, weighed, followed by a re-zeroing of the balance. 62 g (±2.0 g) of solution was then injected into the column and the column was re-weighed. Optimization of saturation was achieved by injecting the solution into the bottom stopcock of the vertical column. Saturation was assumed when the solution escaped at the top stopcock and the potential electrode chambers were filled with solution. Consistent packing was ensured by using a tapping method while adding sand to the column. The columns equilibrated for 15-30 minutes prior to SIP measurement collection.

Systematic error tests were conducted over two days on five columns to check for potential errors due to electrodes, column construction, or packing procedure. As a total of eighteen columns were used during SIP testing, 27.8% of experimental columns were tested for systematic error. Random columns were chosen and filled with equivalent masses of sand and tap water, with random current and potential electrodes. Tap water was pulled from the spigot on day one and was stored in a cubitainer for the remainder of the systematic error tests. Resistance and phase were measured. It was determined that an error of ±5.1% should be considered with the real conductivity data, and ±4.6% error

should be included with the imaginary conductivity data. Data and the method for calculating percent error from the systematic error tests can be found in Appendix A.

Electrical properties were measured with the SIPLab II®, a multi-electrode acquisition system developed by Radic Research, Inc. (Radic Research, 2007) to measure SIP, or more specifically, the impedance magnitude and phase shift of the materials in the column through a spectrum of alternating current frequencies. The SIP equipment generates and transmits a sinusoidal current which can sweep through a range of frequencies from 1 mHz to 12 kHz. The SIPLab II® measures from a 4 electrode configuration, in this case a Wenner array (Figure 10), and has the ability to apply current and measure multiple electrode configurations in quick succession (Radic Research, 2007). Current was applied through the coiled current electrodes, and resistance magnitude and phase shift were recorded between the potential electrodes at 18 logarithmically-spaced frequencies between 0.091 Hz and 12 kHz. The SIPLabII® makes 32 measurements at each frequency. The recorded response is an average of these measurements (Radic, T., personal communication, September 2009).

pH, Dissolved Oxygen, Specific Conductivity

After SIP measurements were completed, the saturated column was attached to a low flow cell to take pH, DO, and specific conductivity measurements. The closed configuration allowed DO measurements by avoiding degassing and mixing with ambient atmospheric conditions. Flow was driven by an Ismatec (IDEX Corporation, 2007) low-flow peristaltic pump through the circuit outlined in Figure 11. The tubing utilized has an inner diameter of 1.6 mm, and the initial flow rate was set at 9.6 mL/min. Flow moved

from a surfactant reservoir per each surfactant concentration, through the saturated column, and into the low flow cell, which housed a Troll 9500®, until the flow cell was completely filled. The Troll 9500®, produced by In-Situ, Inc. (In-Situ, 2008), is a multi-parameter water quality monitoring system with pH, specific conductivity, optical dissolved oxygen, and temperature probes. Temperature was not controlled during these experiments, but was recorded with the water quality measurements in order to identify any changes. It was not analyzed as a parameter of interest. Changes in environmental conditions, particularly ambient temperature, can have large effects on dissolved oxygen and specific conductivity values.

Systematic error tests were conducted on four columns in order to check for potential errors due to column construction or packing procedure. As a total of fifteen columns were used during water quality testing, 26.7% of experimental columns were tested for systematic error. Random columns were chosen and filled with equivalent masses of sand and tap water. Specific conductivity, pH, and dissolved oxygen were measured and recorded. Based on the calculations located in Appendix A, errors of ±0.37% should be applied to the pH parameter, 10.1% to the specific conductivity data, and 4.3% to the dissolved oxygen data. Data and calculation methods used to determine the errors can be found in Appendix A.

The optical DO probe does not utilize ion exchange or consume oxygen, thus allowing accurate conductivity measurements both before and after DO measurements, as the ion concentration in the electrolyte will not change. The flow cell allows more accurate DO measurements by inhibiting degassing of the water and mixing with ambient atmospheric gases, resulting in contamination.

After initiation of circulation by pumping, the low flow cell filled within 70 minutes. Pumping rate was then lowered to 3.0 mL/min, and DO, pH, and conductivity readings were recorded at 0, 15, and 30 minutes. In systematic error tests, measurements were made at 0, 15, 30, 45, and 60 minutes, but it was determined to be unnecessary to continue readings past 30 minutes as readings appeared to change negligibly. Calculated systematic errors, discussed above, can be found in Appendix A.

Time Domain Reflectometry

Time domain reflectometry measurements were performed in a 30.5cm diameter, 30cm tall PVC column. Each column was filled with 8.77 kg (±0.2 kg) of quartzitic sand, and saturated with 1880 mL (±150 mL) surfactant solution from the bottom of the column by gravity flow (Figure 12). The sand used in the TDR experiments is of the same type as described in the Spectral Induced Polarization section above, as are the surfactant solutions. The TDR instrument utilizes a square wave with a period of 1.34 μS, correlating to a frequency of 746 kHz (van Calker, A., personal communication, September 2009). Three readings were taken immediately upon saturation and averaged. The dielectric constant was measured at a 10 ps sampling resolution, through a 10 ns window. At 10 minutes, three more measurements were made and then averaged.

Systematic error tests were conducted on four columns in order to check for potential errors due to column construction and packing procedure. As a total of five columns were used during TDR testing, 80% of experimental columns were tested for systematic error. Columns were chosen and filled with equivalent masses of sand and tap water. Moisture content and dielectric constant were measured. An error of ±3.6% should be

applied to the dielectric constant response. Data from the systematic error tests can be found in Appendix A

Readings were taken using a SoilMoisture, Inc. MiniTrase (Soilmoisture Equipment Corporation, 2005) time domain reflectometer and a 8 cm three-prong uncoated, buriable waveguide (Figure 13) that was inserted vertically into the saturated sand up to its cable attachment.

Statistical Analysis

After completion of the experiments, results were transferred from a written lab notebook to the Stat-Ease program. Statistical analyses were performed separately on each measured response. For each test, the ANOVA table was examined, with particular attention paid to the p-value and three R^2 values. The table contained information including sum of squares, F-value, and p-value. Information was given for the two factors, surfactant and water type, as well as for the model, residuals, and corrected total. The mean, standard deviation, correlation variable, PRESS, and R^2 values were also included. In addition to the ANOVA parameters, a predictive model was presented by the software. The predictive model offered an estimated value of a given parameter based on the measured data set. After the ANOVA output was evaluated, the data was examined graphically for normality and homoscedasticity of variance.

A series of plots using residual data were prepared in order to evaluate the robustness of the data set. The Box-Cox plot was evaluated for the potential use of a data transform, in addition to examining the maximum to minimum ratio of the data set. Typical analysis requires that the data set is normally distributed and homoscedastic. Homoscedasticity is

also referred to as homogeneity of variance, and implies that variance is constant across the data range (Kleinbaum et al., 1998). If these two conditions are not fulfilled, it may be necessary to apply a power transform over the data set. The Box-Cox plot is a tool used in the Stat-Ease software that aids in determining whether a power transformation would be helpful or necessary in the analysis of a set of data, along with suggesting which one should be applied (Stat-Ease, 2007).

On a Box-Cox Plot, the x-axis is Lambda (λ), while the y-axis is the residual sum of squares. Lambda is the power by which a transform would minimize the residual sum of squares. Ideally, the residual sum of squares is minimized, as a totally homoscedastic data set would have a sum of squares equal to zero (Box and Cox, 1964). The lowest point on the plotted curve gives the λ value to use in the power transformation. Transforming the data by the power λ should create the most stable variance over the data set (Stat-Ease, 2007). In the case that a transformation is applied to the data set, either because of a maximum to minimum ratio larger than three or the Box-Cox plot indicates the benefit of one, analyses are repeated with the new conditions.

To determine whether the normality assumption is valid, a plot of residuals versus normal percent probability was evaluated. Ideally, residuals plot along a straight, 45 degree line (Stat-Ease, 2007). If normality was deemed valid, plots were next examined for trends in the data that could be attributed to experimental design or changes in the environment. For example, a plot of the residuals versus run number can help evaluate the potential of instrument drift over the duration of all experiments or between blocks.

A series of influence plots, including Cook's D and leverage, were next evaluated for evidence of any individual runs that were unduly influencing the data set statistics.

Cook's Distance (Cook's D) is a statistical combination of the leverage and t-test influence parameters (Cook, 1977). Like other influence tests, it describes how a single point affects a model and serves as a criterion for exclusion of outlying data (Kleinbaum et al., 1998). The Cook's D for a point is determined by measuring how much a predictive model would change if the data point was removed. Large Cook's D values are generally associated with high leverage values and large studentized residuals (t-test) (Anderson and Whitcomb, 2000). A large relative Cook's D value may indicate an outlier and should be examined further. A large Cook's D alone is not enough reason to exclude a data point. In this project, if outliers were identified, analysis was started over. If an outlier was found in one response, the data for that run was excluded from analyses of all responses.

After confirming normality and other assumptions, plots of the interactions between factor and response were evaluated. Each response had a single interaction graph with the data set divided by water type into two plots. Surfactant treatment was plotted along the x-axis and response on the y-axis.

The goal of this chapter was to provide the reader with the materials and methods used in this project. In addition, the reader should now be aware of which statistical analyses were used and how data was evaluated for robustness.

CHAPTER 4

RESULTS

This chapter presents the results of the previously described experiments. The chapter is separated into sections by measured parameter: real conductivity, imaginary conductivity, pH, specific conductivity, dissolved oxygen, and dielectric constant. Each parameter's section will include ANOVA and predictive model output, along with normality, influence, and interaction plots. Through analysis, a predictive model was proposed for each parameter using Stat-Ease, Inc. Design Expert v 7. The classical Sum of Squares method was utilized for analysis and model development. The model is presented as a final predictive value for each surfactant treatment in each parameter. Each component is described and explained, with discussion to follow in the next chapter. A response table (Table 3) lists, in run order, the unaltered responses of each experimental run.

Data from 11.7 Hz readings was analyzed for the real and imaginary conductivities. While the measured frequency range is between 0.091 Hz and 12 kHz, the frequencies most often used in applications are between 0.1 and 10 kHz (Vanhala, 1997). Frequencies outside of this range have a tendency to produce a large amount of noise that can obscure the true response (Vanhala, 1997). After examining the real and imaginary responses at several frequencies between 1 and 100 Hz, it was determined that 11.7 Hz had the most stable values. For the raw data, please see Appendix B.

Runs 13 and 22 have been omitted from all analyses. In both runs, the imaginary conductivity is negative, a physical impossibility, and correspond to 5% Dowfax, tap and 8% AMA 80-I, tap, respectively. Because of the omissions of these runs, 5% Dowfax,

tap and 8% AMA 80-I, tap statistics were calculated based on two runs of each type rather than three. In the cases where statistics were calculated on two runs, the raw data was examined to determine whether the remaining runs were consistent.

Real Conductivity

The real conductivity response ranges from 12.06 μS/cm to 1910.83 μS/cm, with a maximum to minimum ratio of 158.4. A ratio greater than 10, as seen in this response, may indicate the potential benefit of a transformation (Stat-Ease, 2007). In addition, the Box-Cox plot suggests a log transform (Figure 14), which was performed. Analysis of both $\log_{10}$(real conductivity) and ln(real conductivity) produce the same statistical result. The ANOVA for real conductivity is found in Table 4.

The mean of the untransformed data set is 561.93 μS/cm with a standard deviation of 672.50 μS/cm. The large standard deviation, relative to the mean value, is most likely due to the large range of values in responses. The R^2 value is 0.9997 with a predicted R^2 value, based on the proposed model, of 0.9992. High quality models produce high R^2 values in both categories. These two values are close to 1.0 and in close agreement, indicating that the model may be a good predictor of real conductivity. The modeled values for $\log_{10}$(real conductivity), as well as the untransformed real conductivity response can be found in Tables 5 and 6. The averages and standard deviations of the measured real conductivity values can be found in Table 6.

The data set was next examined graphically to confirm the required normality assumption (Figure 15). The internally studentized residuals were plotted against the normal percent probability. If the residuals lie in a generally straight line, close to 45

degrees, normality can be assumed. If the data displays a pronounced "S" shape, the data may not meet the normality assumption (Stat-Ease, 2007).

A series of plots of residuals versus predicted value, run number, surfactant treatment, and surfactant treatment were evaluated for trends that could possibly be related to experimental or systematic error and could result in exaggerated relationships in the predictive model (Figures 16-19).

The transformed data set was next examined graphically for any design points with potential undue influence over the predictive model. The leverage plot (Figure 20) appears normal, with no runs showing leverage values of concern (none greater than 0.8). Additionally, a plot of the t-test (Figure 21) shows that all of the experimental run values fall within 95% confidence intervals.

The last influence plot to be evaluated was the Cook's Distance, a combination of the t-test and leverage (please see Chapter 3 for full explanation) (Figure 22). The $\log_{10}$(real conductivity) plot does not indicate any runs with large Cook's D values. The successful evaluation of both normality and influence plots suggests that any outliers have been previously removed from the analysis (i.e. runs 13 and 22 as noted above) and further examination of individual runs is not necessary for the real conductivity response.

The real conductivity responses of the experimental treatments appear to be affected by surfactant type, surfactant concentration, and water type. The results are plotted in Figure 23. Overall, tap solutions, regardless of surfactant, had higher real conductivity responses than the corresponding DI solutions. There is a non-linear relationship between surfactant treatments and real conductivity while the difference in real conductivity by water type appears to be smaller and typically constant, although the

difference may be declining with concentration. The data points appear to be well-constrained with small error bars and little overlap among treatments (Figure 24). An error of ±5.1% should be considered with the real conductivity responses as a result of system error assumed to relate to slight packing differences and sand to solution ratio. Please see Appendix A for explanation of this error.

The plot of $\log_{10}$(real conductivity) of tap solutions shows a more moderate increase in real conductivity than what appears in the DI solutions (Figure 24). This apparent discordance may be a result of the log transform of the data. If the untransformed data is plotted (Figure 25), the relationship between surfactant and real conductivity is similar between water types with tap water showing a higher conductance. The real conductivity response does not appear to show frequency dependence (Figure 26) over the measured frequency spectrum. This suggests that polarization is unlikely in this environment, as a frequency-dependent change in real conductivity would likely be associated with a corresponding change in imaginary conductivity as a result of polarization of the fluid-filled medium.

Values at the extreme upper end of the frequency range appear to show a slight drop in real conductivity. This is consistent through the surfactant treatments and water types and is most likely a result of instrument noise. Measurements at frequencies above 10kHz are often affected by considerable noise likely due to interference by instrument wiring (Vanhala, 1997).

Imaginary Conductivity

Imaginary conductivity response ranges from 0.0113 to 0.0412 μS/cm. The maximum to minimum ratio is 3.65. A ratio greater than 10 may indicate the necessity of a data transformation (Stat-Ease, 2007). In addition, the Box-Cox plot does not indicate the use of a power law (Figure 27). The ANOVA for imaginary conductivity is found in Table 7.

The mean of the data is 0.0214 μS/cm with a standard deviation of 0.0067 μS/cm. The R^2 value is 0.530, but the predicted R^2 value, based on the proposed model, is -0.4086. As stated previously, high quality models produce R^2 values approaching 1.0 in both categories. A negative predicted R^2 value as seen here indicates that the mean of the data set may be a better predictor of imaginary conductivity than the proposed model (Stat-Ease, 2007). The modeled values of the imaginary conductivity response, along with the averages and standard deviations of the measured values are found in Table 8.

The data set was next examined graphically to confirm the normality assumption (Figure 28). The internally studentized residuals were plotted against the normal percent probability. As stated in the previous section, if the plot lies in a generally straight line, close to 45 degrees, normality can be assumed. If the data displays a pronounced "S" shape, the data may not meet the normality assumption (Stat-Ease, 2007). In this case, an "S" has not been clearly identified in the data, although a higher number of data points would help clarify the normality assumption.

A series of plots of residuals versus predicted value, run number, surfactant treatment, and water type were evaluated for trends possibly related to experimental or systematic error (Figures 29-32) and that could result in exaggerated relationships in the predictive

model. Run 19, corresponding to 8% AMA 80-I, tap, falls outside of the confidence interval in Figure 29 and is discussed further in the following paragraphs.

The data set was next examined graphically for any design points with potential undue influence over the predictive model. The leverage plot (Figure 33) appears normal, with no runs showing leverage values of concern. Additionally, a plot of the t-test (Figure 34) shows that 29 of the 30 experimental run values fall within 95% confidence intervals. Run#19, corresponding to 8% AMA 80-I, DI, falls below the confidence interval. It should be carefully evaluated as a potential outlier as done below.

The last influence plot to be evaluated was the Cook's Distance, a combination of the t-test and leverage (please see Chapter 3 for full explanation) (Figure 35). The plot does not indicate any runs with problematic Cook's D values. While Run #19 plots higher than the other runs, it is not sufficiently high to omit from analyses. The generally accepted threshold for omission is a Cook's D value approaching 1 or greater (Stat-Ease, 2007). Additionally, there is no record of any data collection problems associated with Run #19 that would warrant removal from analyses. The evaluation of both normality and influence plots suggests that any outliers (i.e. runs 13 and 22) have been removed from the analysis and further examination of individual runs is not necessary in this response.

The imaginary conductivity responses of the experimental treatments do not appear to be significantly affected by either surfactant or water type (Figure 36). There is overlap in response over the treatments as a whole, with large error bars attached to every condition (Figure 37). Furthermore the values are very small suggesting there is little to no polarization or imaginary conductance.

An error of ±4.6% should be considered with the imaginary conductivity responses as a result of system error assumed to relate to slight packing differences and sand to solution ratio. Please see Appendix A for explanation of this error.

Within a specific surfactant type and concentration, the controls, 0.025% Steol, and 5% Dowfax have almost complete overlap with no clear difference between the tap and DI treatments. The 0.5% Dowfax treatments display the most defined gap between the tap and DI samples. The tap solutions and associated error bars are completely separate from the associated DI solutions. The lowest 0.5% Dowfax, tap response is 8.88E-3µS/cm larger than the largest 0.5% Dowfax, DI response.

The 8% AMA 80-I treatments have the opposite relationship with water type. The DI responses were higher than the tap responses. However, the associated error bars are much closer, in comparison to the 0.5% Dowfax, tap treatments. In addition, the measured values are spread apart, with a range of 2.70E-2 µS/cm in the DI measurements and a range of 6.73E-3 µS/cm in the tap measurements. Note also that the larger DI measurement is well outside of its associated upper error bar.

The overall imaginary conductivity response of the system over a range of frequencies is a non-linear increase with increasing frequency (Figure 38). This suggests the imaginary conductivity response is frequency dependent; however the surfactant treatments do not show a significant deviation from the control. With the exception of the 8% AMA 80-I treatments, imaginary conductivity does not vary systematically from surfactant to surfactant or between water types at any given frequency. While the data set varies almost 3 orders of magnitude throughout the frequency range, the experimental solutions containing surfactant do not vary substantially from the control solutions.

The 8% AMA 80-I treatments showed anomalously high imaginary conductivities at low frequencies relative to the control. The very low and very high conductivities showed some scattered data points. Within a more moderate frequency range, from 0.366 to 187.5 Hz (Figure 39), the largest spread between surfactant treatments is 0.034 µS/cm at 5.86 Hz between 8% AMA, tap and 8% AMA, DI.

The 0.5% Dowfax, DI solution produced the largest range of imaginary conductivity between the frequencies 0.366 Hz to 187.5 Hz, while the smallest range of imaginary conductivity corresponded to 0.025% Steol, DI. Within this frequency range, the lowest recorded response was 4.86E-3 µS/cm from the 8% AMA 80-I, tap solution at 5.86 Hz. The highest response corresponded to the 0.5% Dowfax, DI solution at 187.5 Hz.

pH

pH response ranges from 6.16 to 9.44 with a maximum to minimum ratio of 1.53. A ratio greater than 10 may indicate the necessity of a transformation (Stat-Ease, 2007). Because this ratio is not greater than 10, and the Box-Cox plot does not indicate the necessity of a transform (Figure 40), one was not performed. The ANOVA for the pH response is found in Table 9. It is recognized that the analysis of the pH values do not necessarily reflect the analysis of the true activity of the hydrogen ion. Separate analyses would need to be performed after calculating the activity in order to compare the two types of data.

The mean of the data set is 8.06 with a standard deviation of 0.74. The R^2 value is 0.9897, with a predicted R^2 value, based on the proposed model, is 0.9686. High quality models produce high R^2 values in both categories (Stat-Ease, 2007). These two values

are sufficiently high and in close agreement, indicating that the model may be a good predictor of pH. Modeled pH values, as well as the averages and standard deviations of the measured values, are found in Table 10.

The data set was next examined graphically to confirm the normality assumption (Figure 41). As in the previous parameters, the internally studentized residuals were plotted against the normal percent probability. The plot was generally linear, indicating normality in the data set, although a small subset of the data showed minor variation. Additionally, a series of plots of residuals versus run number, water type, and surfactant treatment were evaluated for trends possibly related to experimental or systematic error (Figures 42-45).

The data set was evaluated graphically for any design points with potential undue influence over the predictive model. The leverage plot (Figure 46) appears normal, with no runs showing leverage values of concern. Additionally, a plot of the t-test (Figure 47) shows that all 30 of the experimental run values fall within the 95% confidence interval.

The last influence plot to be evaluated was the Cook's Distance, a combination of the t-test and leverage (see Chapter 3 for full explanation). The pH plot does not indicate any runs with large Cook's D values (Figure 48).

The successful evaluation of both normality and influence plots suggests that any outliers have been previously removed from the analysis and further examination of individual runs is not necessary.

The pH responses of the experimental treatments appear to be affected by surfactant and water type, as well as the interaction of the two factors (Figures 49-51). In the low concentration treatments, the pH values of the DI solutions are appreciably higher than

the tap solutions. The 8% AMA 80-I treatments are the exceptions, with the tap solution measuring a higher pH than the DI solution. The pH of each solution is fairly well-constrained. The largest range within a single treatment is a pH difference of 0.51 in the 5% Dowfax, DI solution.

Within the DI solutions, the control, 0.025% Steol, and 0.5% Dowfax solutions are similar, with some range overlap. 5% Dowfax shows a slight decrease in pH in comparison to the lower concentration solutions, and 8% AMA 80-I shows a sharp decrease in pH. Within the tap solutions, there is response overlap in all treatments except 5% Dowfax. This solution showed the highest average pH response at 8.33 with a standard deviation of 0.08.

An error of ±0.37% should be considered with the pH responses as a result of system error assumed to relate to instrument error. Please see Appendix A for explanation of this error.

Specific Conductivity

Specific conductivity response ranges from 18.38 to 8963.62 μS/cm with a maximum to minimum ratio of 487.68. A ratio greater than 10 may indicate a positive response to a transformation (Stat-Ease, 2007). In this case, the Box-Cox plot indicated the potential of using a square root transform (Figure 52), which was performed. The transform is referred to as sqrt(specific conductivity) in the associated tables and plots. The ANOVA for the specific conductivity response is found in Table 11.

The mean of the entire data set is 1568.95μS/cm with a standard deviation of 3052.58 μS/cm. The large standard deviation, relative to the mean value is most likely due to the

large range of values in responses. The R^2 value is 0.9999, with a predicted R^2 value, based on the proposed model, is 0.9998. As discussed previously, high quality models produce R^2 values approaching 1.0 in both categories. These two values are sufficiently high and in close agreement, indicating that the model may be a good predictor of specific conductivity. The modeled values for sqrt(specific conductivity) are found in Table 12. The untransformed modeled values, as well as the averages and standard deviations of the measured specific conductivity values are located in Table 13.

The data set was next examined graphically to confirm the normality assumption (Figure 53). The internally studentized residuals were plotted against the normal percent probability, as discussed in the previous sections. A series of plots of residuals versus predicted, run number, surfactant treatment, and water type were evaluated for trends possibly related to experimental or systematic error (Figures 54-57). A wider range of residuals appears in low predicted values, DI solutions, and the control groups.

The transformed data set was evaluated graphically for any design points with potential undue influence over the predictive model. The leverage plot (Figure 58) appears normal, with no runs showing leverage values of concern. Additionally, a plot of the t-test (Figure 59) shows that all of the experimental run values fall within 95% confidence intervals. The last influence plot to be evaluated was the Cook's Distance (please see Chapter 3 for full explanation) (Figure 60). The sqrt(specific conductivity) plot does not indicate any runs with large Cook's D values (greater than 0.95).

The evaluation of both normality and influence plots suggests that any outliers have been removed from the analysis previously and further examination of individual runs is not necessary for the specific conductivity response.

The specific conductivity responses of the experimental treatments appear to be affected by both surfactant and water type (Figure 61). There is a non-linear positive correlation between surfactant, concentration, water type and specific conductivity (Figure 62).

Overall, tap solutions had higher specific conductivity than the corresponding DI solutions. The plot of square root of specific conductivity shows similar increases in both tap and DI solutions as surfactant concentration increases (Figure 62). A plot of the untransformed data show similar trends (Figure 63, 64).

Each treatment is well-constrained with small error bars and very little overlap. Specific conductivity appears to be more strongly influenced by surfactant treatment and concentration than by water type. The difference in specific conductivity between the tap and DI solutions of a specific surfactant treatment averages 907 μS/cm, with a standard deviation of 180. The difference appears to decline with increasing surfactant concentration. While this is far from a constant difference, it is smaller than the averaged and standard deviations of the surfactant treatments relative to each other. The DI solutions measured on average 2208 μS/cm with a standard deviation of 3565. The tap solutions measured on average 3081 μS/cm with a standard deviation of 3387.

An error of ±10.1% should be considered with the specific conductivity responses as a result of systematic error assumed to relate to instrument error and slight variations in solution temperature. Please see Appendix A for explanation of this error.

Dissolved Oxygen

Dissolved oxygen response ranged from 4375.5 to 8644 µg/L with a maximum to minimum ratio of 1.98. A ratio greater than 10 may indicate the necessity of a transform, but a power transform generally has little to no effect on ratios less than 3 (Stat-Ease, 2007). As the dissolved oxygen ratio is low, no transform was performed. In addition, the Box-Cox plot does not recommend the use of a power law (Figure 65). The ANOVA for the DO response is found in Table 14.

The mean of the data set is 7394.88 µg/L with a standard deviation of 832.46. The R^2 value is 0.6710, with a predicted R^2 value, based on the proposed model, of 0.0432. High quality models produce high R^2 values in both categories. The values for dissolved oxygen are neither maximized or in close agreement. The proposed model is unlikely to be a good predictor for dissolved oxygen. Modeled values are found in Table 15, along with the averages and standard deviations of the measured DO values.

The data set was examined graphically to confirm the normality assumption (Figure 66). The internally studentized residuals were plotted against the normal percent probability, and an "S" shape was interpreted. Because of this, the assumption of normality may not be met in this data set, although the same analyses were completed for dissolved oxygen as for the other parameters.

A series of plots of residuals versus predicted values, run number, surfactant treatment, and water type were evaluated for trends possibly related to experimental or systematic error that could result in poor relationship prediction by the model (Figures 67-70). The 0.025% Steol, tap treatment appeared to show the most range in of residuals throughout the plots. The transformed data set was evaluated graphically for any design

points with potential undue influence over the predictive model. The leverage plot (Figure 71) appears normal, with no runs showing leverage values of concern. Additionally, a plot of the t-test (Figure 72) shows that 29 of the 30 experimental run values fall within 95% confidence intervals. Run #9, 0.025% Steol, tap, lies well outside, while Run 15, 0.025% Steol, tap solution, lies just inside the lower boundary.

The last influence plot to be evaluated was the Cook's Distance, a combination of the t-test and leverage (please see Chapter 3 for full explanation) (Figure 73). The dissolved oxygen plot does not indicate any runs with very large Cook's D values. While Run 9 and 15 are higher than most, it is not sufficient to omit the data points from the analysis; Nothing unusual was noted during the experimental runtime, including temperature fluctuation or substantial amounts of air entering the flow cell. In addition, measurements of other parameters, taken simultaneously using the same equipment, do not reflect the same outlier potential. The successful evaluation of both normality and influence plots suggests that any outliers have been previously removed from the analysis and further examination of individual runs is not necessary.

The dissolved oxygen responses do not appear to be significantly affected by either surfactant or water type (Figure 74, 75). With the exception of the tap water control, there is overlap in the measured responses across all experimental treatments. The lowest measured tap control responses are 222 μg/L higher than any other measured responses. The largest range is in the 0.025% Steol, tap treatment, of 3274 μg/L. The other treatments average a range almost one magnitude smaller, at 330.6 μg/L with a standard deviation of 157.9 (Figure 75).

With the exception of 0.025% Steol, tap treatment, there is overlap across the modeled responses. The 0.025% Steol, tap treatment is modeled much lower than the other treatments. Despite the very large range in its measured responses, the error bar attached to the 0.025% Steol, tap treatment is the same size as the other treatments.

In the associated bar graph (Figure 76), there is overlap in response over the treatments as a whole, which is consistent with the previous plot. Furthermore, the error bar associated with 0.025% Steol, tap in this plot is substantially larger than the error bars associated with the other experimental treatments. The large error bar here is most likely due to Run 9, as discussed above. While most of the treatments appear to be well-constrained, there is overlap in all treatments except the tap control.

An error of ±4.3% should be considered with the DO responses as a result of system error assumed to relate to instrument error and slight temperature variation. Please see Appendix A for explanation of this error.

Dielectric Constant

Dielectric constant response ranges from 21.03 to 25.07, with a maximum to minimum ratio of 1.19. Ratios greater than 10 may indicate the necessity of a data transform. Because this ratio is low and the Box-Cox plot does not suggest a transform (Figure 77), one was not performed on the data set. The ANOVA for the specific conductivity response is found in Table 16.

The mean of the data set is 23.5 with a standard deviation of 1.10. The R^2 value is 0.4618, with a predicted R^2 value, based on the proposed model, of -0.5449. High quality models produce high R^2 values in both categories. A negative predicted R^2 value as seen

here indicates that the mean of the data set may be a better predictor of dielectric constant than the proposed model. Modeled values are found in Table 17, along with the averages and standard deviations of the measured dielectric constants.

As with the previous parameters, the data set was examined graphically to confirm the normality assumption with a plot of the internally studentized residuals plotted against the normal percent probability (Figure 78). Identification of an "S" shape in the plot may suggest that the data set does not meet the normality requirements (Stat-Ease, 2007).

A series of plots of residuals versus predicted value, run number, surfactant treatment, and water type were evaluated for trends possibly related to experimental or systematic error that could result in significant errors in predictive models (Figures 79-82).

The data set was evaluated graphically for any design points with potential undue influence over the predictive model. The leverage plot (Figure 83) appears normal, with no runs showing leverage values greater than 0.8. Additionally, a plot of the t-test (Figure 84) shows that all the experimental run values fall within 95% confidence intervals.

The last influence plot to be evaluated was the Cook's Distance, a combination of the t-test and leverage (please see Chapter 3 for full explanation) (Figure 85). The dielectric constant plot does not indicate any runs with large Cook's D values.

The evaluation of both normality and influence plots suggests that any outliers have been removed from the program previously and further examination of individual runs is not necessary for the dielectric conductivity response.

The dielectric constant responses of the experimental treatments do not appear to be statistically significant effects as a results of either surfactant or water type (Figure 86). All dielectric responses overlap among the treatments. None of the treatments are well-constrained, with large error bars in both measured and modeled data (Figure 87).

In the associated bar graph (Figure 88), there is overlap in response over the treatments as a whole, consistent with the previous plots (Figure 86, 87). Again, none of the treatments are well-constrained. There do not appear to be any trends in dielectric constant based on water type, surfactant type, or concentration.

An error of ±3.6% should be considered with the dielectric constant responses as a result of system error assumed to relate to instrument error, slight packing differences, and the sand to solution ratio. Please see Appendix A for explanation of this error.

Results Summary

Table 18 outlines the overall responses of each experimental treatment. Real and specific conductivities, along with pH, produced models with the highest R^2 and R^2_{pred} values, suggesting that these three parameters have the most predictable response in a quartz sand-water environment of the parameters measured. Imaginary conductivity and dissolved oxygen have negative R^2_{pred} values, indicating that those parameters may be better predicted by the mean of the data set than by the proposed models.

CHAPTER 5

DISCUSSION

In the previous chapter, the measured responses were described, along with the analyses used to determine the robustness of data. This chapter will discuss the results in more detail and attempt to place the parameter responses in a broader context while proposing possible explanations for each parameter's behavior.

Geoelectrical Measurements

There is a clear correlation between surfactant and real conductivity, and to a lesser extent, water type and real conductivity. Real conductivity response appears as a logarithmic increase with increasing surfactant concentration, which suggests that surfactant concentration is the key to real conductivity response.

After the conclusion of the initial 30-run experiment plan, real and imaginary conductivity values were measured for 8% DI solutions of Steol CS-330 and Dowfax 8390, in addition to the original 8% Aerosol MA 80-I experiments in order to determine if the conductivity could be linked to either the surfactant's chemical make-up or the actual solution concentration. These experiments were performed identically to the SIP experiments described in Chapter 3. If concentration is the controlling factor of real conductivity response, all three of the 8% solutions should show similar real conductivity measurements. The real conductivity measurements at 8% were compared to the real conductivity value of a DI control. Because the Steol and Dowfax 8% runs took place after the conclusion of the experimental runs, they were compared to a different DI control than the original 8% AMA runs (Table 19). Comparisons were made by

calculating a percent difference (Eqn 16) between the DI control and the experimental solution.

$$PercentDifference = \frac{\sigma'_{DI} - \sigma'_{\exp}}{\sigma'_{DI}} * 100 \quad (16)$$

Percent Difference is the calculated percent difference between the DI control and the experimental solution, σ'_{DI} is the real conductivity value of the measured DI control, and $\sigma'_{\exp}$ is the real conductivity of the experimental surfactant treatment.

The 8% Steol solution averaged a real conductivity value of 497.5 ±14.1 μS/cm, which corresponds to a 1234% increase from the DI control value. The 8% Dowfax treatment averaged a real conductivity value of 714.2 ±8.8 μS/cm, which corresponds to a 1816 % increase from the DI baseline. These two solutions are somewhat comparable, suggesting that real conductivity is affected more by surfactant concentration than surfactant brand or molecular make-up. However, there is still a difference of 582% between the two surfactants that is most likely explained by differences in chemical composition and structure. The 8% AMA 80-I solution averaged 1793.6 ±58.35 μS/cm, corresponding to a 13945% increase from the DI control. This is significantly larger than the values of the other two surfactants, thus there is likely a different cause for the conductivity measurement than concentration alone.

Additionally, the specific conductivity of a 0.5% AMA 80-I, DI solution was measured in an effort to clarify the role of concentration on the geoelectrical responses. The responses were compared to the 0.5% Dowfax, DI solution response recorded during the initial experiments. The 0.5% Dowfax solution averaged a specific conductivity value of 123.75 ±4.08 μS/cm, which corresponds to a 1337% increase from the DI

control. The 0.5% AMA 80-I solution, however, averaged 199.02 ±0.11µS/cm, corresponding to a 9506% increase from the DI control. The substantially larger percent increase of the 0.5% AMA 80-I solution compared to the Dowfax solution is in close agreement with the findings from the 8% solution experiments described above. Concentration cannot account for the entire difference in the conductivity responses among surfactant treatments.

The three surfactant formulas, Steol CS-330, Dowfax 8390, and Aerosol MA 80-I are all anionic, suggesting that this property cannot be cited as a reason for differences in conductivity. The molecular formula of Steol, primarily sodium laureth sulfate (Stepan Company, 2005) , is $C_{12}H_{25}(C_2H_4O)_3O_4S^-$ (Karapanagioti et al., 2005), and its structure can be found in Figure 89. The molecular formula of Dowfax 8390, or alkyldiphenyl oxide disulfonate (Dow Chemical Company, 2009), is $C_{28}H_{40}O_7S_2^{2-}$ (Karapanagioti et al., 2005), and it's structure can be viewed in Figure 90. AMA 80-I, or dihexyl sulfosuccinate, has a molecular formula of $C_{16}H_{29}O_7NaS$ (Cytec Industries, 1994). This particular surfactant contains the alcohol isopropanol (isopropyl alcohol), and its structure is found in Figure 91.

It seems apparent that some surfactant formulations act as stronger electrolytes than others when in solution. There are several potential mechanisms to explain this effect. They include differences in dissociation constant, as well as differences in the number of dissociable ions on an individual molecule. The use of cosolvents and other additives could also affect differences in conductivities among surfactant formulations.

It is possible that the increase in pore fluid conductivity is related to the number of easily dissociable ions in a surfactant molecule. The dissociated ions would increase the

real and specific conductivity by increasing the total dissolved solids and salts in the electrolyte, and thus the number of dissociating ions would control the degree of conductivity increase. If one assumes that the number of sodium ions corresponds to the number of dissociable ions on a surfactant molecule, Dowfax has two, while Aerosol MA 80-I and Steol have only one. Therefore it is unlikely that the number of sodium ions in a surfactant is the controlling factor on conductivity.

A somewhat related possibility is tied to the dissociation constant of each surfactant. A dissociation constant describes a compounds ability to break apart into smaller components. Due to complex chemical properties, some compounds dissociate more easily in polar solvents than others. While Aerosol MA 80-I may have fewer dissociable ions, its dissociation constant may be higher, resulting in more complete dissociation when in solution. This could result in higher electrolytic conductivity. Additionally, Aerosol MA 80-I includes isopropanol, an alcohol, in its formulation, which may affect its geoelectrical properties. However, research has found that alcohols have low conductivity relative to the specific conductivity responses of the surfactant solutions (Prego et al., 2000). This suggests that the isopropanol in the Aerosol MA 80-I solutions does not account for the significantly higher conductivity responses in comparison to the surfactant solutions that do not contain the alcohol.

Water type appears to affect real conductivity as a semi-constant, with an average of 175.8 µS/cm (standard deviation 44.7 µS/cm) separating the tap and DI measurements of a specific surfactant treatment. The semi-constant gap appears to increase with increasing surfactant concentration. While the standard deviation initially seems large, in comparison to the difference in response between the surfactant treatments it is not.

This semi-constant separation is likely a result of the differences in starting conductivity of the two water types, rather than an effect of interactions with either surfactant or aquifer solids. The starting specific conductivity of the DI water was measured at 3.8 µS/cm, while the tap water measured 1025 µS/cm, which is a substantial difference. This hypothesis, that intial differences in water type are important, is supported by the specific conductivity response, which also indicates a semi-constant gap between the correlated tap and DI measurements.

In addition, the semi-constant state of the difference between the DI and tap solutions is likely a result of the size of the role played by the water type in real conductivity. When the surfactant concentration is low, the measured conductivity is due to the water type. As the surfactant concentration increases, it is likely the result of a change in the dominant conductivity source at different concentrations of surfactant. At low concentrations, the conductivity of the water dominates the response, while at high concentrations, the conductivity of the surfactant is dominant.

Imaginary conductivity does not appear to have the same relationships with either surfactant treatment or water type as seen in real and specific conductivities. The difference between the control and surfactant treatments is minimal, with little to no significant correlation. This finding implies that the main electrical conduction mechanism in the tested environment is electrolytic, and there is little to no surface conduction that results from the presence of surfactants in a saturated quartzitic sand environment. Because specific conductivity is a single component of real conductivity, it is expected that any change in conduction mechanism, via polarization or increased surface conductivity, would alter the real conductivity response, while the specific

conductivity remained unaffected. Because the measured real and specific conductivity responses in this thesis follow the same trend throughout the surfactant treatments, it suggests that changes in the real conductivity are related to changes in the specific conductivity. This leads to the conclusion that electrolytic conductivity is the main conduction mechanism.

While real conductivity shows no significant value change across the measured frequency range, imaginary conductivity values display an overall increase with increasing frequency. This frequency effect does not appear to be dependent upon surfactant treatment or water type, however. Both controls and all surfactant treatments display the same general trend through the frequency spectrum. In addition, all treatments lie within one order of magnitude from one another and have fairly large standard deviations, indicating there is overlap among treatments.

There is a clear correlation of surfactant treatment to real conductivity (Table 6) and specific conductivity (Table 13) while there is no clear correlation of imaginary conductivity (Table 8) to the presence of surfactant in a quartz sand-water environment. The behaviors of the real, specific, and imaginary conductivities in the presence of surfactant in quartz sand-water environment suggests that the geoelectrical conduction mechanism is primarily electrolytic and a function of pore fluid chemistry in this particular set of conditions. This supports the findings of Werkema (2008) that there is an increase in pore fluid conductivity in relation to surfactant presence (Figure 92).

Water Quality Measurements

The water quality measurements of pH, specific conductivity, and dissolved oxygen (DO) display varying responses to surfactant presence in a quartz sand-water environment. The pH and specific conductivity parameters appear to repond in a statistically significant manner to both surfactant treatment and water type. Dissolved oxygen does not show the same correlation, and statistical analysis did not meet the required normality assumption. Because of this, statistical significance could not be assessed in this parameter and will therefore not be discussed in depth.

pH

The pH is affected by the water type, as well as the interaction between water type and surfactant treatment (Table 21). The response can be broken into two parts: the response of tap solutions versus DI solutions and the response of the high concentration solutions (5%, 8%) versus the low concentration solutions (control, 0.025%, 0.5%).

With the exception of the 8% AMA 80-I solution, the DI solutions measured higher pH values than the tap solutions. This is likely a result of the pH of the water that was mixed with the surfactant, rather than a comment on the surfactants themselves. This is concluded due to the higher pH values measured in the DI control in relative to the tap water control. The gap between the tap and DI solutions at low surfactant concentrations averages 1.57 with a standard deviation of 0.25. The larger concentration solutions do not appear to have the same relationship with each other. While pH of the tap solutions appear to be moderated or perhaps buffered by the tap water itself, the high concentration DI solutions, particularly 8% AMA 80-I, show a precipitous decrease in pH. The reason for this response may be related to the molecular structure of the surfactant, including the

presence of the isopropyl alcohol. Some ions may be more readily dissociated in DI water than in tap water, driving a decrease in pH. It may be reasonable to hypothesize that solutions of Steol and Dowfax at 8% concentration may measure similar decreased pH values due to similar surfactant structures. Alternately, if dissociation constants are more of a controlling factor, then one may expect variation in pH values among the different surfactant formulations. As noted in the Geoelectrical Measurements section, AMA 80-I contains isopropanol, which may also explain the decrease in pH associated with that surfactant.

Specific Conductivity

As discussed in the Geoelectrical Measurements section earlier in this chapter, specific conductivity response suggests a statistically significant link exists between surfactant treatment and specific conductivity, as well as water type and specific conductivity.

The general relationships seem to mirror that of real conductivity, indicating that ionic conductivity is likely the primary conduction mechanism in the saturated sand analog aquifer. The DI solutions display overall lower specific conductivity measurements than the associated tap solutions. The difference between the two is a semi-constant averaging 873 μS/cm with a standard deviation of 184. Low concentration treatments have substantially lower specific conductivity values than the higher concentration treatments. Potential mechanisms for this behavior are discussed above in the Geoelectrical Measurements section.

A simple comparison of the findings of this research to the findings of Werkema (2008) yields the plot in Figure 85. This comparison clearly shows that the trends of

specific conductivity organized by surfactant type and concentration are similar in the two works. The slight differences between the two may be related to the starting specific conductivity value of the DI water used in solution. There is also the potential that the sand matrix used in this research contributed dissolved solids and ions to the electrolyte, increasing the specific conductivities in the higher concentration solutions. Investigating what effects the matrix has on the geoelectrical response was a main goal of the thesis research.

Dissolved Oxygen

Dissolved oxygen is a difficult parameter to measure and can be affected by temperature, flow velocity, or outside air leaking into the system. The raw data suggests that dissolved oxygen response does not change significantly with surfactant presence. Although the 0.025% Steol, tap solutions appear to show a significantly lower response than the other surfactant treatments as well as its associated DI solution, further testing could not replicate the low numbers. In addition, statistical analysis suggests that the normality assumption is not valid, leaving any proposed model in an uncertain state.

Dielectric Constant

Dielectric constant response to surfactants in a quartz sand-water environment shows little response. One suggestion to explain this is insufficient instrument sensitivity. The sensitivity for the MiniTrase is ±2% moisture content, equivalent to a dielectric constant of 3.27, using a standard waveguide (Soilmoisture Equipment Corporation, 2005). It should be noted that the experiments performed in this project used a shorter waveguide than is standard. A standard waveguide is 15 cm. The experiments in this research

utilized an 8 cm waveguide. It is expected that this would increase error. The expected error overshadows the relatively small response differences among surfactant treatments in the time domain reflectometry experiments. Additionally, the surfactant molecules may be too large to "twist," a behavior necessary to the relaxation phenomenon on which time domain reflectometry response depends (Endres, A.L., personal communication, December 2008).

In addition, the typical dielectric constant values for saturated sand are between 20 and 30 (Kirsch, 2006). All of the values measured in this project fall in that category, suggesting that dielectric constant may be more strongly impacted by the matrix materials and moisture content than the solution itself in the experimental quartzitic sand environment.

While dielectric response of surfactant-quartz sand-water may not be significant, this does not rule out the potential of GPR as a surfactant monitoring method, as the method is also affected by the conductivity of the surveyed area. As demonstrated in this project, the conductivity measurements are affected by the surfactant solutions.

CHAPTER 6

CONCLUDING REMARKS

The research presented in this thesis has provided further information to the scientific community, as well as indicating potential directions for future work. Increased real and specific conductivities associated with surfactants used in SEAR support the work of Werkema (2008), and indicate that the geoelectrical responses in quartz sand-water environments may be useful in monitoring subsurface surfactants with geophysical methods. Resistivity surveys in particular show potential as the real and specific conductivities can show a strong response to surfactant treatments.

The positive correlation between real and specific conductivities suggests that electrolytic conduction is the primary electrical conduction mechanism in quartz sand-water environments. A lack of significant imaginary conductivity response supports this suggestion, and rules out substantial conduction via surface or electronic conduction.

The pH response also appears to be affected by surfactant presence in a quartz sand-water environment. High surfactant concentrations appear to decrease the pH value of the environment. If this response is scaled to a field environment, there is a potential to negatively affect subsurface organisms, including bacteria and microbes that are actively aiding in bioremediation.

The dissolved oxygen and dielectric constant parameters do not appear to be significantly affected by the presence of surfactants in a quartz sand-water environment. The possible reasons for this are discussed in Chapter 5.

Future work should continue to increase both the scale of experimentation, as well as the complexity. Studies will need to incorporate heterogeneous solid materials, including

clays. The presence of clay in the subsurface is likely to increase the imaginary conductivity response, as well as providing sorption sites for surfactant. The surfactants may also interact with clay particles, resulting in changes to the geoelectrical responses. The introduction of clays to the experimental environment will likely increase the imaginary conductivity component of the geoelectrical response, possibly masking any surfactant-related response.

Increasing the complexity of the experimental electrolyte will also be important for future work. SEAR is only used in environments containing contaminants. It will be important to include potential contaminants, like tetrachloroethylene, in the saturating solutions in order to observe any interactions between surfactants and DNAPL. Chlorinated solvents such as tetrachloroethylene (PCE) and trichloroethylene (TCE) have been associated with decreased conductivity in field studies (Chambers et al., 2004) and would therefore be expected to buffer the increased conductivity responses shown with surfactant presence. Additionally, DNAPL contaminants have low dielectric constants, generally below 10 (Ajo-Franklin et al., 2006). The interactions of DNAPL and surfactant may result in measurable changes to dielectric constant.

The geoelectrical response should also be investigated for changes related to temporal variations. The experiments presented in this research concentrate on readings made within an hour of saturation. Field applications require a substantially larger time scale, stretching beyond a full year and up to several years. Dissolved oxygen, while not responding to the surfactants over the time scale used in this research, may react differently over a longer period of time.

This research also utilized a fully-saturated environment. However, responses to surfactants within a more complex saturation profile should also be investigated in an effort to bring the complexity of the environment closer to the scale of a field application. It is expected that decreasing saturation will lower both the conductivity and dielectric constant of an environment.

In conclusion, geophysical, and particularly geoelectrical, methods have the potential to monitor surfactants in the subsurface. A substantial amount of future work must increase the scale and complexity of the experimental conditions in order to determine the true feasibility. Ultimately, the ability to monitor surfactants in the subsurface could result in more efficient and effective groundwater remediation, which will be beneficial to all living organisms.

EXHIBITS

TABLES AND FIGURES

Table 1. Experimental Treatments.

Surfactant	Concentration	Water Type
None	-	DI
None	-	Tap
Steol CS-330	0.025%	DI
Steol CS-331	0.025%	Tap
Dowfax 8390	0.5%	DI
Dowfax 8390	0.5%	Tap
Dowfax 8390	5%	DI
Dowfax 8390	5%	Tap
Aerosol MA 80-I	8%	DI
Aerosol MA 80-I	8%	Tap

Table 2. Specific Conductivity results from Werkema 2008.

	Specific Conductivity (µS/cm)
Control	3.93
Steol CS-330	16.35
0.5% Dowfax 8390	405.74
5% Dowfax 8390	2465.86
8% Aerosol MA 80-I	7232.65

Table 3. Run order and response of each experimental treatment at 11.7Hz. Runs 13 and 22 are lined out as they were not included in analyses. Real, imaginary, and specific conductivity are reported in μS/cm. Units for dissolved oxygen (DO) are μg/L.

Run	Block	Surfactant	Water	Real	Imaginary	Sp Cond	DO	Dielectric	pH
1	1	0.5 Dowfax	DI	123.07	1.71E-02	385.4	7420.5	22.3	9.44
2	1	5 Dowfax	Tap	925.945	3.61E-02	3048.44	7859	22.73	8.37
3	1	5 Dowfax	DI	733.025	2.82E-02	2223	7453	22.2	9.12
4	1	None	Tap	324.395	2.56E-02	1019.95	8507	23.86	7.65
5	1	.025 Steol	DI	23.57	3.38E-02	32.92	7383	23.1	9.39
6	1	8 AMA 80-I	DI	2630.775	5.15E-02	8352.18	7406	21.03	6.36
7	1	8 AMA 80-I	Tap	2865.44	2.15E-02	8963.62	7313	21.5	7.76
8	1	0.5 Dowfax	Tap	409.755	4.15E-02	1254.36	7817.5	23.13	7.85
9	1	.025 Steol	Tap	346.285	2.87E-02	1053.65	7649.5	23.83	7.71
10	1	None	DI	19.285	2.53E-02	24.48	7158.5	23.96	9.34
11	2	None	DI	18.275	3.48E-02	18.38	7676	23.33	9.095
12	2	8 AMA 80-I	Tap	2895.2	3.17E-02	8924.695	7565	22.26	7.8
~~13~~	~~2~~	5 Dowfax	~~Tap~~	1033.475	-6.00E-02	~~3136.585~~	~~7646.5~~	~~23.67~~	~~8.235~~
14	2	.025 Steol	DI	22.4	2.28E-02	35.665	7683	24.37	9.17
15	2	.025 Steol	Tap	353.21	3.33E-02	1069.095	4375.5	21.97	7.32
16	2	0.5 Dowfax	DI	129.985	2.80E-02	364.48	7141.5	24.17	9.14
17	2	5 Dowfax	DI	707.755	3.69E-02	2250.5	7293.5	23.3	8.78
18	2	None	Tap	333.77	2.30E-02	1048.77	8081	22.5	7.625
19	2	8 AMA 80-I	DI	2649.57	2.17E-02	8369.16	7470.5	23.13	6.33
20	2	0.5 Dowfax	Tap	425.545	4.43E-02	1254.86	7555.5	24.17	8.025
21	3	None	DI	19.92	3.67E-02	34.6	7560.5	21.9	9.26
~~22~~	~~3~~	8 AMA 80-I	~~Tap~~	2786.67	-1.20E-01	~~9038.49~~	~~7567.5~~	~~23.43~~	~~7.88~~

23	3	.025 Steol	Tap	354.245	2.79E-02	1079.77	5179.5	24.23	7.37
24	3	.025 Steol	DI	21.835	3.51E-02	32.46	7442.5	25.07	9.28
25	3	None	Tap	332.89	3.19E-02	1076.01	8644	21.57	7.6
26	3	8 AMA 80-I	DI	2790.92	6.25E-02	8371.99	7348	22.13	6.16
27	3	0.5 Dowfax	DI	119.55	2.39E-02	363.89	7190	23.9	9.19
28	3	5 Dowfax	Tap	982.845	3.38E-02	3129.63	7503	22.57	8.38
29	3	5 Dowfax	DI	763.405	2.32E-02	2272.47	7408.5	23.27	8.61
30	3	0.5 Dowfax	Tap	399.545	4.77E-02	1279.93	7425	24.67	8.07

Table 4. ANOVA of Real Conductivity; Classical Sum of Squares, Type II. Units are μS/cm.

	Sum of Squares	F-factor	p-value
Surfactant	10.23	11222.87	<.0001
Water Type	3.07	13482.86	<.0001
Model	14.14	6898.72	<.0001

Mean	561.93	**C.V.**	0.66
Standard Deviation	672.50	$\mathbf{R^2}$	0.9997
Maximum	1910.83	$\mathbf{R^2_{adj}}$	0.9996
Minimum	12.06	$\mathbf{R^2_{pred}}$	0.9992

Table 5. Modeled values of $\log_{10}$ (real conductivity) values.

	DI	Tap
Control	1.11	2.34
0.025% Steol	1.18	2.37
0.5% Dowfax	1.92	2.44
5% Dowfax	2.69	2.80
8% AMA 80-I	3.25	3.28

Table 6. Modeled and average measured real conductivity values for DI and tap solutions. Modeled values do not include standard deviations. Units are μS/cm.

	DI		Tap	
Modeled	**Mean ±5.1%**	**Std Dev**	**Mean ±5.1%**	**Std Dev**
Control	12.88	-	218.78	-
0.025% Steol	15.14	-	234.42	-
0.5% Dowfax	83.18	-	275.42	-
5% Dowfax	489.78	-	630.96	-
8% AMA 80-I	1778.3	-	1905.5	-
Measured				
Control	12.77	0.55	220.23	3.45
0.025% Steol	15.07	0.59	234.17	2.89
0.5% Dowfax	82.80	3.54	274.41	8.73
5% Dowfax	489.82	18.58	653.84	35.86
8% AMA 80-I	1793.6	58.36	1899.4	37.39

Table 7. ANOVA of Imaginary Conductivity; Classical Sum of Squares, Type II. Units are in μS/m

	Sum of Squares	**F-factor**	**p-value**
Surfactant	1.241E-4	0.91	0.4796
Water Type	4.855E-6	0.14	0.7102
Model	6.115E-4	2.00	0.1081

Mean	0.0214	**C.V.**	26.97%
Standard Deviation	0.0067	$\mathbf{R^2}$	0.5297
Maximum	0.0113	$\mathbf{R^2_{adj}}$	0.2652
Minimum	0.0412	$\mathbf{R^2_{pred}}$	-0.4086

Table 8. Modeled and average measured imaginary conductivity values for DI and tap solutions. Standard deviations are included for measured values. The predictive model did not produce standard deviations for the modeled values. Units are in μS/cm.

	DI		Tap	
Modeled	**Mean ±4.6%**	**Std Dev**	**Mean ±4.6%**	**Std Dev**
Control	0.02148	-	0.01786	-
0.025% Steol	0.02035	-	0.01997	-
0.5% Dowfax	0.01533	-	0.02965	-
5% Dowfax	0.01960	-	0.02279	-
8% AMA 80-I	0.03004	-	0.01868	-
Measured				
Control	0.0215	0.0041	0.0179	0.0031
0.025% Steol	0.0204	0.0045	0.0200	0.0019
0.5% Dowfax	0.0153	0.0037	0.0296	0.0021
5% Dowfax	0.0196	0.0046	0.0241	-
8% AMA 80-I	0.0300	0.0140	0.0177	0.0048

Table 9. ANOVA of pH; Classical Sum of Squares, Type II. pH units are used.

	Sum of Squares	**F-factor**	**p-value**
Surfactant	12.21	185.04	<.0001
Water Type	5.01	303.69	<.0001
Model	25.43	171.34	<.0001

Mean	8.25	**C.V.**	1.56%
Standard Deviation	0.13	$\mathbf{R^2}$	0.9897
Maximum	9.44	$\mathbf{R^2_{adj}}$	0.9840
Minimum	6.16	$\mathbf{R^2_{pred}}$	0.9686

Table 10. Modeled and average measured pH values for DI and tap solutions. Measured values also include standard deviations. The predictive model did not produce standard deviations for the modeled values. pH units are used.

	DI		Tap	
Modeled	**Mean ±0.37%**	**Std Dev**	**Mean ±0.37%**	**Std Dev**
Control	9.23	-	7.63	-
0.025% Steol	9.28	-	7.47	-
0.5% Dowfax	9.26	-	7.98	-
5% Dowfax	8.84	-	8.35	-
8% AMA 80-I	6.28	-	7.76	-
Measured				
Control	9.34	0.01	7.63	0.03
0.025% Steol	9.39	0.03	7.47	0.18
0.5% Dowfax	9.44	0.02	7.99	0.11
5% Dowfax	9.13	0.01	8.33	0.07
8% AMA 80-I	6.54	0.3	7.81	0.06

Table 11. ANOVA of Specific Conductivity; Classical Sum of Squares, Type II. Data is presented in μS/cm.

	Sum of Squares	**F-factor**	**p-value**
Surfactant	21568.38	48626.39	<.0001
Water Type	2065.97	18631.12	<.0001
Model	23256.34	23303.08	<.0001

Mean	1568.95	**C.V.**	0.84%
Standard Deviation	3052.58	$\mathbf{R^2}$	0.9999
Maximum	8963.62	$\mathbf{R^2_{adj}}$	0.9999
Minimum	18.38	$\mathbf{R^2_{pred}}$	0.9998

Table 12. Modeled values of Sqrt (Specific Conductivity).

	DI	Tap
Control	5.039	32.38
0.025% Steol	5.802	32.67
0.5% Dowfax	19.27	35.54
5% Dowfax	47.42	55.52
8% AMA 80-I	91.46	94.69

Table 13. Modeled and average measured specific conductivity values. Standard deviations are listed with the associated measurement. Units are μS/cm.

	DI		Tap	
Modeled	**Mean ±10.1%**	**Std Dev**	**Mean ±10.1%**	**Std Dev**
Control	25.39	-	1048.14	-
0.025% Steol	33.66	-	1067.46	-
0.5% Dowfax	371.33	-	1263.09	-
5% Dowfax	2248.66	-	3082.47	-
8% AMA 80-I	8364.93	-	8966.2	-
Measured				
Control	23.87	6.75	1048.18	24.08
0.025% Steol	32.79	2.06	1066.37	11.36
0.5% Dowfax	367.99	10.46	1262	13.35
5% Dowfax	2248.8	21.5	3102.63	42.32
8% AMA 80-I	8363.52	8.64	8971.09	49.17

Table 14. ANOVA of Dissolved Oxygen; Classical Sum of Squares, Type II. Data is presented in μg/L.

	Sum of Squares	F-factor	p-value
Surfactant	5.39E6	3.77	0.0242
Water Type	29854.07	0.083	0.7763
Model	1.17E7	3.63	0.0121

Mean	7375.34	**C.V.**	8.11%
Standard Deviation	597.95	$\mathbf{R^2}$	0.6710
Maximum	8644	$\mathbf{R^2_{adj}}$	0.4859
Minimum	4375.5	$\mathbf{R^2_{pred}}$	0.0432

Table 15. Modeled and average measured dissolved oxygen values for DI and tap solutions. Measured values include associated standard deviations. Values are presented in μg/L.

	DI		Tap	
Modeled	**Mean ±4.3%**	**Std Dev**	**Mean ±4.3%**	**Std Dev**
Control	7465	-	8410.7	-
0.025% Steol	7502.8	-	5734.8	-
0.5% Dowfax	7250.7	-	7599.3	-
5% Dowfax	7385	-	7607.8	-
8% AMA 80-I	7408.2	-	7402.2	-
Measured				
Control	7468.22	228.49	8430.22	257.02
0.025% Steol	7495.67	116.92	5708.56	1517.22
0.5% Dowfax	7290.22	135.5	7633.78	170.63
5% Dowfax	7401.13	78.52	7692.33	161.4
8% AMA 80-I	7442.33	80.18	7508	129.04

Table 16. ANOVA of Dielectric Constant; Classical Sum of Squares, Type II. Dielectric constant is dimensionless.

	Sum of Squares	F-factor	p-value
Surfactant	11.52	3.02	0.0495
Water Type	0.33	0.35	0.5650
Model	13.10	1.53	0.2210

Mean	23.08	**C.V.**	4.23%
Standard Deviation	0.98	R^2	0.4618
Maximum	25.07	R^2_{adj}	0.1590
Minimum	21.03	R^2_{pred}	-0.5449

Table 17. Modeled and average measured dielectric constant values of DI and tap solutions. Standard deviations are shown with their associated measured value. The data is dimensionless.

	DI		Tap	
Modeled	**Mean ±3.6%**	**Std Dev**	**Mean ±3.6%**	**Std Dev**
Control	23.06	-	22.64	-
0.025% Steol	24.18	-	23.34	-
0.5% Dowfax	23.46	-	23.99	-
5% Dowfax	22.92	-	22.74	-
8% AMA 80-I	22.1	-	21.93	-
Measured				
Control	23.2	1.045579	23.0	0.818176
0.025% Steol	24.4	0.828358	23.6	1.239808
0.5% Dowfax	23.8	0.96962	24.5	0.49405
5% Dowfax	23.2	0.787588	23.4	0.584103
8% AMA 80-I	22.6	1.206789	22.6	0.889812

Table 18. Results summary of the mean measured responses over all experimental treatments. Real, imaginary, and specific conductivity are reported in μS/cm. Units for dissolved oxygen (DO) are μg/L.

	Water	Real Cond ±5.1%	Imaginary Cond ±4.6%	pH ±0.37%	Specific Cond ±10.1%	Dissolved Oxygen ±4.3%	Dielectric ±3.6%
Control	DI	12.77	0.0215	9.23	25.39	7465	23.06
	Tap	220.23	0.0179	7.63	1048.14	8410.7	22.64
0.025% Steol	DI	15.07	0.0204	9.28	33.66	7502.8	24.18
	Tap	234.17	0.0200	7.47	1067.46	5734.8	23.34
0.5% Dowfax	DI	82.80	0.0153	9.26	371.33	7250.7	23.46
	Tap	274.41	0.0296	7.98	1263.09	7599.3	23.99
5% Dowfax	DI	489.82	0.0196	8.84	2248.66	7385	22.92
	Tap	653.84	0.0241	8.35	3082.47	7607.8	22.74
8% AMA 80-I	DI	1793.6	0.0300	6.28	8364.93	7408.2	22.1
	Tap	1899.4	0.0177	7.76	8966.2	7402.2	21.93
R^2	-	0.9997	0.5297	0.9897	0.9999	0.6710	0.4618
R^2_{pred}	-	0.9992	-0.4086	0.9686	0.9998	0.0432	-0.5449

Table 19. Summarized Response of 8% Surfactant Solutions and Percent Change from Control. Control 1 is the DI control measured during the main 30 run experimental program. Control 2 is a second DI control that was measured to coincide with the 8% Steol and 8% Dowfax measurements. Percent change calculations were made using the associated DI control. Means and standard deviations are in µS/cm. % Change is in percent.

	Mean	Std Dev	% Change
Control 1	12.77	0.55	N/A
AMA 80-I	1793.6	58.35	13945
Control 2	37.27	1.4	N/A
Steol	497.5	14.1	1234
Dowfax	714.2	8.8	1816

Table 20. Summarized specific conductivity response of 0.5% surfactant solutions. Control 1 is the DI control measured during the main 30 run experimental program. Control 2 is a second DI control that was measured to coincide with the 0.5% AMA 80-I measurements. Percent change calculations were made using the associated DI control. Mean and standard deviation are reported in µS/cm. % Change is reported in percent.

	Mean	Std Dev	% Change
Control 1	8.61	2.73	NA
0.5% Dowfax	123.75	4.08	1337.86
Control 2	2.07	1.06	NA
0.5% AMA 80-I	199.02	0.11	9506.72

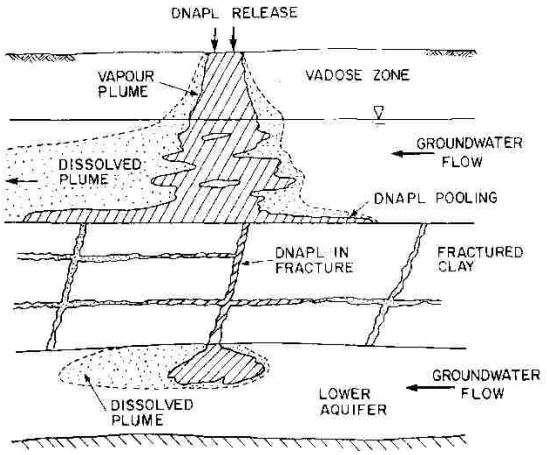

Figure 1. Schematic of a typical DNAPL release. Free phase DNAPL moves through vadose zone, past the water table and through the saturated zone. DNAPL can flow through fractures to contaminate lower strata, as well as pooling up-hydraulic-gradient. A dissolved plume is pictured in the vadose zone, upper aquifer, and lower aquifer (After Kueper and McWhorter, 1991).

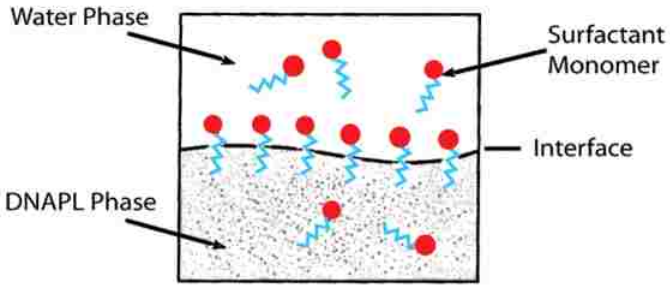

Figure 2. Surfactants accumulating at water-DNAPL interface. Monomers amass at the interface between the aqueous and NAPL phases. The hydrophilic head locates to the water phase while the hydrophobic tail is in the NAPL phase (After Lowe et al., 1999).

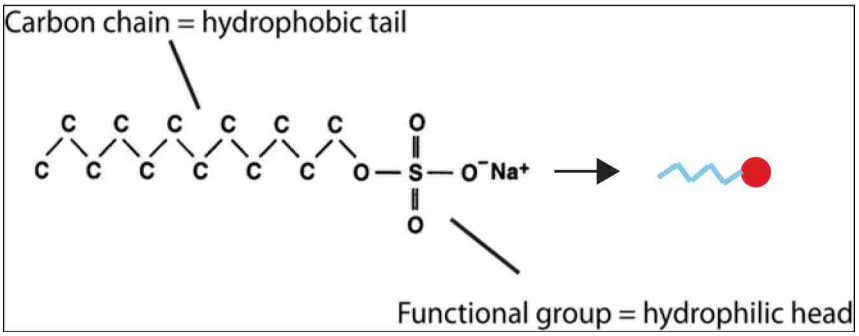

Figure 3. Surfactant monomer. The carbon chain acts as the hydrophobic group while the functional group acts as the hydrophilic group. A schematic of the monomer is shown to the left of the arrow (After Lowe et al., 1999).

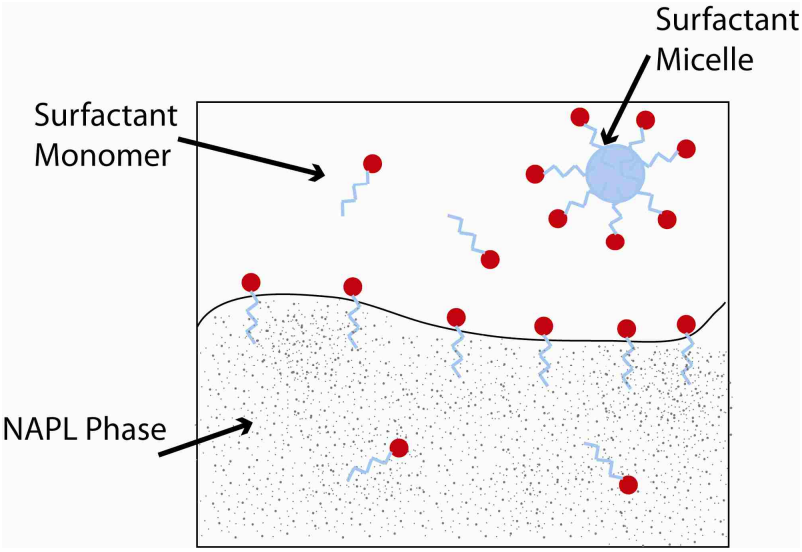

Figure 4. Surfactant micelle. Surfactant micelles form when the concentration of surfactant added reaches the critical micelle concentration (CMC). Surfactant monomers cluster together to form structures with hydrophobic interiors and hydrophilic exteriors. NAPL contaminant molecules can collect in the interiors while the micelle itself is soluble in the aqueous phase. This process effectively increases the solubility of the contaminant (After Lowe et al., 1999).

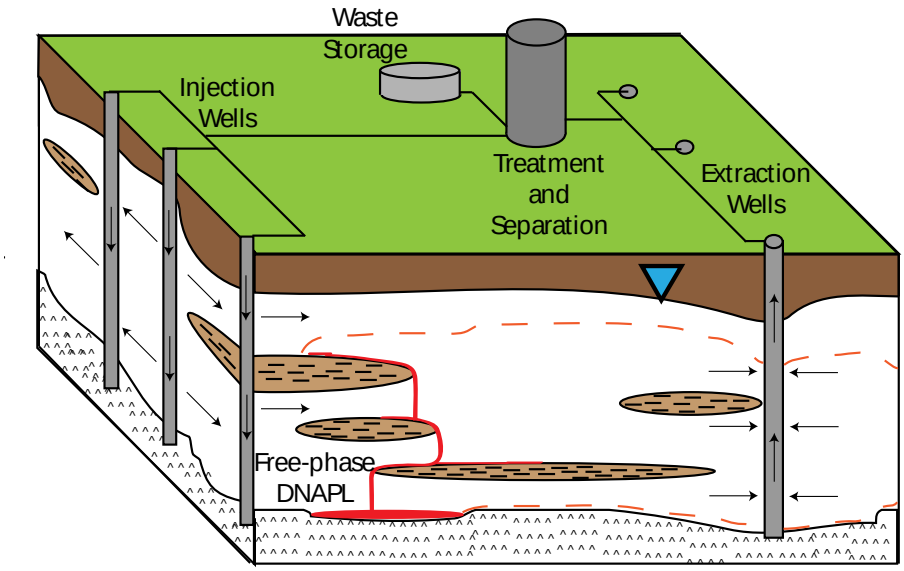

Figure 5. Schematic of surfactant-enhanced aquifer remediation. Free-phase DNAPL is removed from the site using a traditional pump-and-treat method. Surfactant solution is then injected into the subsurface via injection wells. The solution moves through the contaminant plume (outlined in red dashed line), and the solubilized or mobilized contaminant is extracted through a series of extraction wells. The extract is sent for treatment and separation of the surfactant from the rest of the solution for continued use. The brown shaded areas with dashed lines are lenses of low permeability material. Free-phase DNAPL is shown in solid red. After Battelle and Duke Engineering Services, 2002.

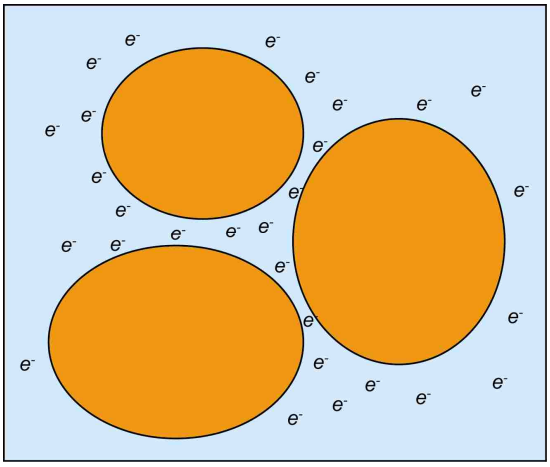

Figure 6. Schematic of ionic conduction, which is a mechanism of electrical conduction in which ions move through the pore spaces between grains via the pore fluid. Grains are represented by orange spherical shapes, pore fluid is in blue.

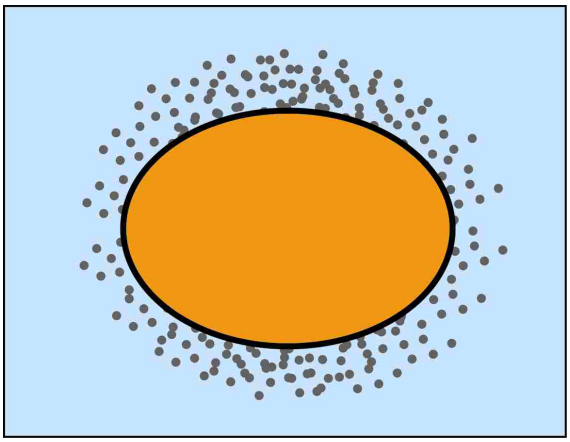

Figure 7. Schematic of an Electrical Double Layer (EDL). The EDL commonly occurs around clay grains. A fixed layer of charged ions is adhered to the grain surface, while a diffuse layer of charged ions is located adjacent to the grain surface, in the pore fluid. The concentration of charged ions in the diffuse layer decreases with distance from the grain surface. Grains are represented by orange spherical shapes, pore fluid is in blue.

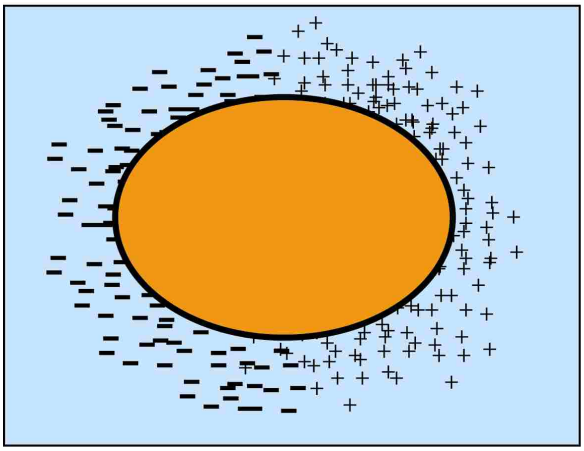

Figure 8. Schematic of polarization of ions at the fluid-grain interface. Inducing an electrical current at some frequency can cause polarization of ions in some materials. The ions within the electrical double layer (EDL) and pore fluid segregate into positive and negative groups on opposite sides of the fluid-grain interface, and slowly reintegrate with the removal of the electrical current. Grains are represented by orange spherical shapes, pore fluid is in blue.

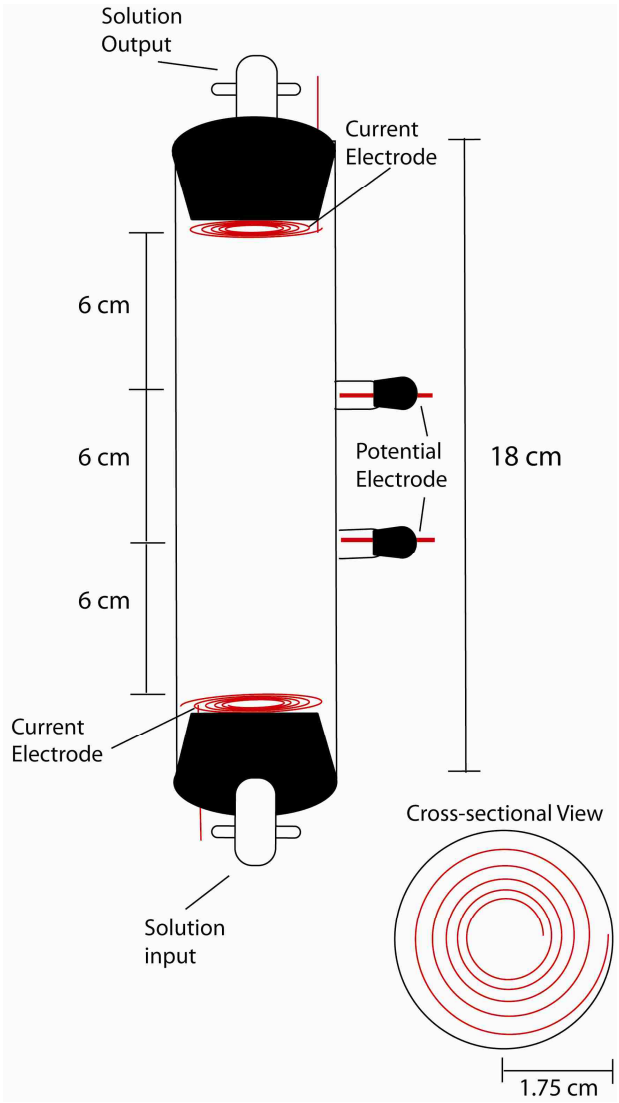

Figure 9. Diagram of experimental PVC apparatus. Diagram shows the layout of the PVC apparatus, including locations of electrodes and input/output. The column is 18 cm long and 6 cm is the spacing between electrodes. The column radius is 1.75 cm.

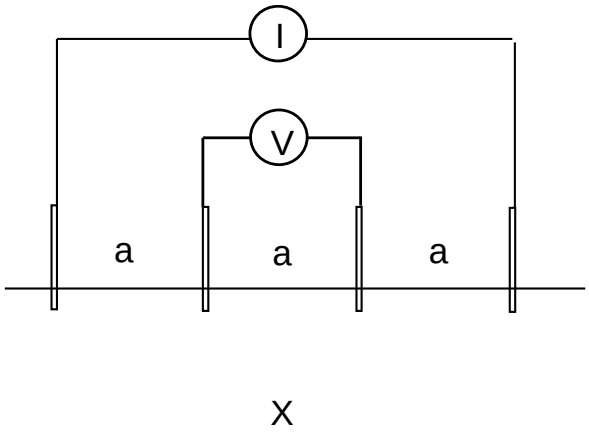

Figure 10. Schematic of Wenner array. Four electrodes are separated by spacing "a". The two current electrodes are located on the outside, with 2 potential electrodes located between them. The recorded measurement represents conditions at location X.

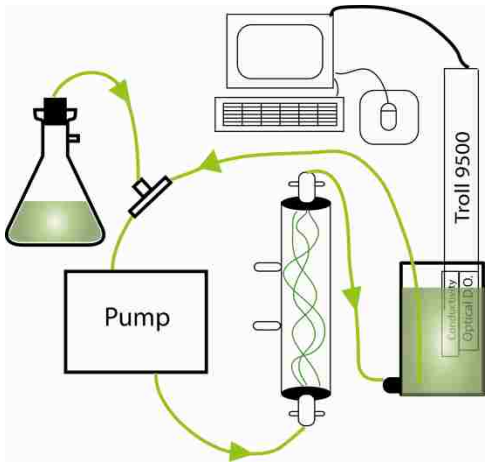

Figure 11. Schematic of flow system. Surfactant solutions will flow in a closed loop between a peristaltic pump, the PVC apparatus, and the flow cell. A T-valve exists in the line between the pump and flow cell in order to add more surfactant solution from an Erlenmeyer flask if necessary. If additional solution is not required to fill the flow cell, the valve is closed. In the flow cell, the Troll 9500 will make DO, conductivity, and pH measurements and relay them to a computer. Figure is not to scale.

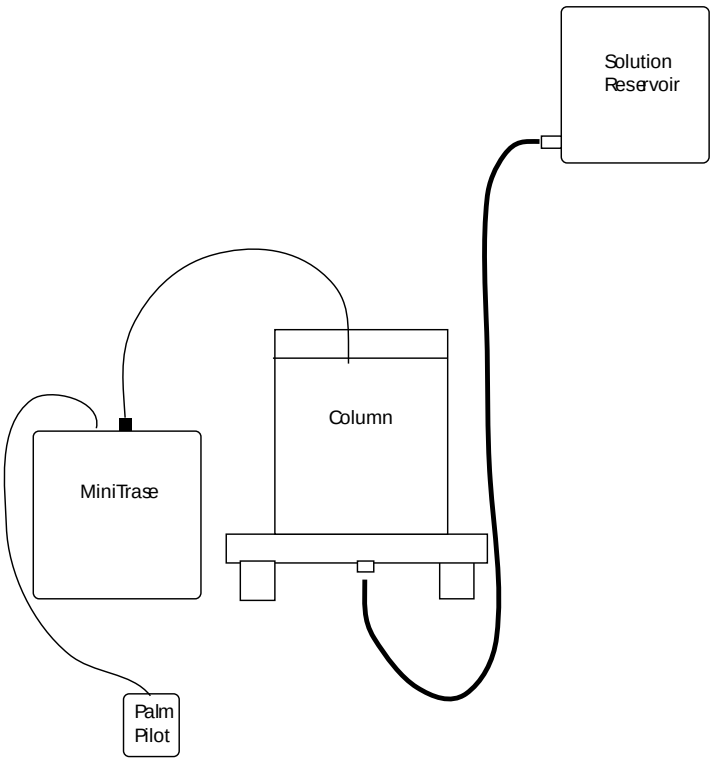

Figure 12. Schematic of time domain reflectometry laboratory set-up. The column is filled with sand, after which solution flowed from the reservoir into the column by gravity feed. After saturation was complete, measurements were taken using the MiniTrase.

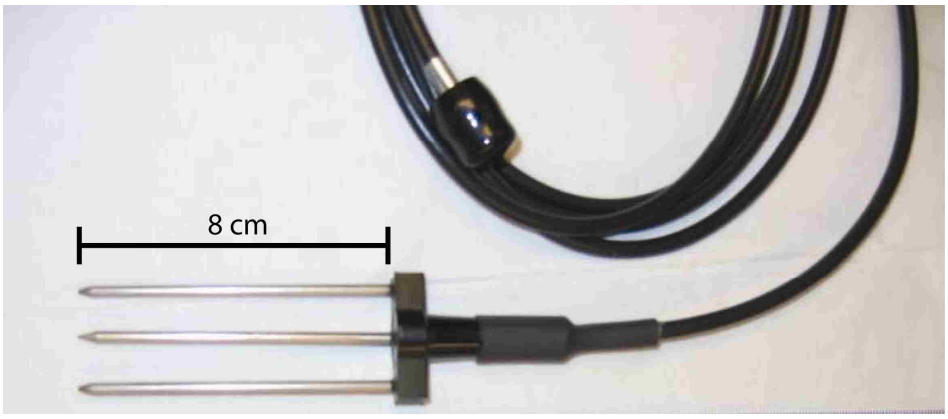

Figure 13. Photo of TDR waveguide. The waveguide is a buriable, 8cm long model. There is a 1cm between each prong.

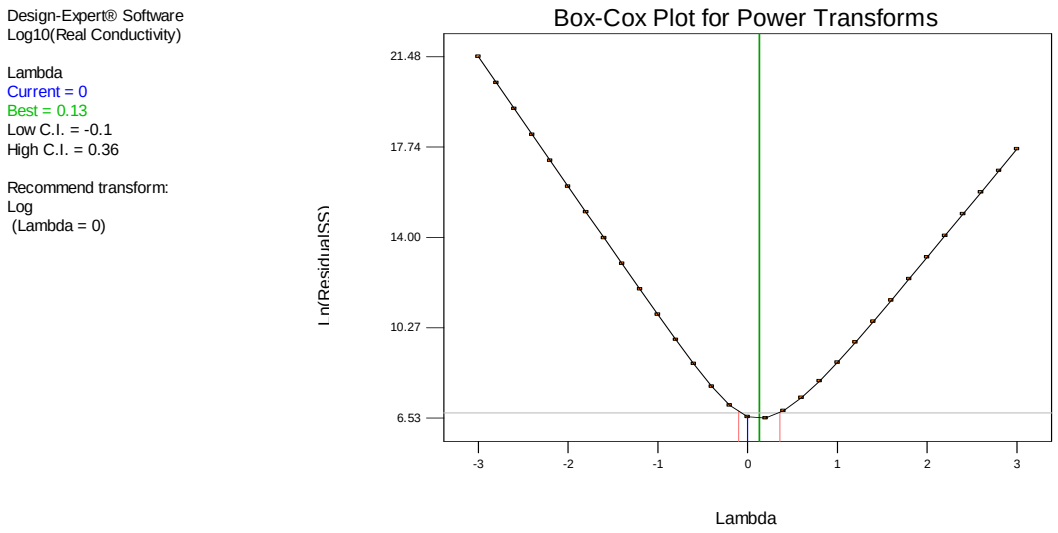

Figure 14. Box-Cox Plot of Real Conductivity. This plot indicates that a log transform of the real conductivity may be beneficial to minimizing and stabilizing the data residuals**.**

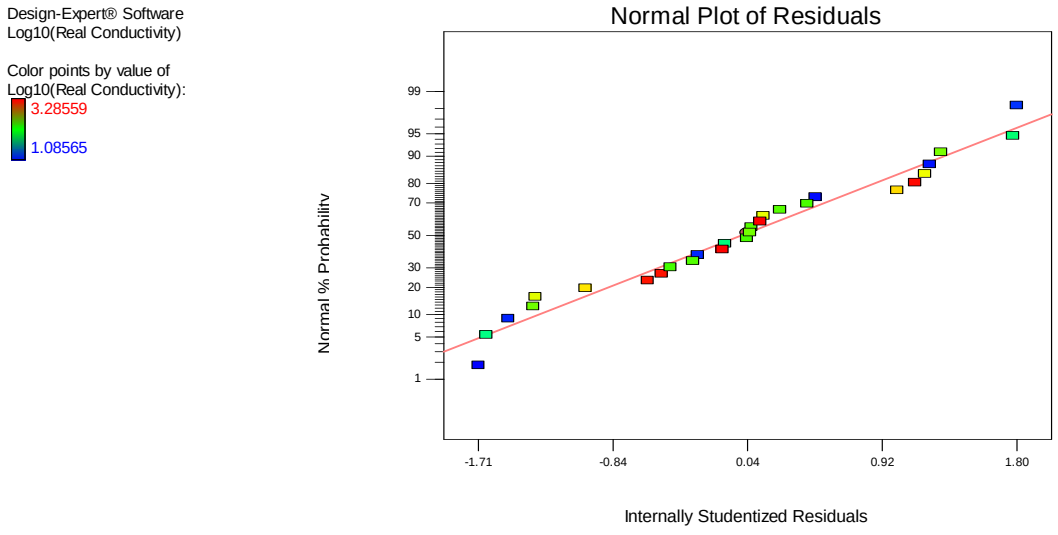

Figure 15. Scatter plot of residuals versus the normal percent probability of $\log_{10}$ (real conductivity). To verify the normality assumption, this plot should show a close fit of the residuals to the red straight line. An indication of poor normality would be an "S" shape. This plot appears to verify the normality assumption.

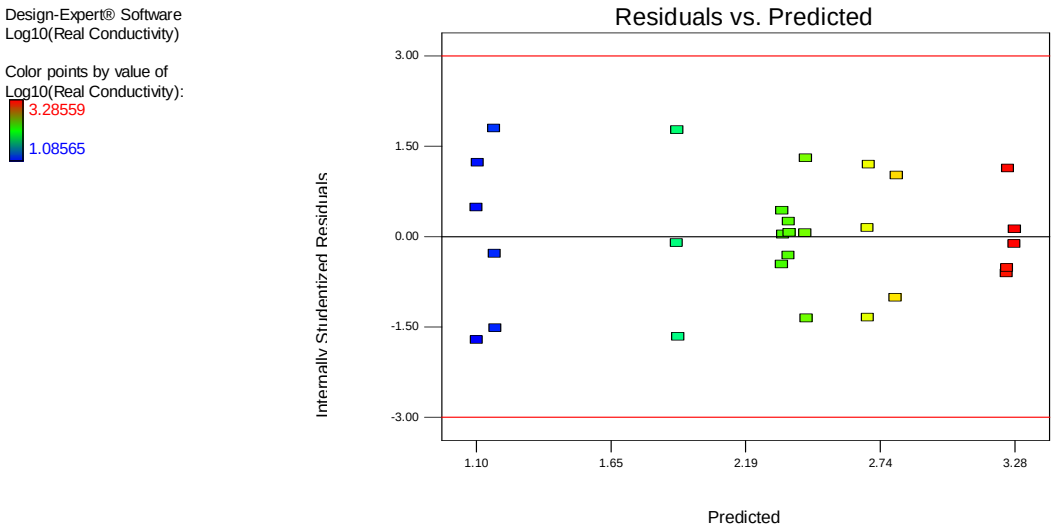

Figure 16. Scatter plot of internally studentized residuals versus the predicted real conductivity. This plot should show random scatter, indicating that the variance is constant over the predicted range. There do not appear to be any trends in the residuals.

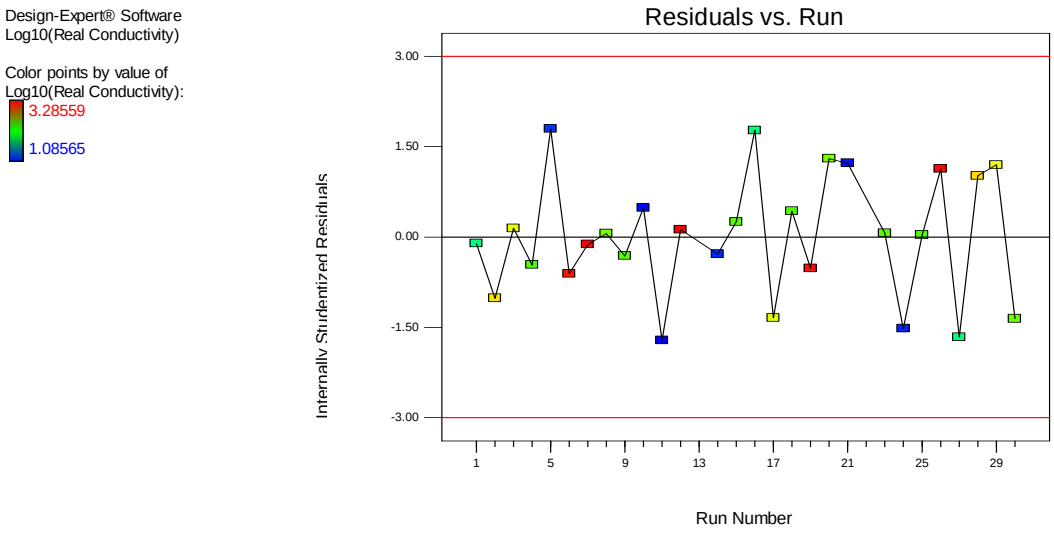

Figure 17. Scatter plot of internally studentized real conductivity residuals versus run number. Residual values below ±3.00 indicate that the proposed model of real conductivity is fairly good. Random scatter indicates that the variance is constant over all runs with no trends between residual and run number. All of the runs lie within the confidence interval, and there do not appear to be any trends in the residuals based on run order.

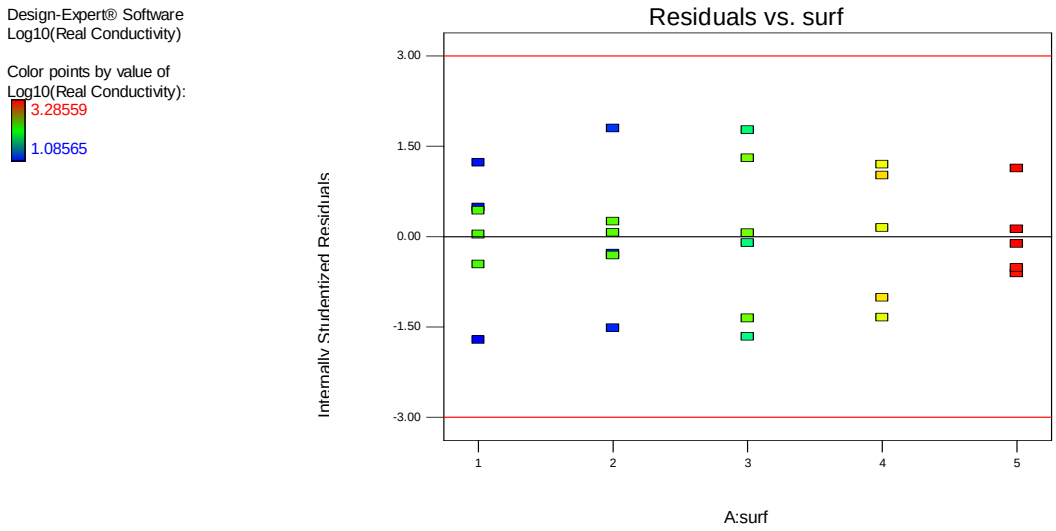

Figure 18. Plot of real conductivity residuals by surfactant type and concentration. This plot should show fairly consistent residual range across the 5 surfactant treatments. The overall fit of the data is good.

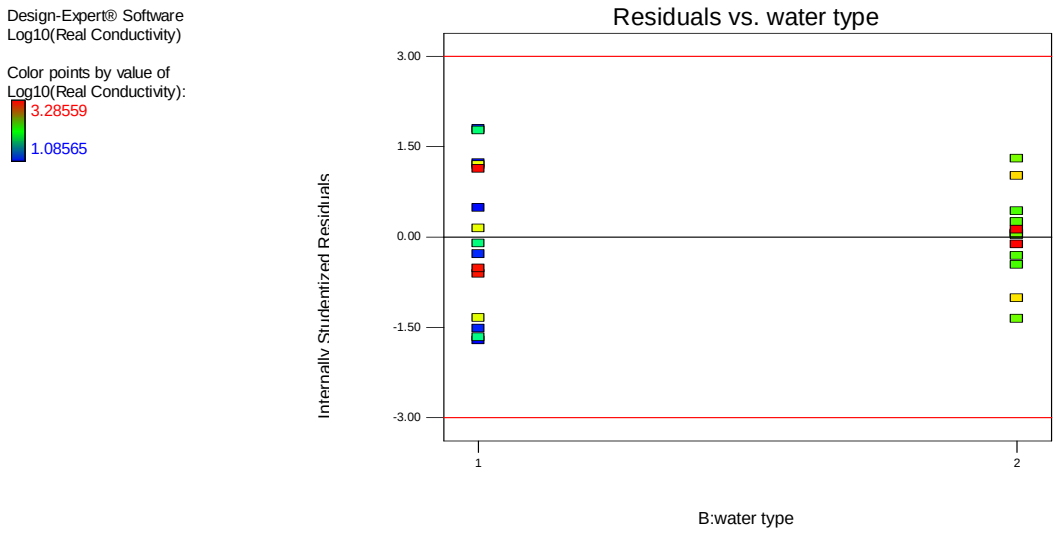

Figure 19. Plot of real conductivity residuals by water type. This plot should show fairly consistent residual range between the two water types. The overall fit of the data is good.

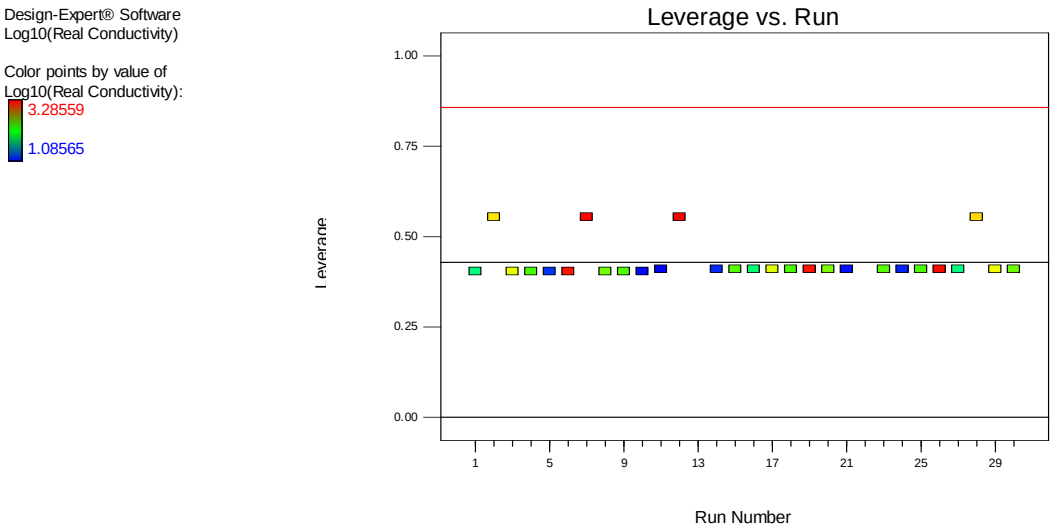

Figure 20. Leverage versus Run Number of Log_{10} (Real Conductivity). Leverage values at or above 2 times the leverage average may unduly influence at least one model parameter. The log_{10} (real conductivity) plot does not appear to show any points with exceptional leverage.

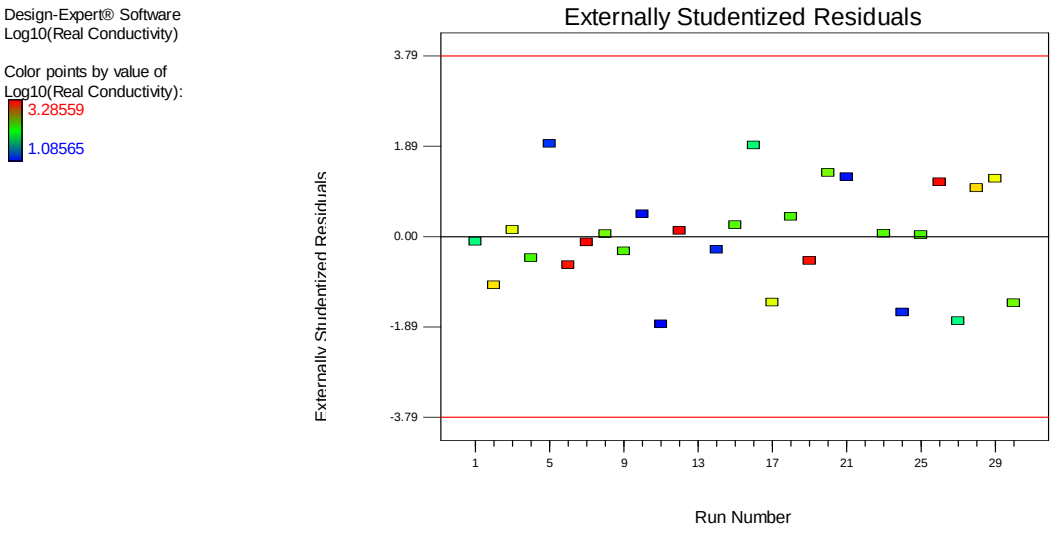

Figure 21. Externally Studentized Residuals versus Run Number of Log_{10} (Real Conductivity). This plot is used to indicate whether data falls inside of the 95% confidence interval (t-test). All runs lie inside the confidence interval.

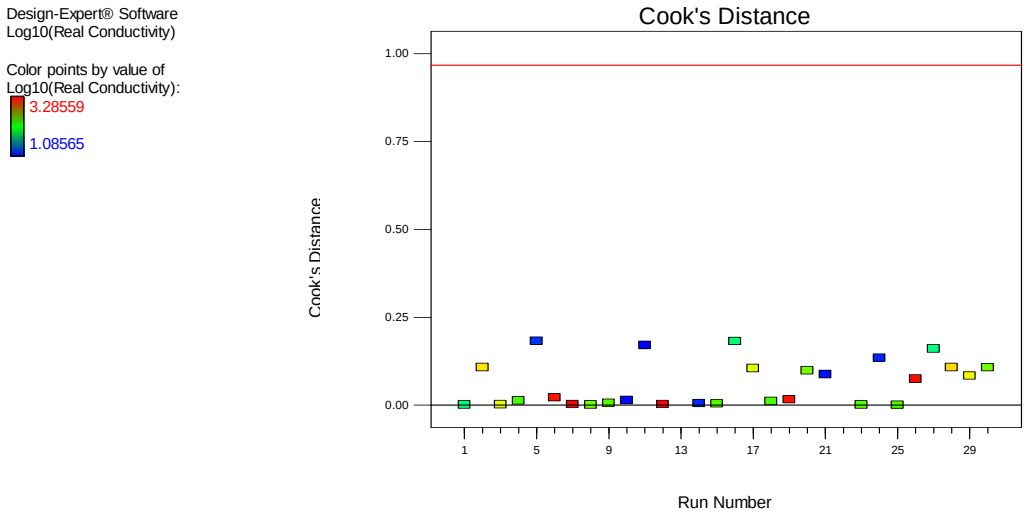

Figure 22. Cook's Distance of Log_{10} (Real Conductivity). It is a measure of how much the estimated parameter, in this case log_{10} (real conductivity), would change if a particular run was omitted, and can be used to identify potential outliers. This plot does not appear to identify any potential outliers.

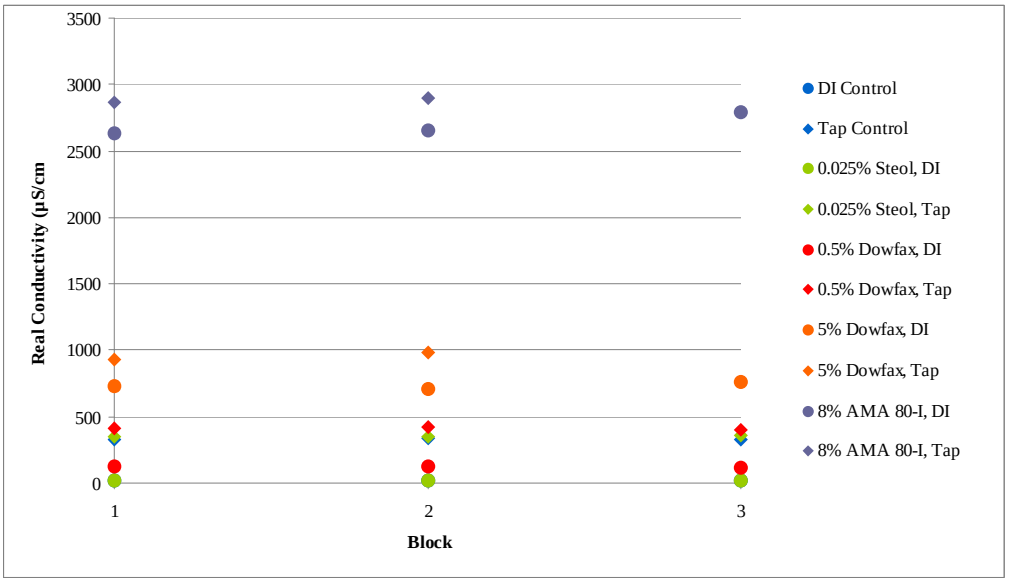

Figure 23. Plot of real conductivity results by block. The plot indicates that real conductivity values for individual surfactant treatments are consistent through all three runs.

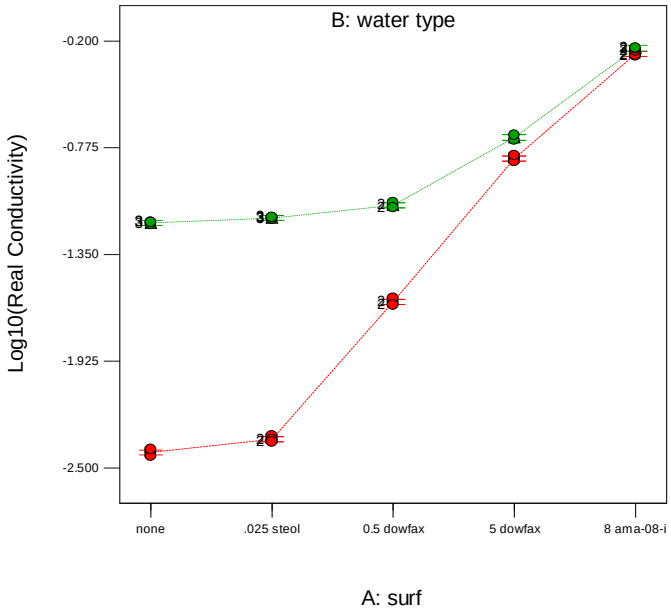

Figure 24. Plot of modeled and measured data of $\log_{10}$ (real conductivity). The green triangles and error bars connected with a dotted line represents the modeled real conductivity in tap water solutions. The green circles represent the measured data. The red square and error bars connected with a dashed line represent the modeled real conductivity in DI solutions. The red circles represent the measured data.

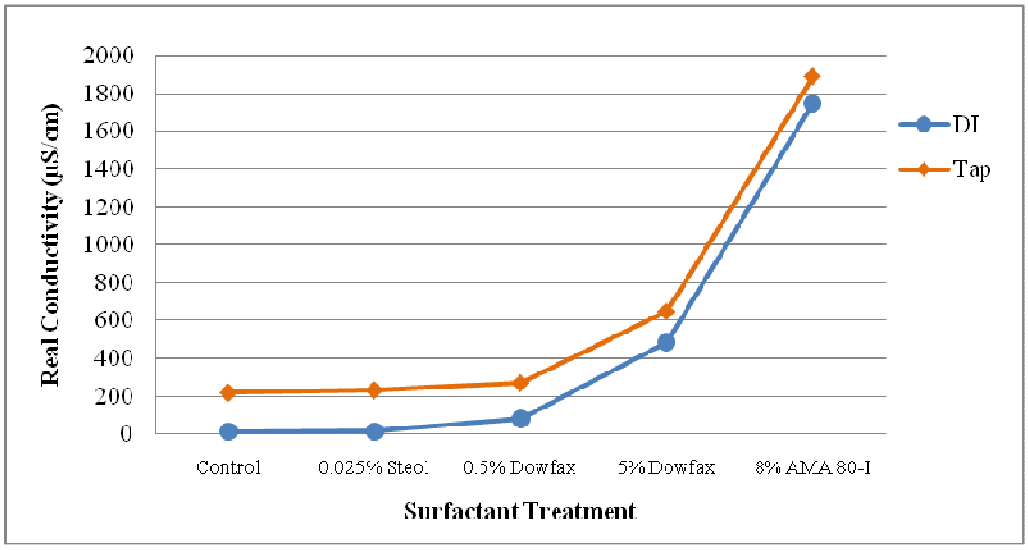

Figure 25. Plot of Real Conductivity versus Surfactant Treatment. Data in blue represents the untransformed real conductivity values of DI solutions. The data in orange represent the tap solutions.

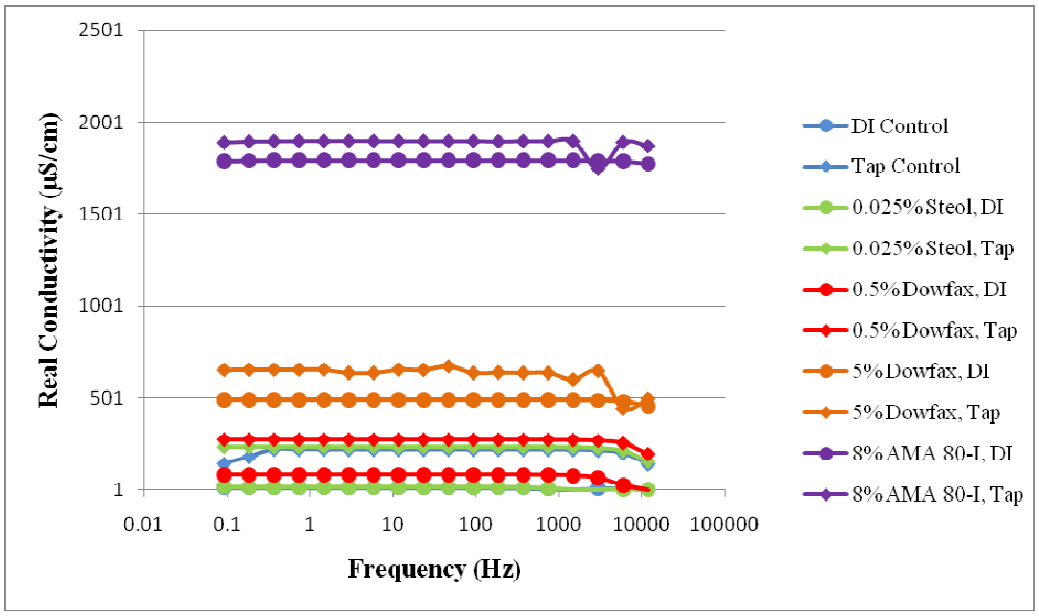

Figure 26. Real conductivity responses of each surfactant treatment over the range of measured frequencies (12000-0.091Hz). Response does not appear to be greatly affected by frequency over the measured frequencies, although there does appear to be a slight drop in value at the uppermost end of the frequency spectrum. This is most likely a result of instrument noise.

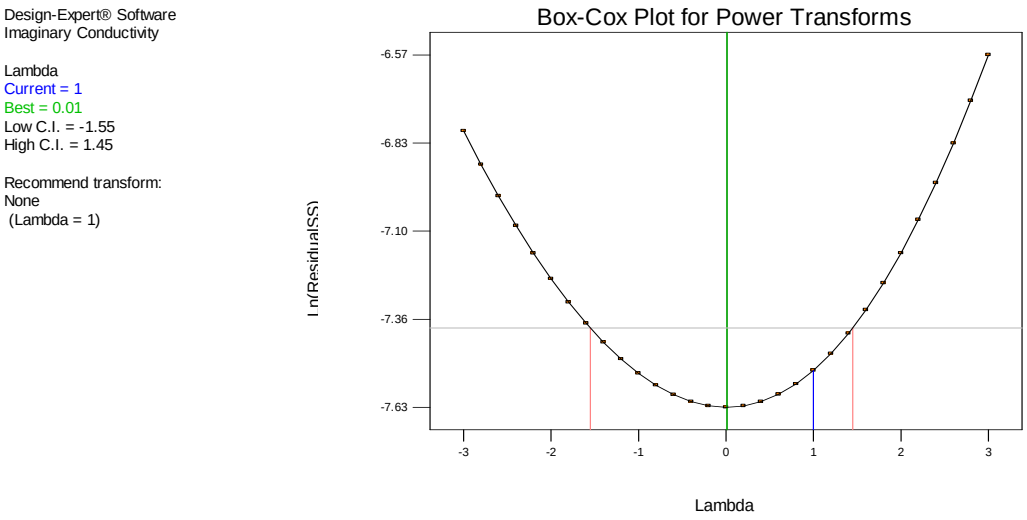

Figure 27. Box-Cox Plot of Imaginary Conductivity. This plot indicates a transform of the imaginary conductivity response is unlikely to aid in minimizing and stabilizing the data residuals.

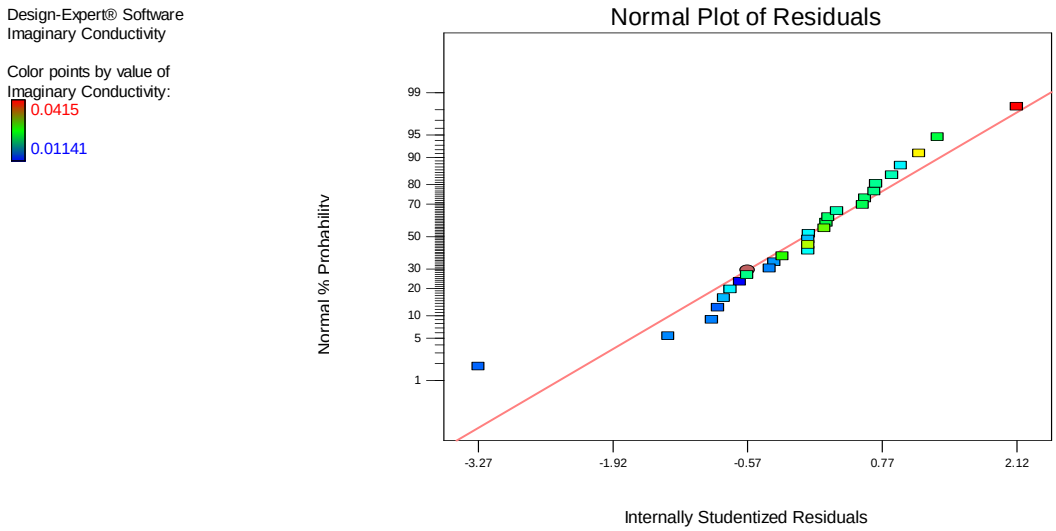

Figure 28. Scatter plot of residuals versus the normal percent probability of imaginary conductivity. To verify the normality assumption, this plot should show a close fit of the residuals to the red straight line. An indication of poor normality would be an "S" shape. This plot appears to verify the normality assumption.

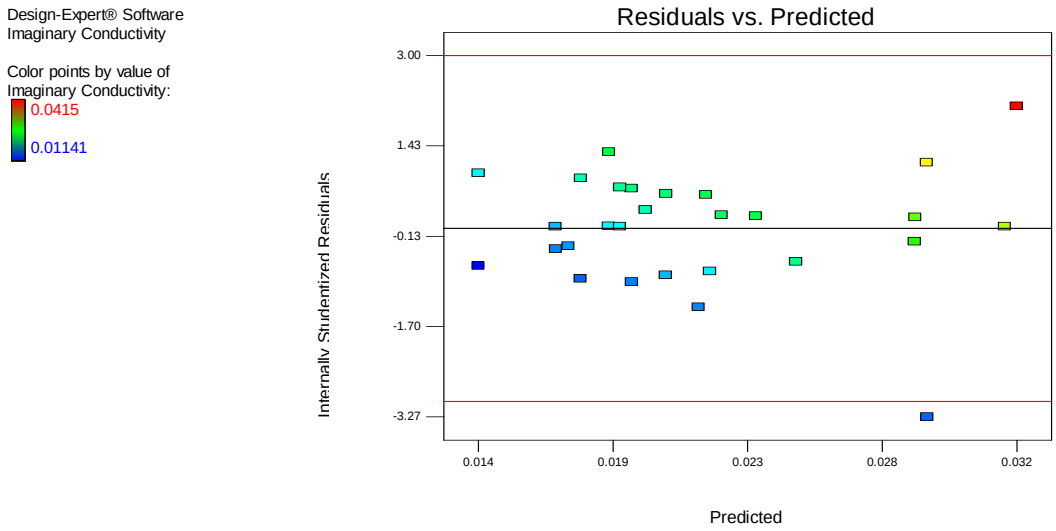

Figure 29. Scatter plot of internally studentized residuals versus the predicted imaginary conductivity. This plot should show random scatter, indicating that the variance is constant over the predicted range. There do not appear to be any trends in the residuals although Run #19 (8AMA, DI) is outside of the confidence interval.

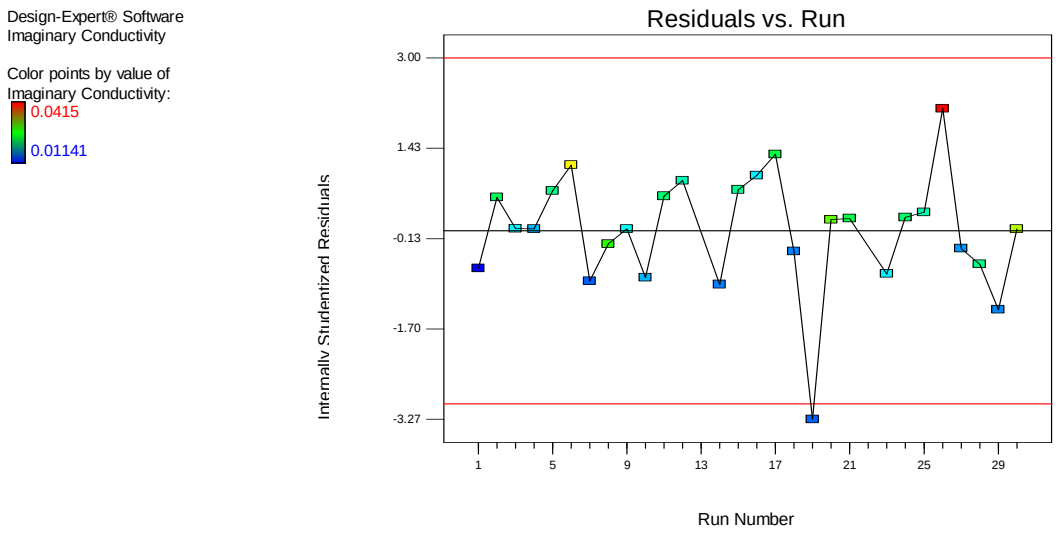

Figure 30. Scatter plot of internally studentized residuals versus run number. Residual values below ±3.00 indicate that the proposed model of imaginary conductivity is good. Random scatter indicates that variance is constant over all runs with no apparent trends. All but one of the runs lies within the confidence interval, and there are no apparent trends in the residuals. Run #19 is outside the confidence interval.

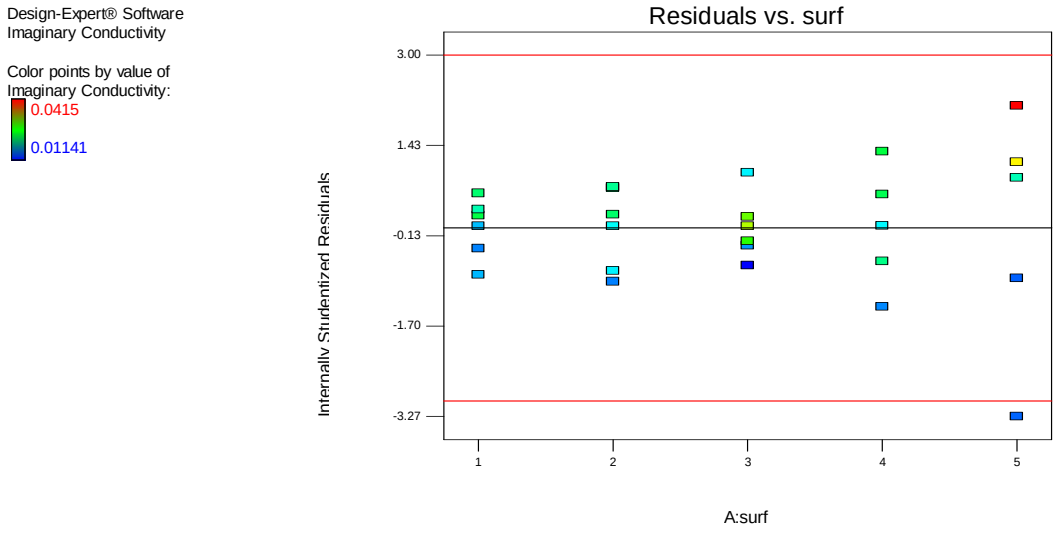

Figure 31. Plot of residuals by surfactant type and concentration. This plot should show fairly consistent range across the 5 surfactant treatments. The overall fit is good, although there appears to be a slight megaphone shape towards the higher surfactant concentrations.

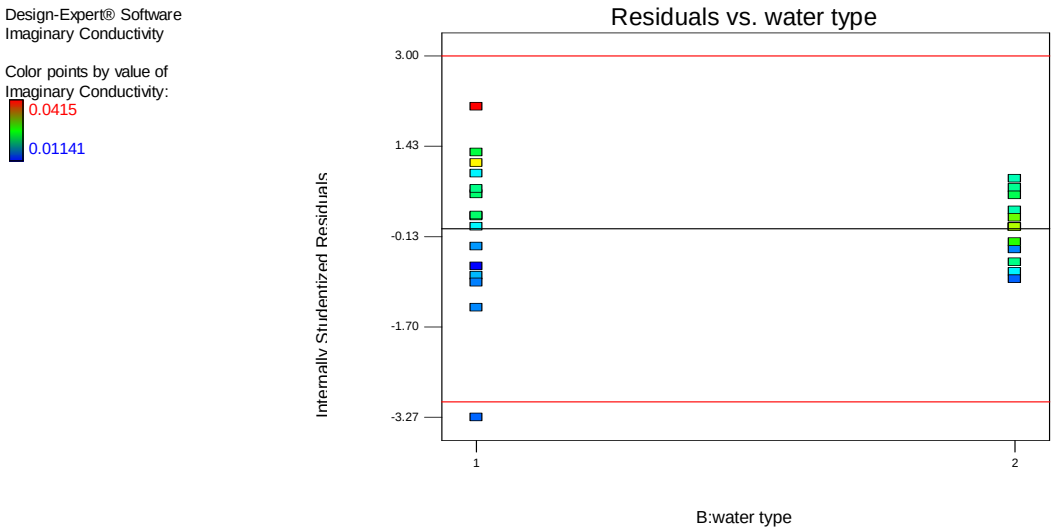

Figure 32. Plot of residuals by water type. This plot should show fairly consistent residual range between the 2 water types. DI (type 1) displays a larger range of residuals than tap (type 2). However, if the most negative residual, Run #19 is removed, the 2 water types show much greater consistency.

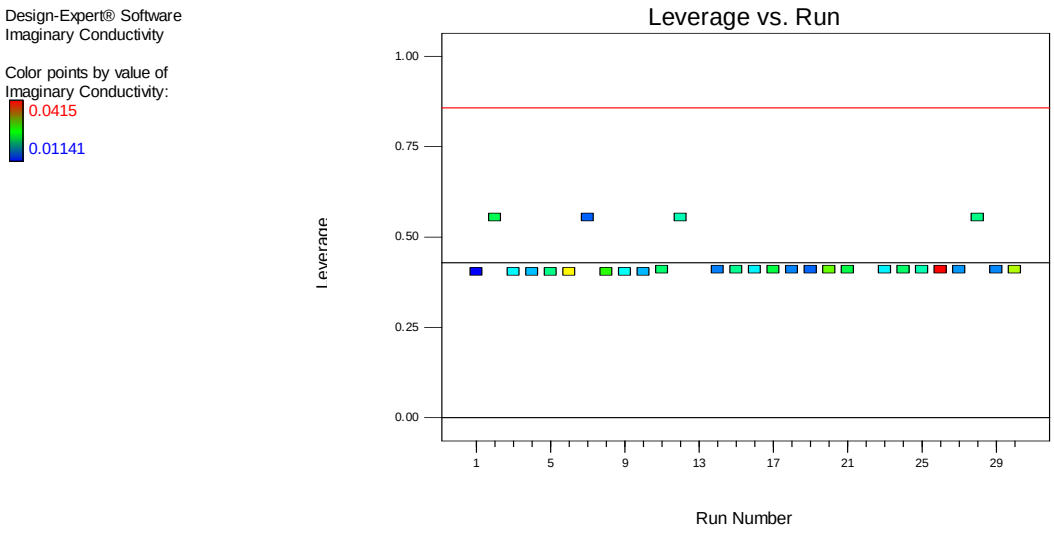

Figure 33. Leverage versus Run Number of Imaginary Conductivity. Leverage values at or above 2 times the leverage average may unduly influence at least one model parameter. The imaginary conductivity plot does not appear to show any points with exceptional leverage.

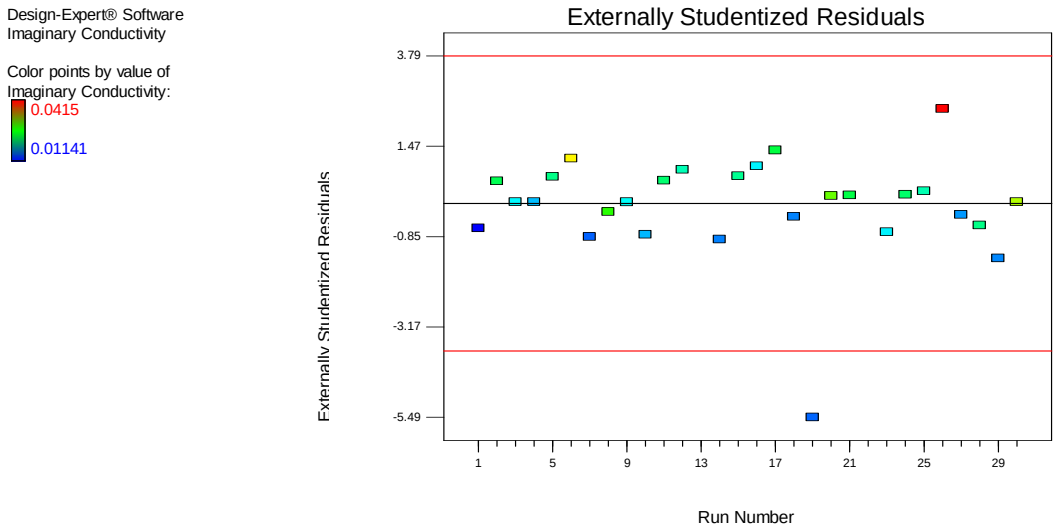

Figure 34. Externally Studentized Residuals versus Run Number of Imaginary Conductivity. This plot is used to indicate whether data falls inside of the 95% confidence interval (t-test). All runs except one lie inside the confidence interval. Run 19, 8% AMA, tap, lies outside. It should be carefully evaluated for outlier potential.

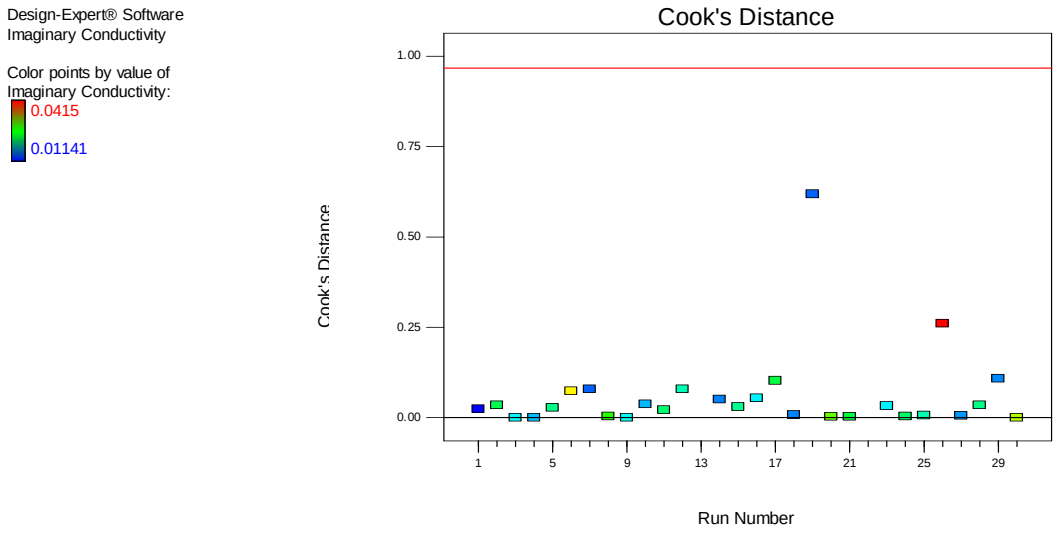

Figure 35. Cook's Distance of Imaginary Conductivity. It is a measure of how much the estimated parameter, in this case imaginary conductivity, would change if a particular run was omitted, and can be used to identify potential outliers. This plot, as in the t-test, identifies Run 19 as being a potential outlier. The Cook's D is not sufficiently high to omit from analyses.

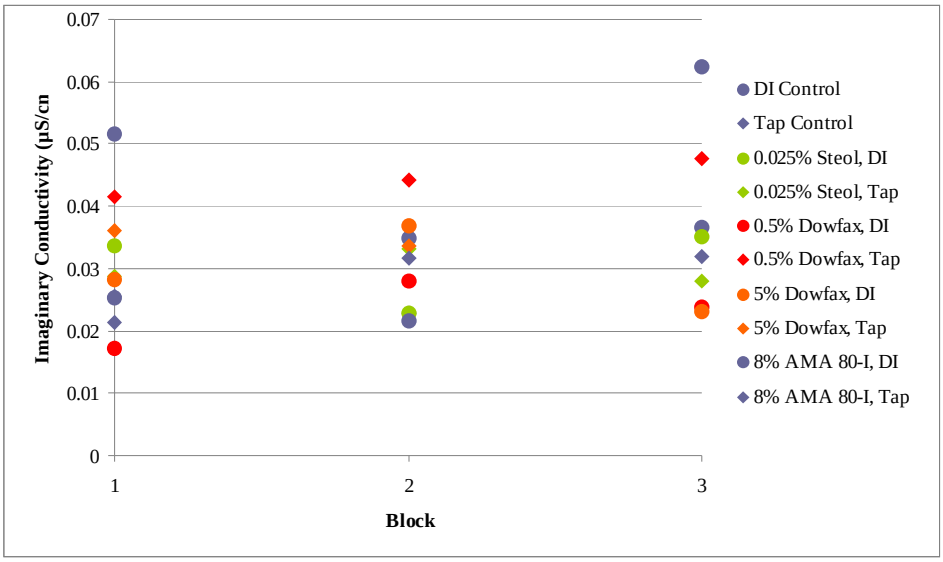

Figure 36. Plot of imaginary conductivity results by block. The plot indicates that imaginary conductivity values for individual surfactant treatments are inconsistent through all three runs.

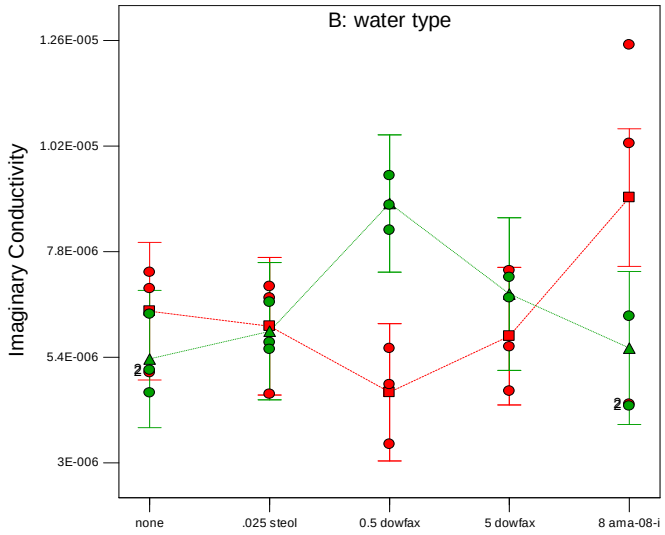

Figure 37. Plot of modeled and measured data of imaginary conductivity. The green triangles and error bars connected with a dotted line represents the modeled imaginary conductivity in tap water solutions. The green circles represent the measured data. The red square and error bars connected with a dashed line represent the modeled imaginary conductivity in DI solutions. The red circles represent the measured data.

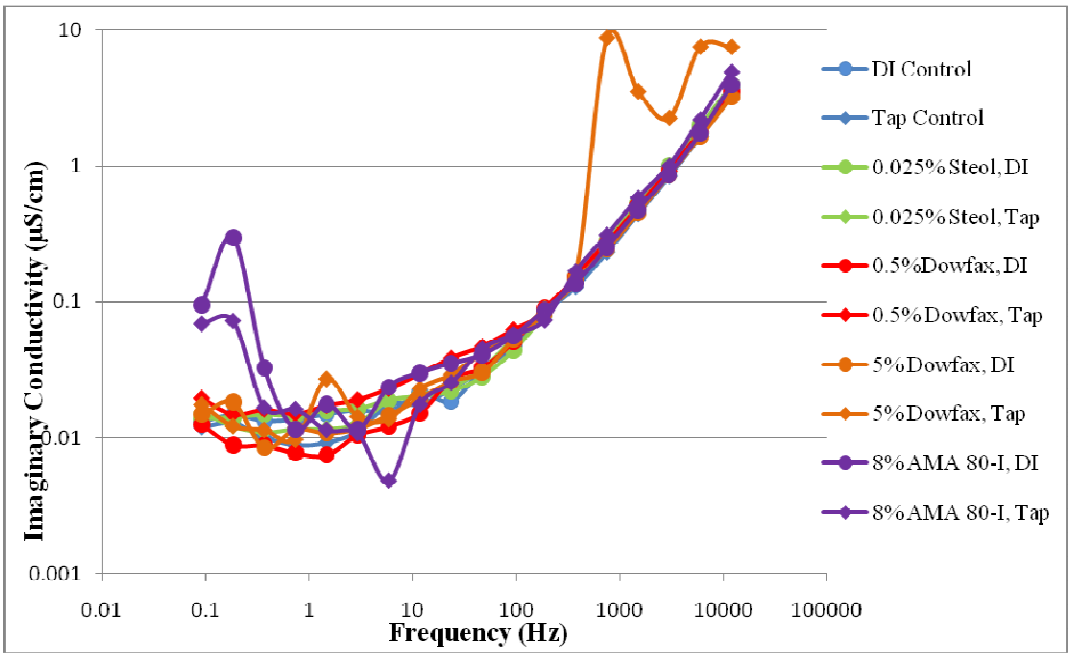

Figure 38. Imaginary conductivity responses of each surfactant treatment over the range of measured frequencies (0.091 Hz-12 kHz).

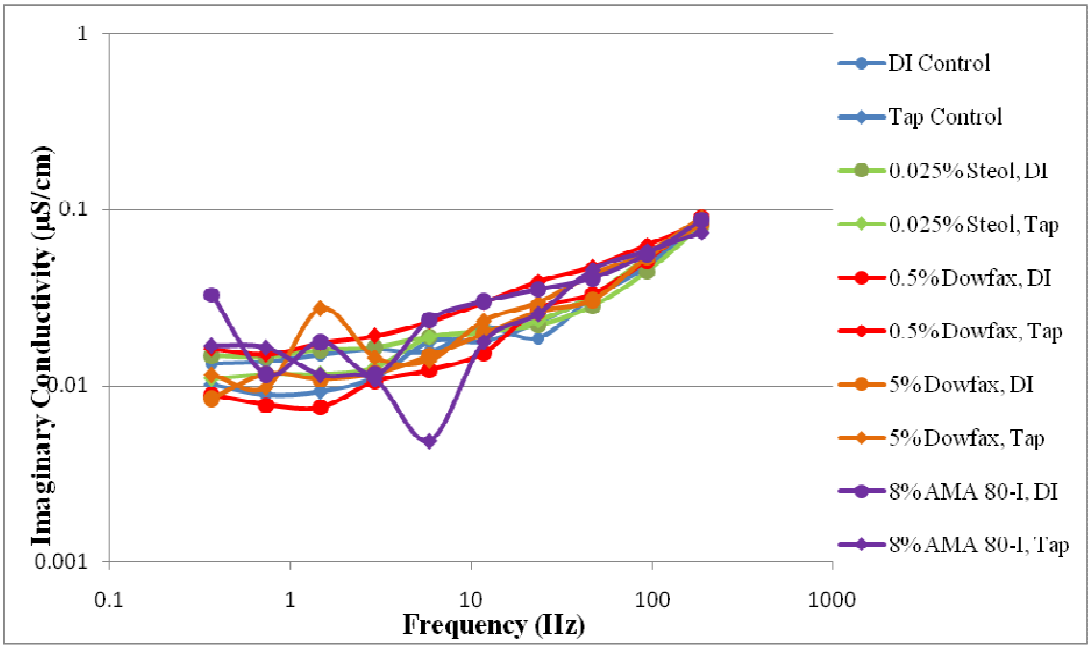

Figure 39. Imaginary conductivity responses of each surfactant treatment over a limited frequency range (0.366-187.5 Hz).

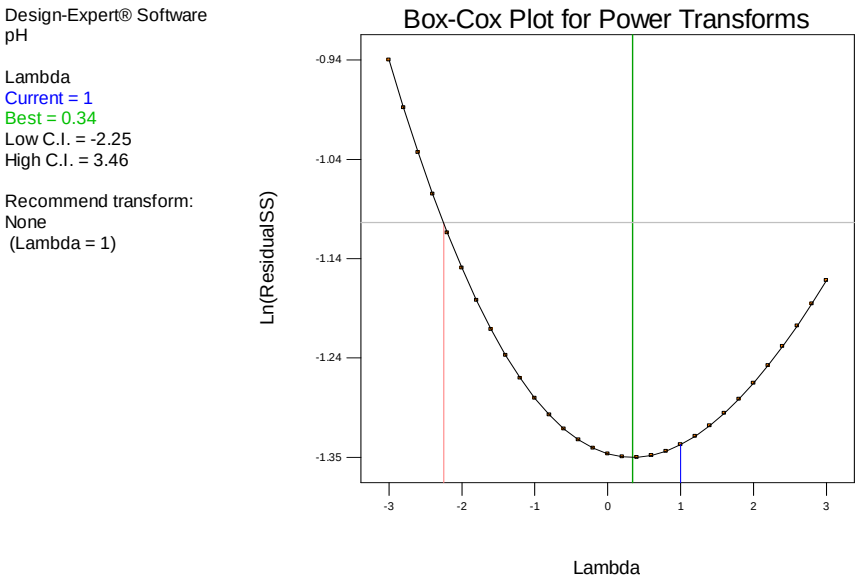

Figure 40. Box-Cox Plot of pH. This plot indicates a transform of the pH is unlikely to aid in minimizing and stabilizing the data residuals**.**

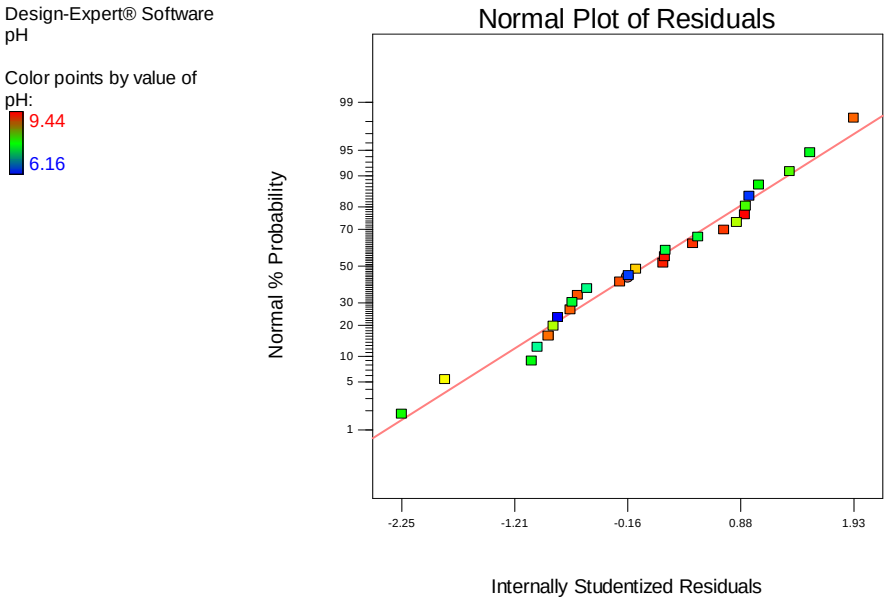

Figure 41. Scatter plot of residuals versus the normal percent probability of pH. To verify the normality assumption, this plot should show a close fit of the residuals to the red straight line. An indication of poor normality would be an “S” shape. This plot appears to verify the normality assumption.

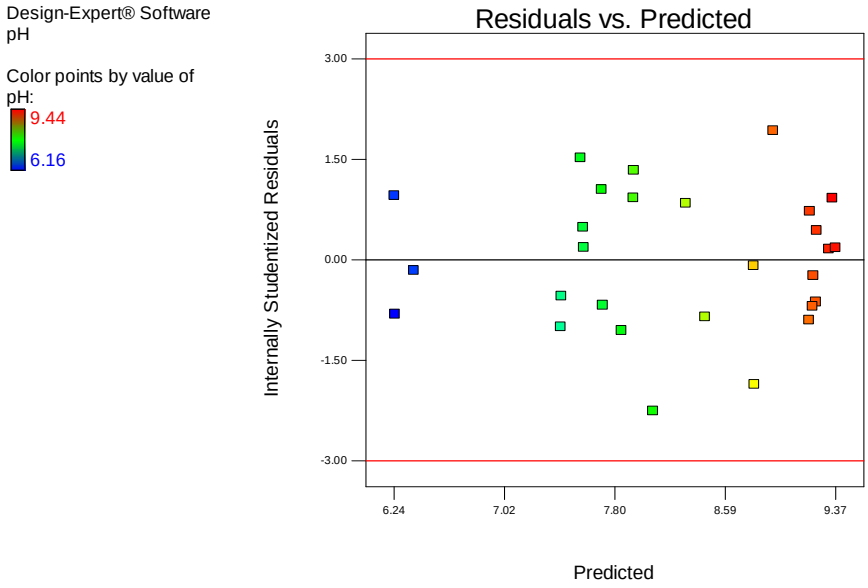

Figure 42. Scatter plot of internally studentized residuals versus the predicted pH. This plot should show random scatter, indicating that the variance is constant over the predicted range. There do not appear to be any trends in the residuals.

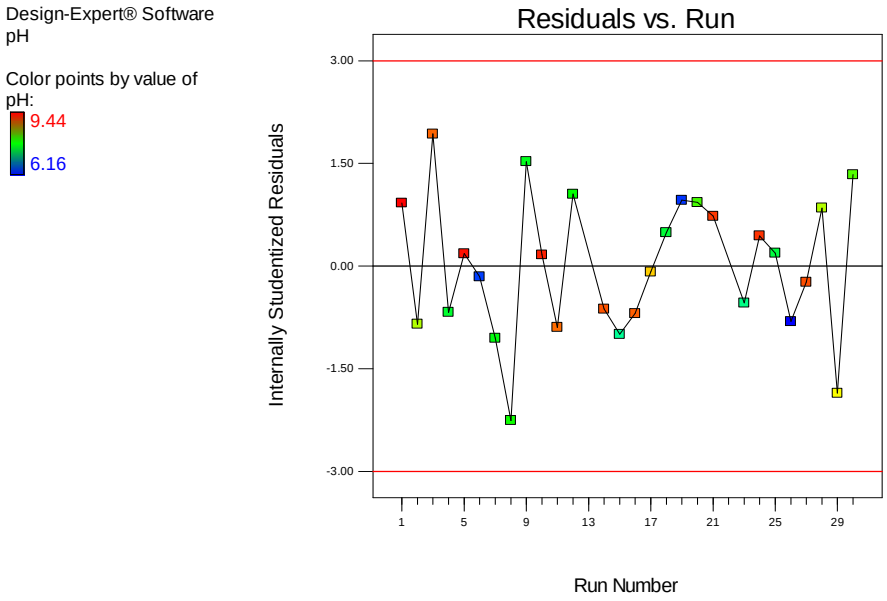

Figure 43. Scatter plot of internally studentized residuals versus run number. Residual values below ±3.00 indicate that the proposed model of pH is fairly good. Random scatter indicates that the variance is constant over all runs with no trends between residual and run number. All of the runs lie within the confidence interval, and there do not appear to be any trends in the residuals based on run order.

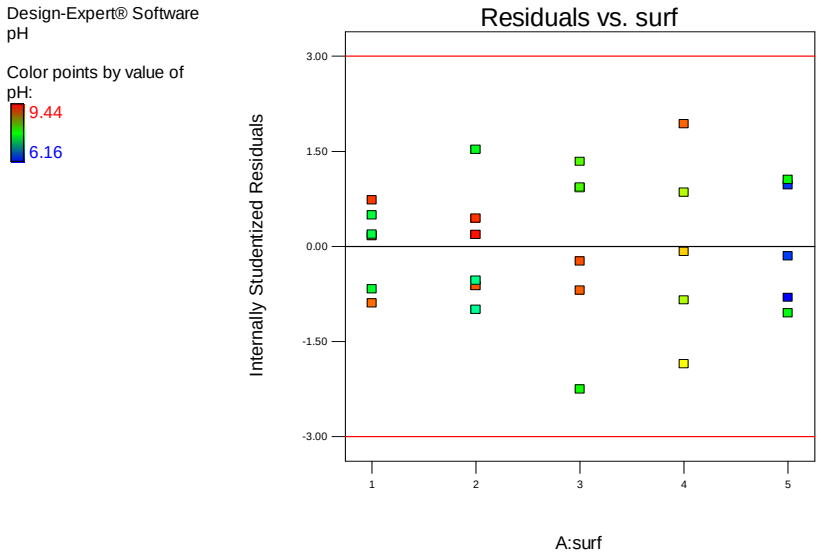

Figure 44. Plot of residuals by surfactant type and concentration. This plot should show fairly consistent residual range across the 5 surfactant treatments. The Dowfax treatments (3 and 4) have slightly larger ranges, but still fall within the confidence interval.

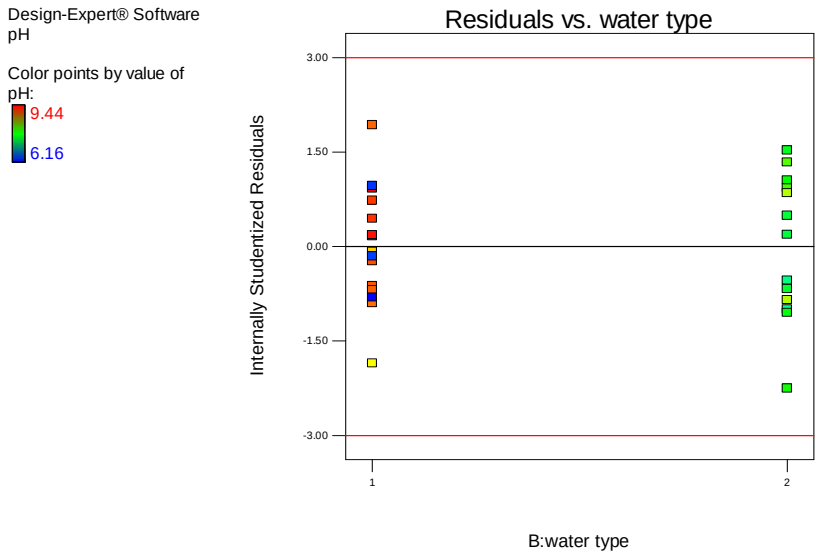

Figure 45. Plot of residuals by water type. This plot should show fairly consistent residual range between the two water types. The overall fit of the data is good, with fairly consistent spreads and all data points within the confidence interval. Note that the measured pH values of the DI solutions (water type 1) read both the highest and lowest, while the tap solutions (water type 2) appear to lie in the middle values.

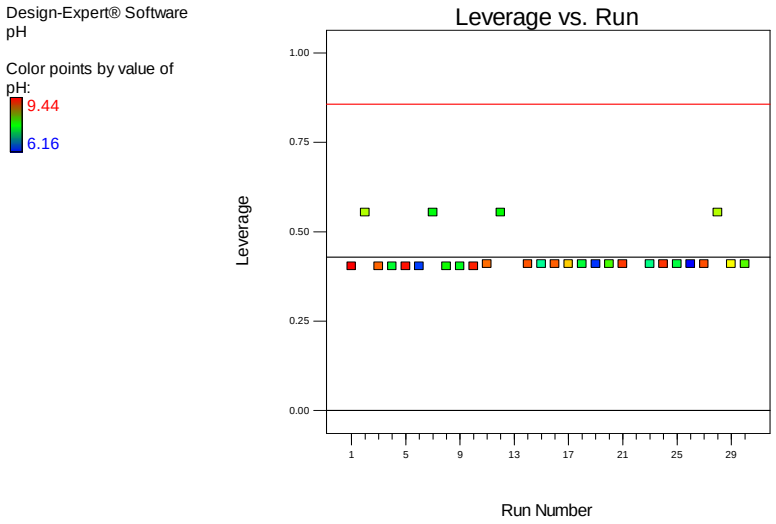

Figure 46. Leverage versus Run Number of pH. Leverage values at or above 2 times the leverage average may unduly influence at least one model parameter. The pH plot does not appear to show any points with exceptional leverage.

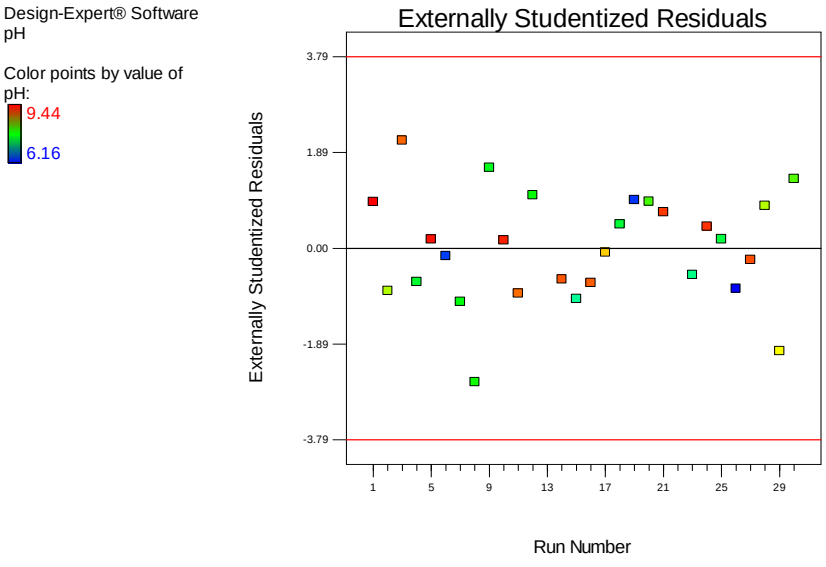

Figure 47. Externally Studentized Residuals versus Run Number of pH. This plot is used to indicate whether data falls inside of the 95% confidence interval (t-test). All runs lie inside the confidence interval.

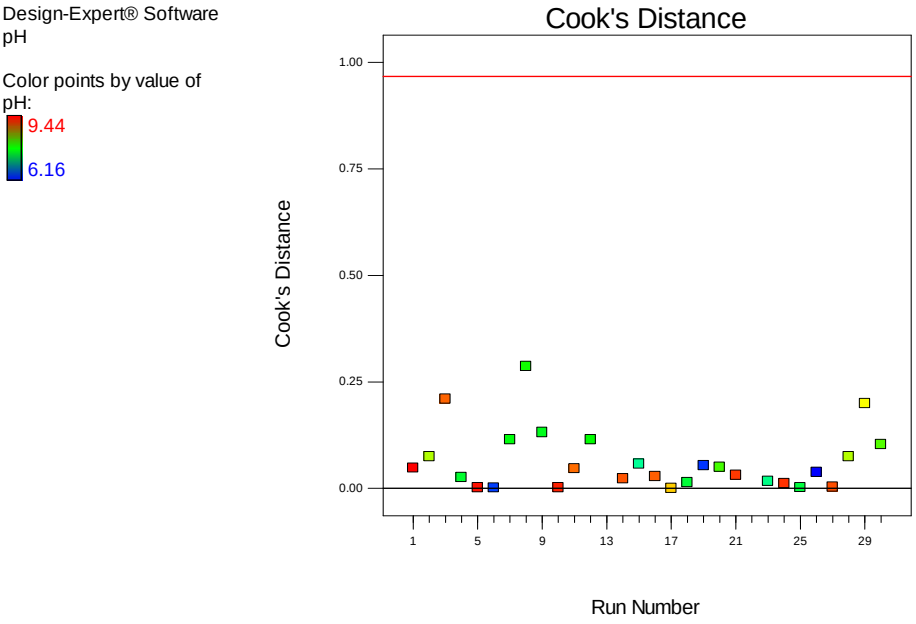

Figure 48. Cook's Distance of pH. It is a measure of how much the estimated parameter, in this case imaginary conductivity, would change if a particular run was omitted, and can be used to identify potential outliers. The plot does not indicate any potential outliers.

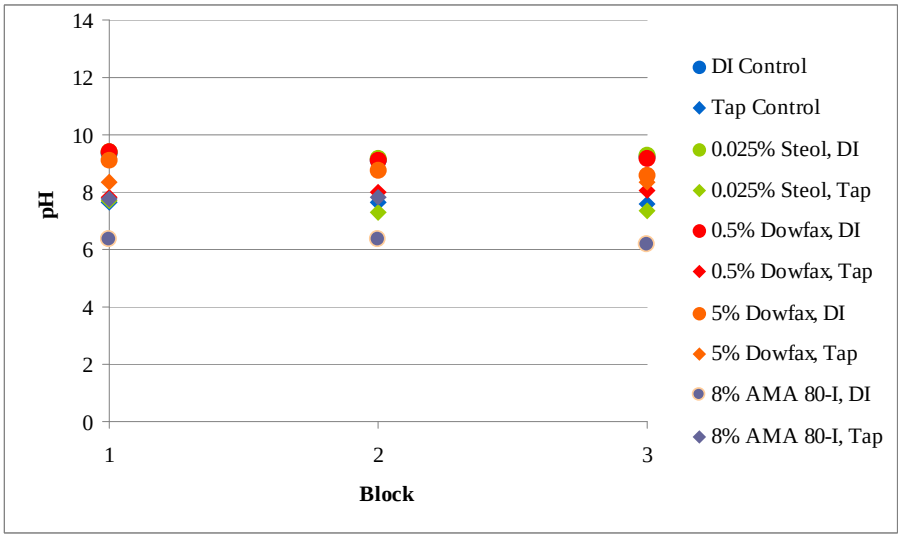

Figure 49. Plot of pH results by block. The plot indicates that pH values for individual surfactant treatments are consistent through all three runs, although there is significant overlap among treatments.

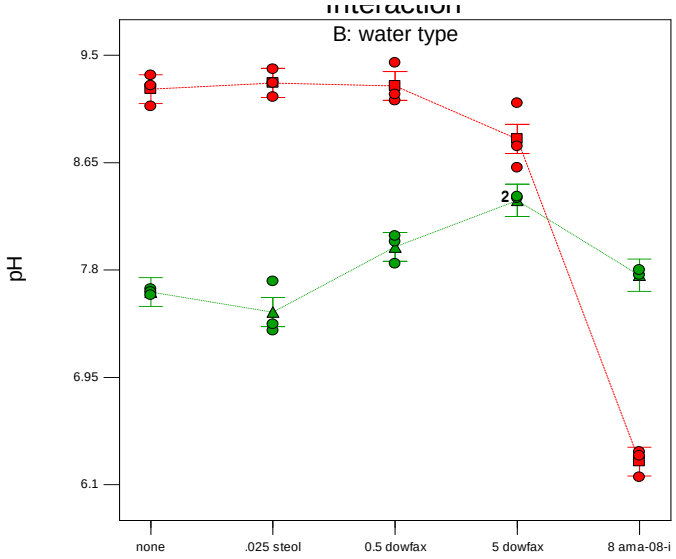

Figure 50. Plot of modeled and measured data pH. The green triangles and error bars connected with a dotted line represents the modeled pH in tap water solutions. The green circles represent the measured data. The red square and error bars connected with a dashed line represent the modeled pH in DI solutions. The red circles represent the measured data.

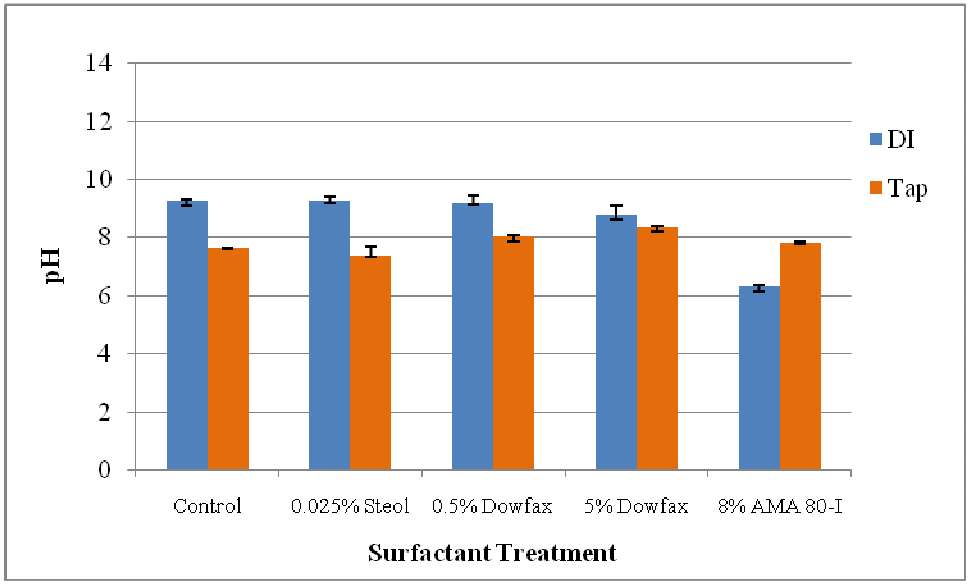

Figure 51. Bar graph of measured pH responses. The bar represents the median value, while the upper error bar is the treatment's maximum, and the lower error bar is the minimum.

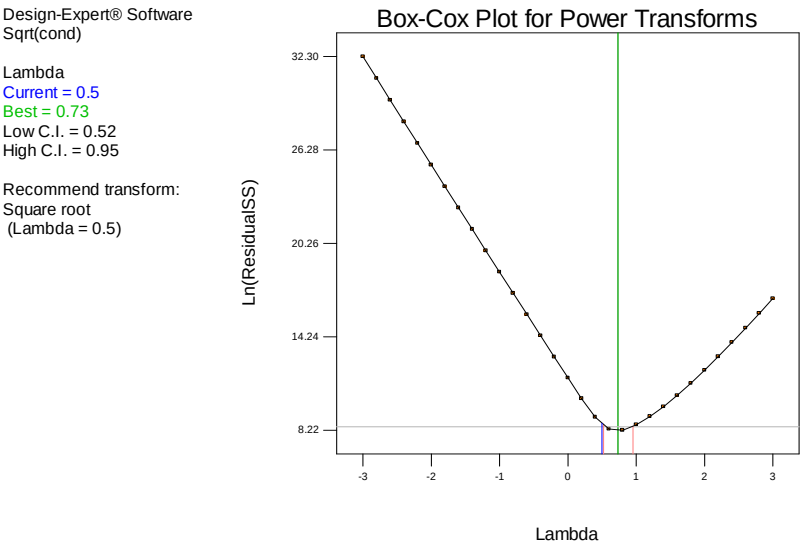

Figure 52. Box-Cox Plot of Specific Conductivity. This plot indicates that a square root transform of the specific conductivity may be beneficial to minimizing and stabilizing the data residuals**.**

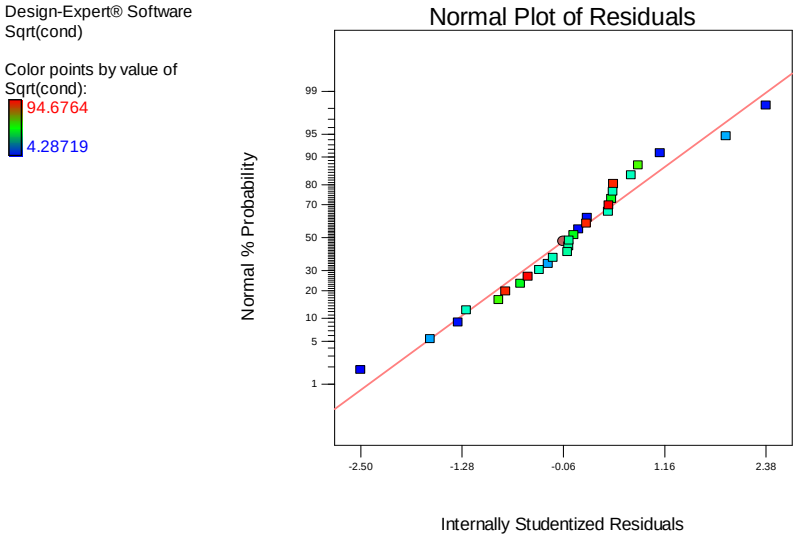

Figure 53. Scatter plot of residuals versus the normal percent probability of sqrt (specific conductivity). To verify the normality assumption, this plot should show a close fit of the residuals to the red straight line. An indication of poor normality would be an "S" shape. This plot appears to verify the normality assumption.

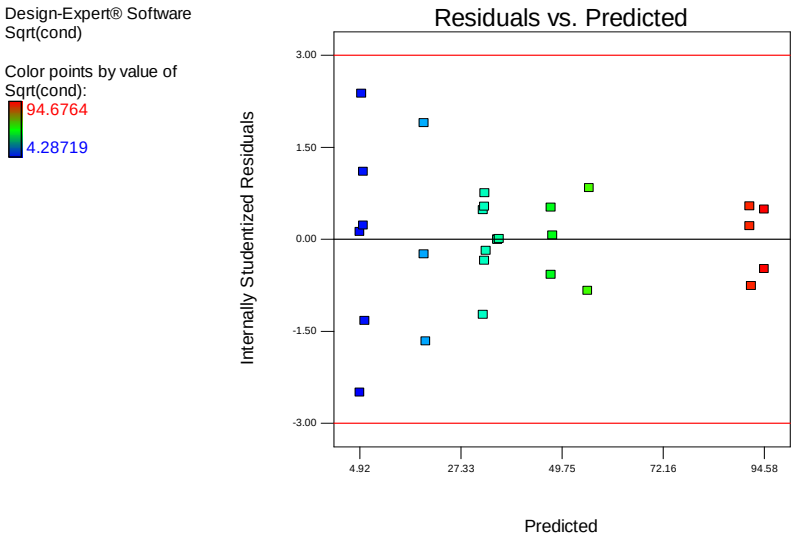

Figure 54. Scatter plot of internally studentized residuals versus the predicted sqrt (specific conductivity). This plot should show random scatter, indicating that the variance is constant over the predicted range. There is a megaphone shape to the plot, with the largest range of residuals appearing in the lowest values predicted conductivity. This may be a function of normal variation in the DI water used in the experiments.

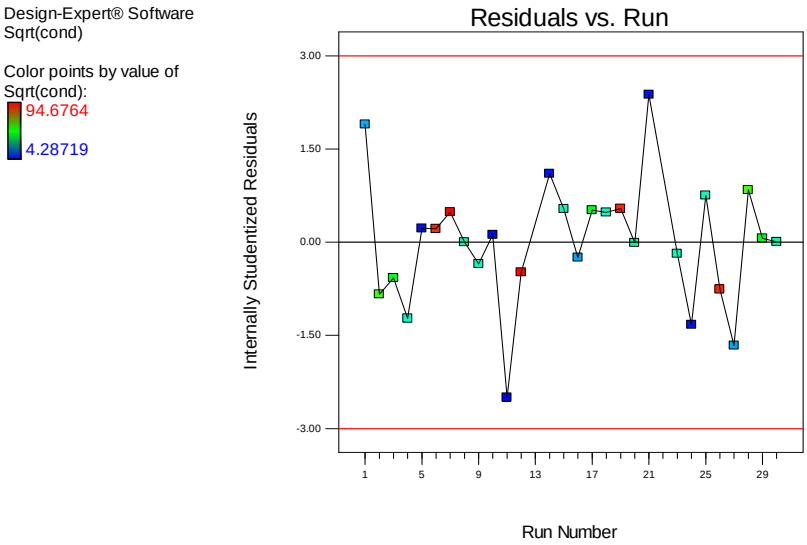

Figure 55. Scatter plot of internally studentized residuals versus run number. Residual values below ±3.00 indicate that the proposed model of sqrt (specific conductivity) is fairly good. Random scatter indicates that the variance is constant over all runs with no trends between residual and run number. All of the runs lie within the confidence interval, and there do not appear to be any trends in the residuals based on run order.

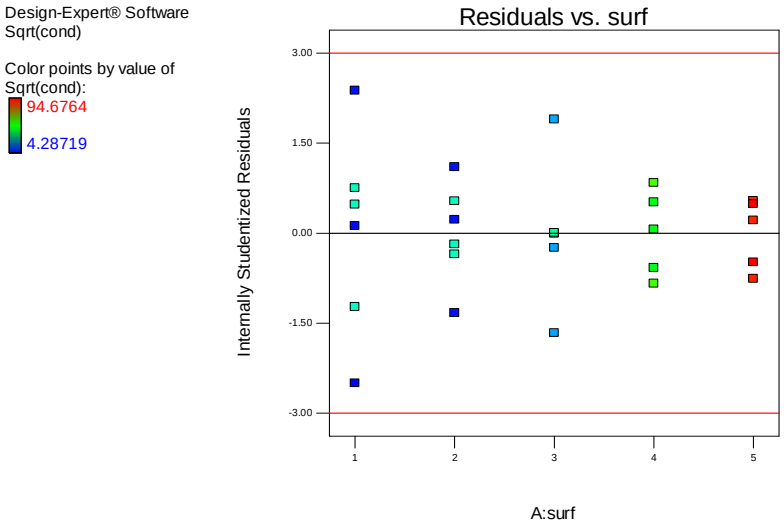

Figure 56. Plot of residuals by surfactant type and concentration. This plot should show fairly consistent residual range across the 5 surfactant treatments although the control groups (no surfactant) appear to have larger residual ranges.

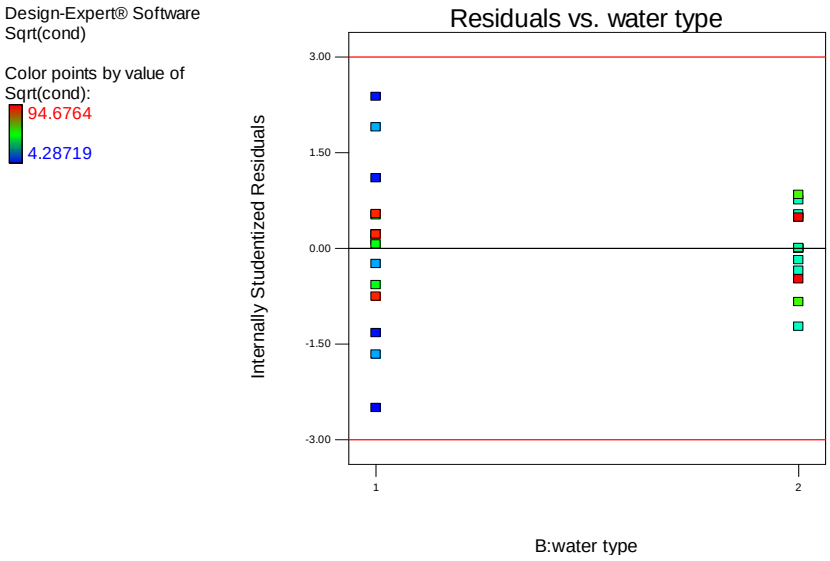

Figure 57. Plot of residuals by water type. This plot should show fairly consistent residual range between the two water types. DI (type 1) has a much larger range of residuals than the tap treatments (type 2).

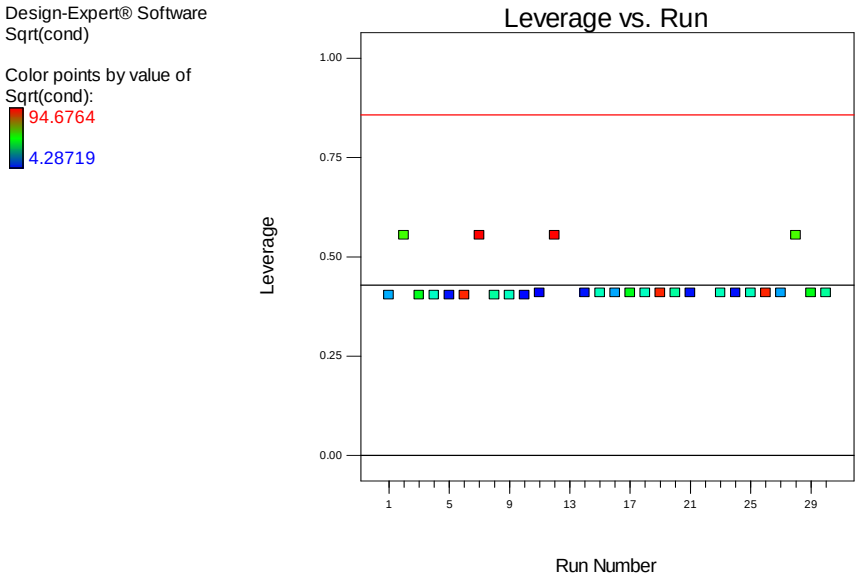

Figure 58. Leverage versus Run Number of Sqrt (Specific Conductivity). Leverage values at or above 2 times the leverage average may unduly influence at least one model parameter. The sqrt (specific conductivity) plot does not appear to show any points with exceptional leverage.

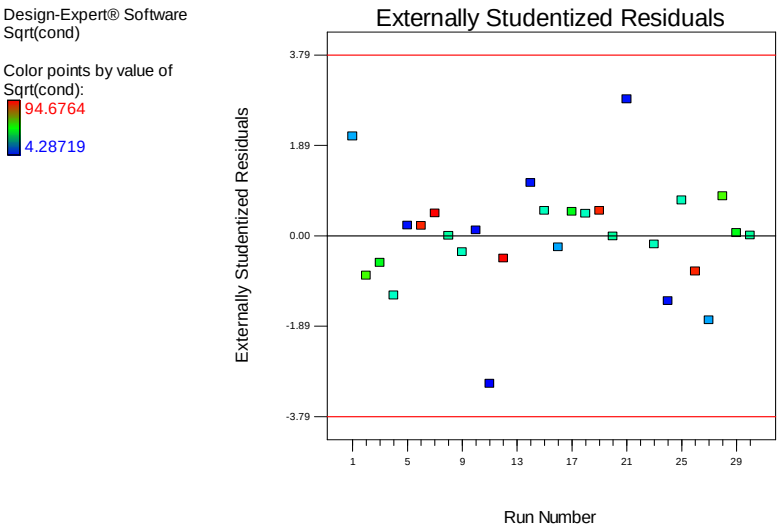

Figure 59. Externally Studentized Residuals versus Run Number of Sqrt (Specific Conductivity). This plot is used to indicate whether data falls inside of the 95% confidence interval (t-test). All runs lie inside the confidence interval.

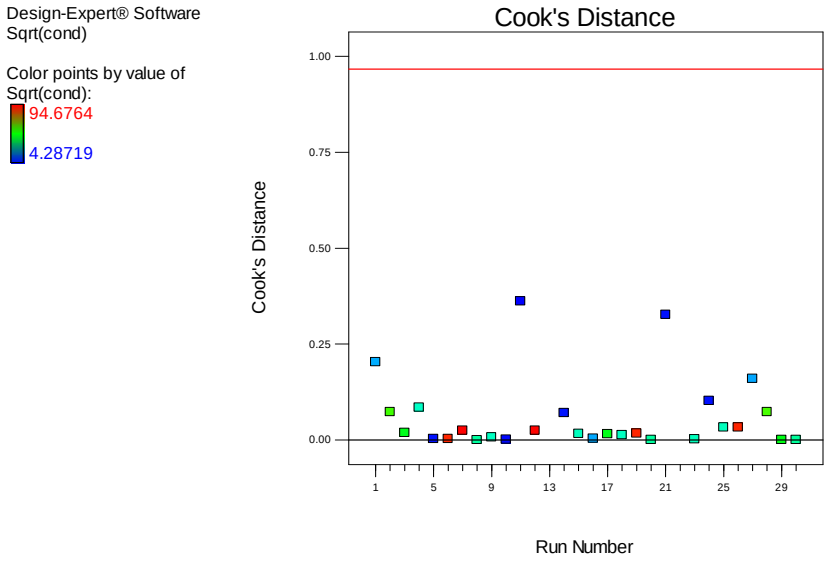

Figure 60. Cook's Distance of Sqrt (Specific Conductivity). It is a measure of how much the estimated parameter, in this case sqrt (specific conductivity), would change if a particular run was omitted, and can be used to identify potential outliers. This plot does not appear to identify any potential outliers.

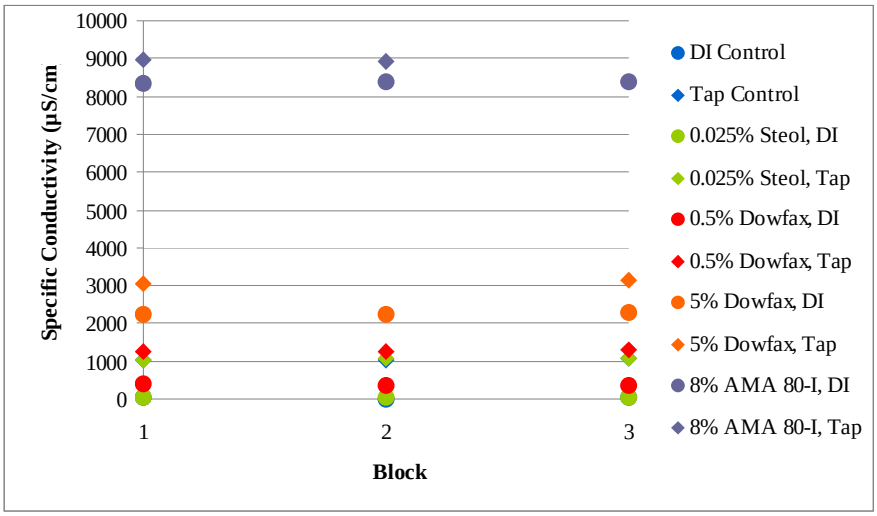

Figure 61. Plot of specific conductivity by block. The plot indicates that specific conductivity values for individual surfactant treatments are consistent through all three runs.

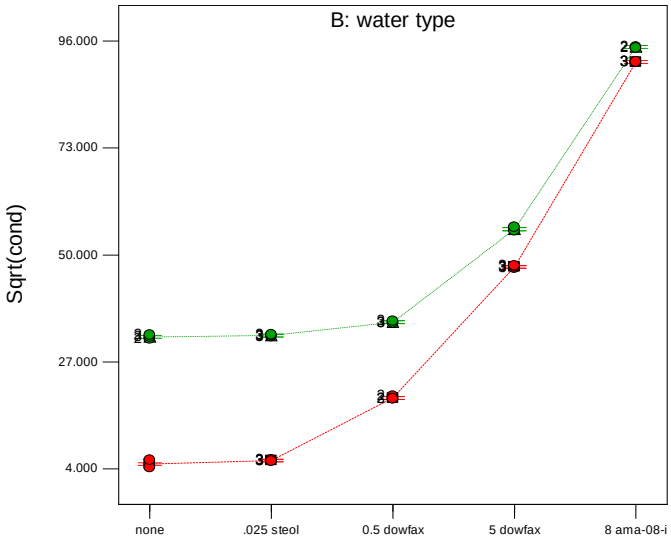

Figure 62. Plot of modeled and measured data of sqrt (specific conductivity). The green triangles and error bars connected with a dotted line represents the modeled specific conductivity in tap water solutions. The green circles represent the measured data. The red square and error bars connected with a dashed line represent the modeled specific conductivity in DI solutions. The red circles represent the measured data.

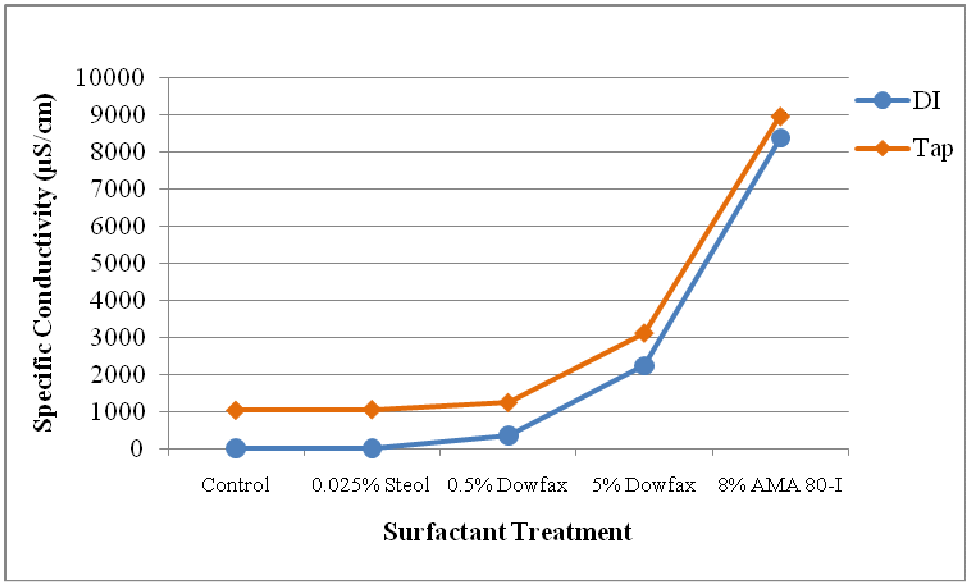

Figure 63. Plot of Specific Conductivity versus Surfactant Treatment. Data in blue represents the untransformed specific conductivity values of DI solutions. The data in orange represent the tap solutions.

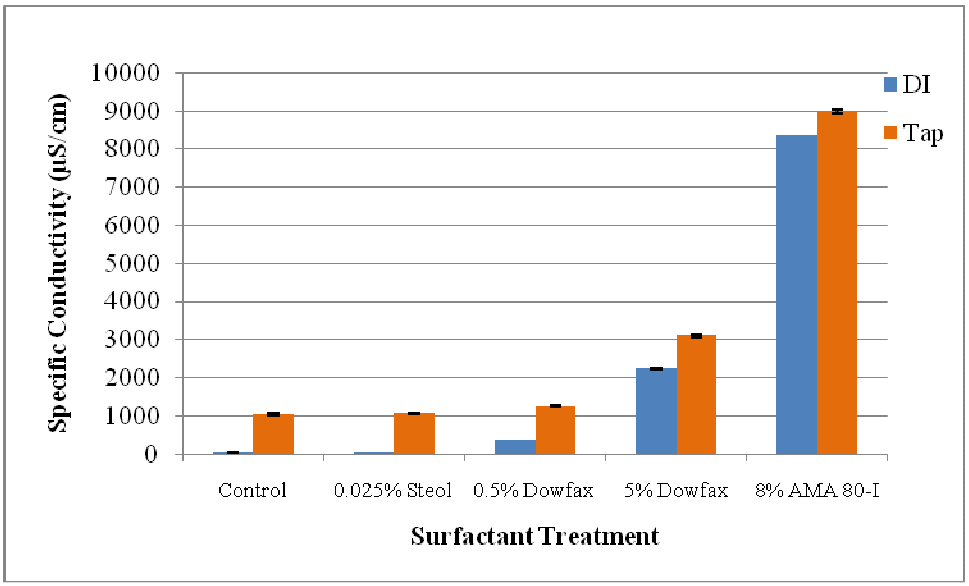

Figure 64. Bar graph of specific conductivity. The bar represents the median value, while the upper error bar is the treatment's maximum, and the lower error bar is the minimum.

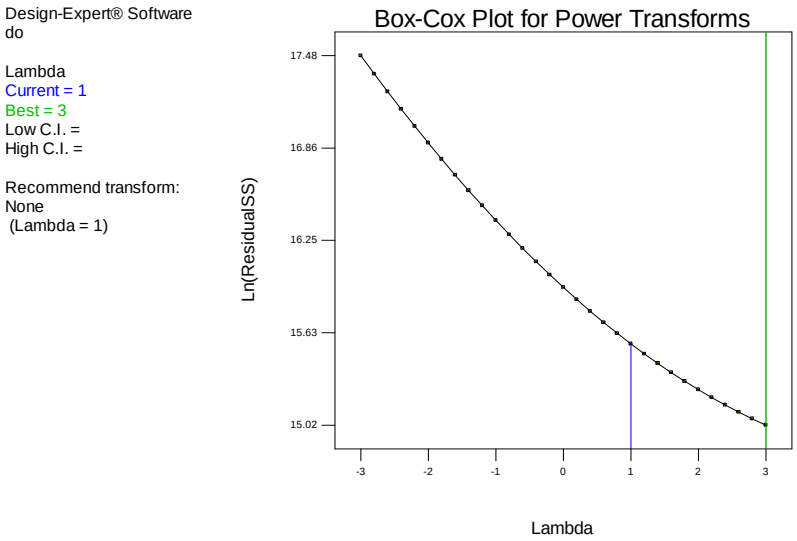

Figure 65. Box-Cox Plot of Dissolved Oxygen. This plot indicates a transform of the dissolved oxygen is unlikely to aid in minimizing and stabilizing the data residuals**.**

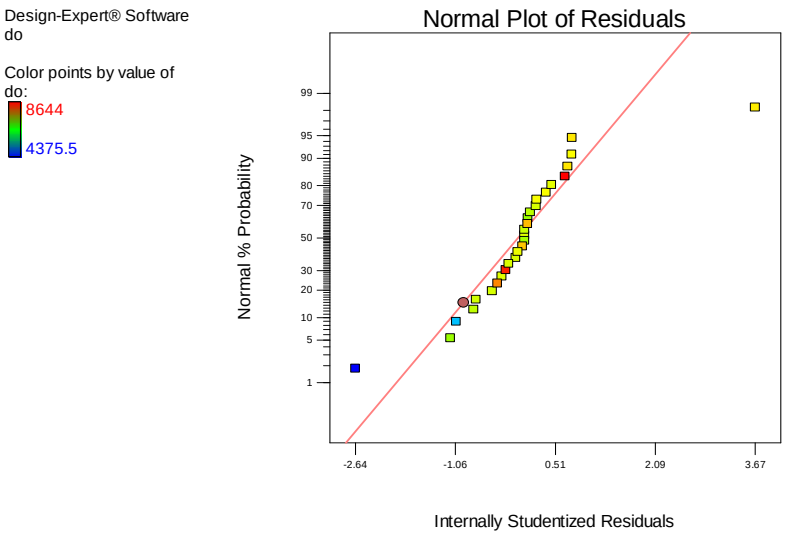

Figure 66. Scatter plot of residuals versus the normal percent probability of dissolved oxygen. To verify the normality assumption, this plot should show a close fit of the residuals to the red straight line. An indication of poor normality would be an "S" shape. This plot does not appear to verify the normality assumption.

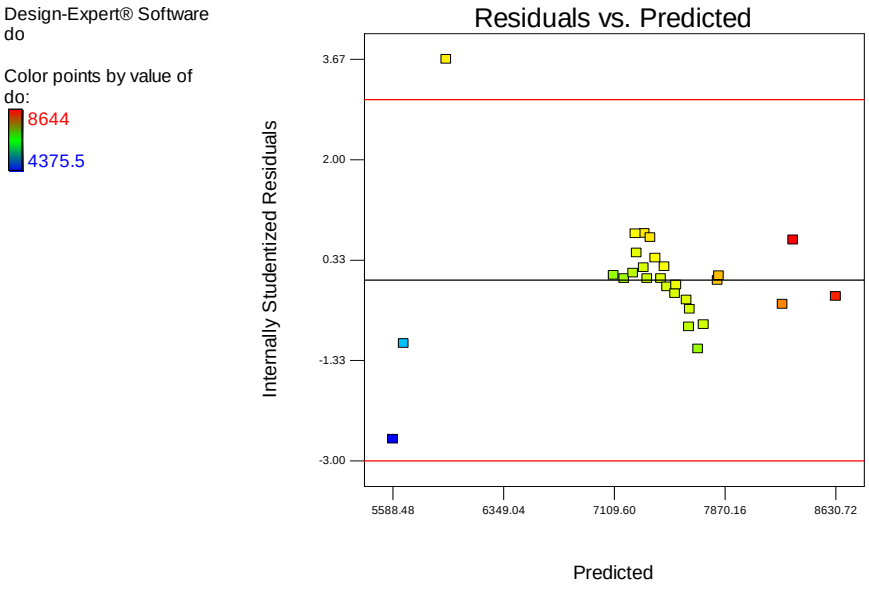

Figure 67. Scatter plot of internally studentized residuals versus the predicted dissolved oxygen. This plot should show random scatter, indicating that the variance is constant over the predicted range. While the high predicted values appear to have randomly scatter residuals, the low predicted values have a much larger range. This may correspond to the anomalously low measured dissolved oxygen values in the 0.025% Steol, tap experimental treatment.

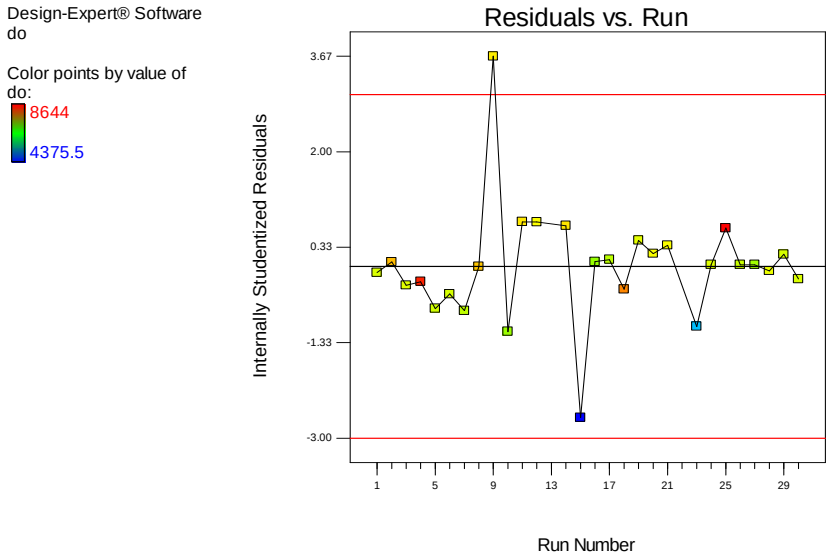

Figure 68. Scatter plot of internally studentized residuals versus run number. Residual values below ±3.00 indicate that the proposed model of dissolved is fair. Random scatter indicates that variance is constant over all runs with no apparent trends. Run #9 lies outside of the confidence interval, which corresponds to a 0.025% Steol, tap treatment DO value that is much higher than other similar treatments.

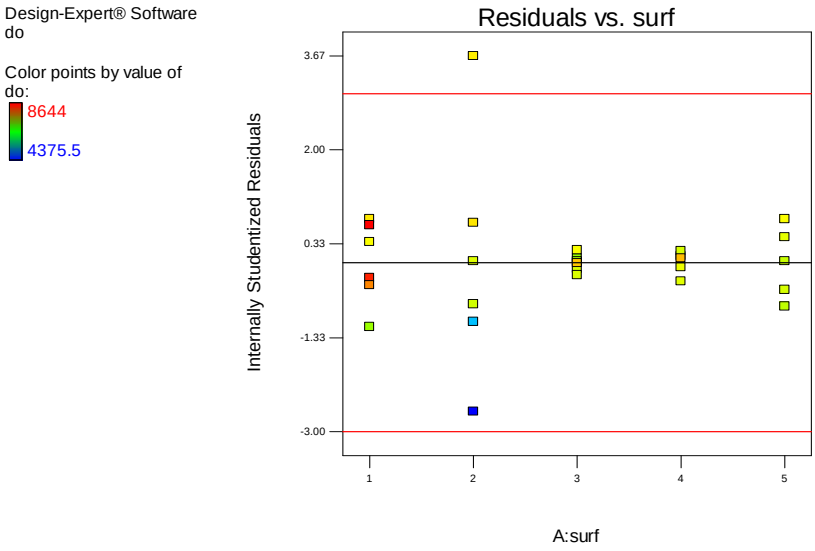

Figure 69. Plot of residuals by surfactant type and concentration. This plot should show fairly consistent range across the 5 surfactant treatments. With the exception of Run #9 and Run #15, both corresponding to 0.025% Steol, the overall fit of the data is good.

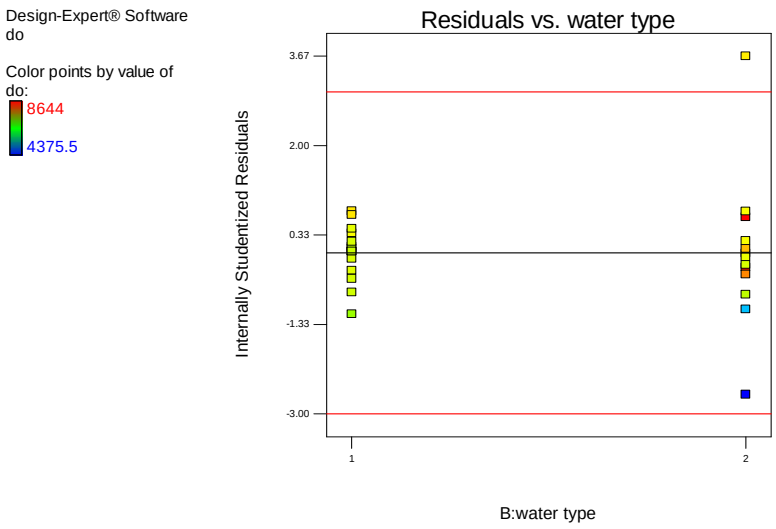

Figure 70. Plot of residuals by water type. This plot should show fairly consistent residual range across the two water types. With the exception of Run #9 and Run #15, both in tap water (type 2), the overall fit of the data is good.

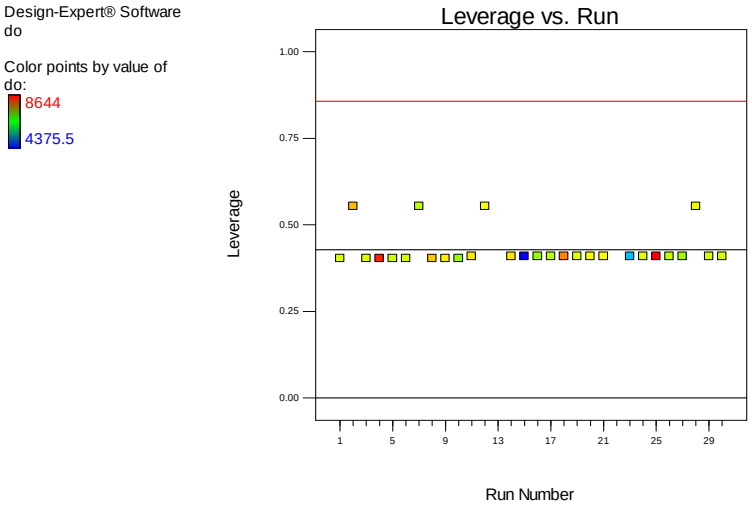

Figure 71. Leverage versus Run Number in Dissolved Oxygen. Leverage values at or above 2 times the leverage average may unduly influence at least one model parameter. The dissolved oxygen plot does not appear to show any points with exceptional leverage.

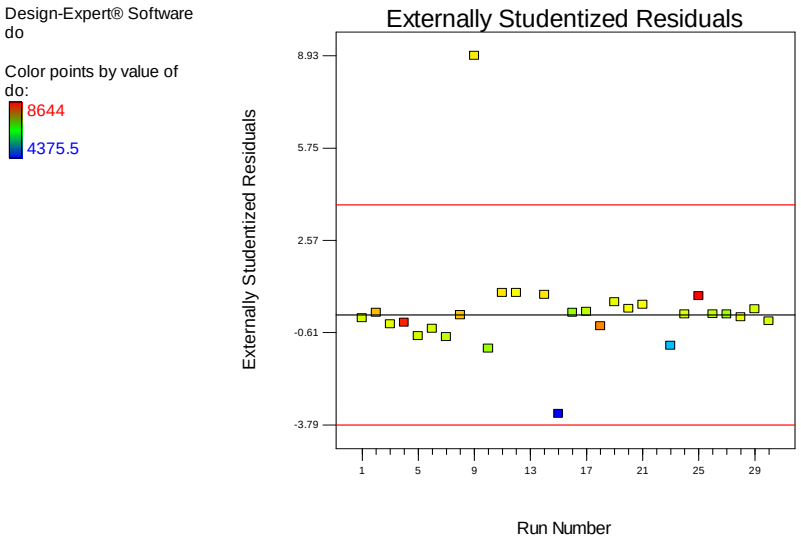

Figure 72. Externally Studentized Residuals versus Run Number of Dissolved Oxygen. This plot is used to indicate whether data falls inside of the 95% confidence interval (t-test). Run 9, corresponding to 0.025% Steol, tap, is well outside of the confidence interval.

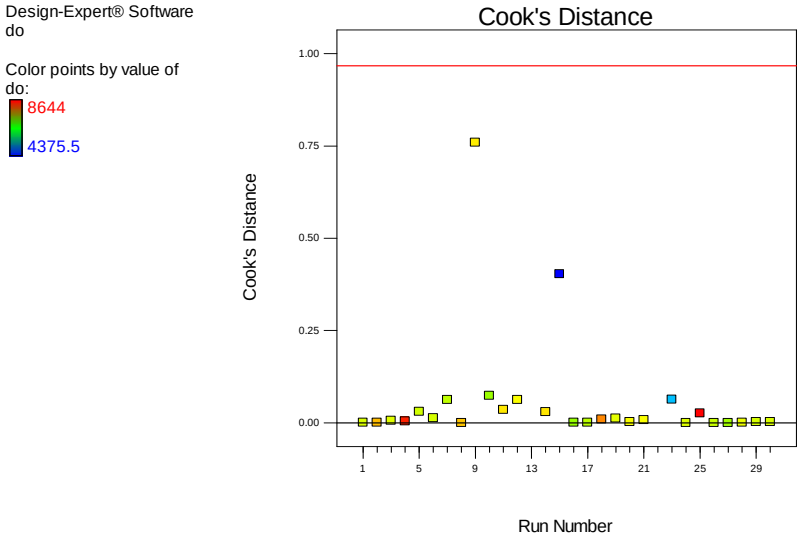

Figure 73. Cook's Distance of Dissolved Oxygen. It is a measure of how much the estimated parameter, in this case dissolved oxygen, would change if a particular run was omitted, and can be used to identify potential outliers. This plot, as in the t-test, identifies Run 9 as being a potential outlier. The Cook's D is not sufficiently high to omit from analyses. Run 9 corresponds to 0.025% Steol, tap.

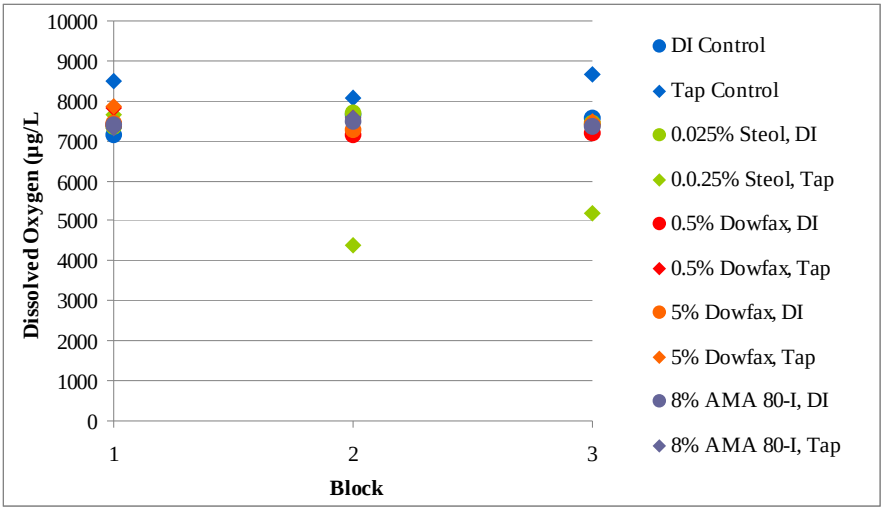

Figure 74. Plot of dissolved oxygen by block. Plot indicates that there is significant overlap among treatments. The tap control is consistently higher than the other treatments over all three runs, while the 0.025% Steol, tap treatment is substantially lower in blocks 2 and 3 than in block 1.

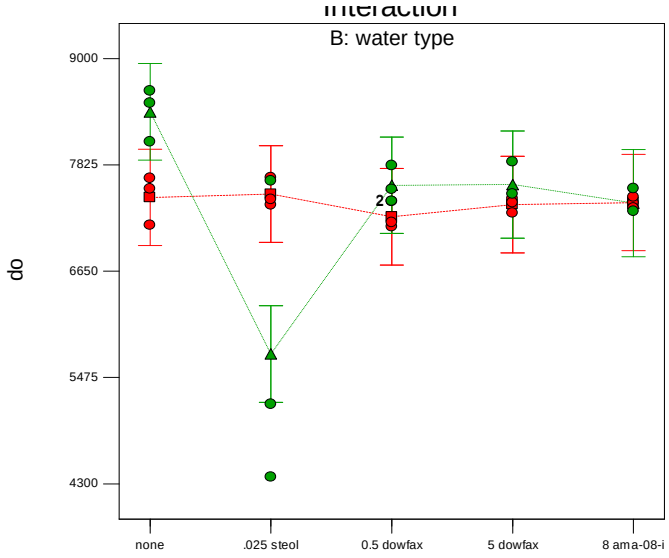

Figure 75. Plot of the modeled and measured dissolved oxygen. The green triangles and error bars connected with a dotted line represent the modeled dissolved oxygen in tap water solutions. The green circles represent the measured data. The red square and error bars connected with a dashed line represent the modeled dissolved oxygen in DI solutions. The red circles represent the measured data.

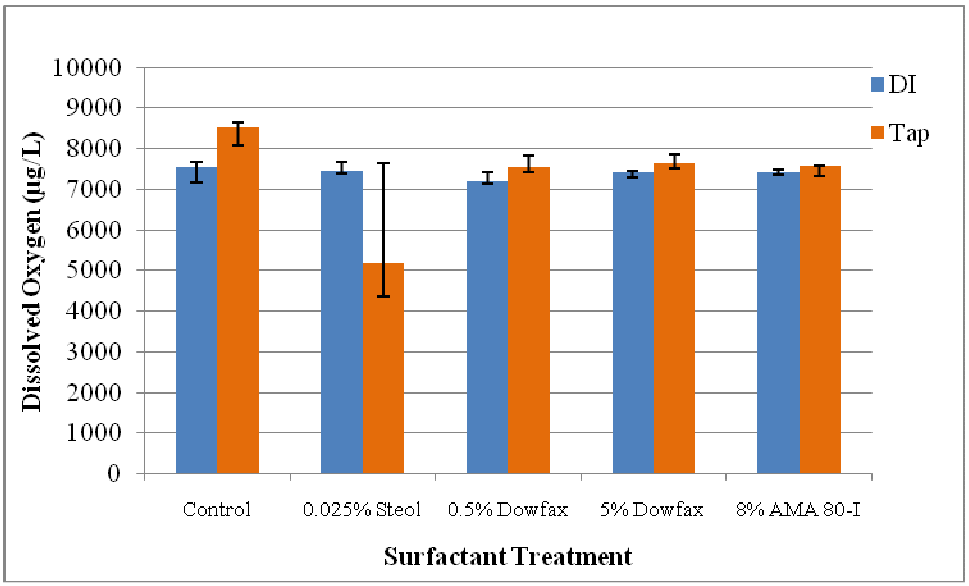

Figure 76. Bar graph of measured dissolved oxygen responses. The bar represents the median value, while the upper error bar is the treatment's maximum, and the lower error bar is the minimum.

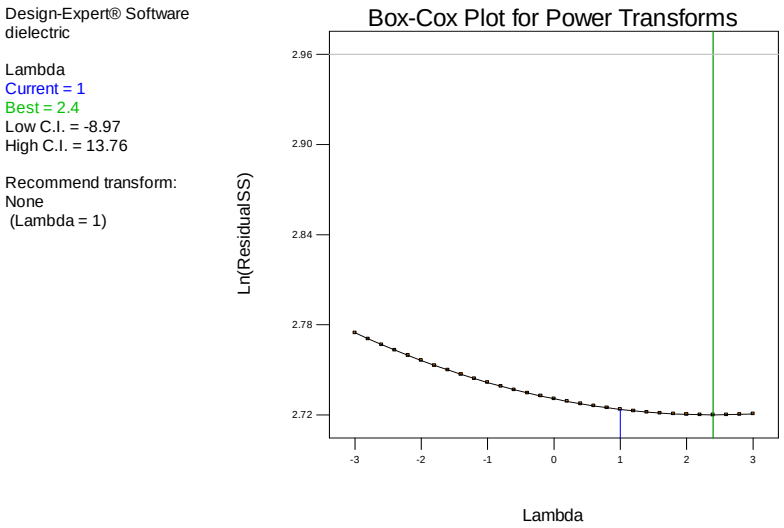

Figure 77. Box-Cox Plot of Dielectric Constant. This plot indicates a transform of the dielectric constant is unlikely to aid in minimizing and stabilizing the data residuals**.**

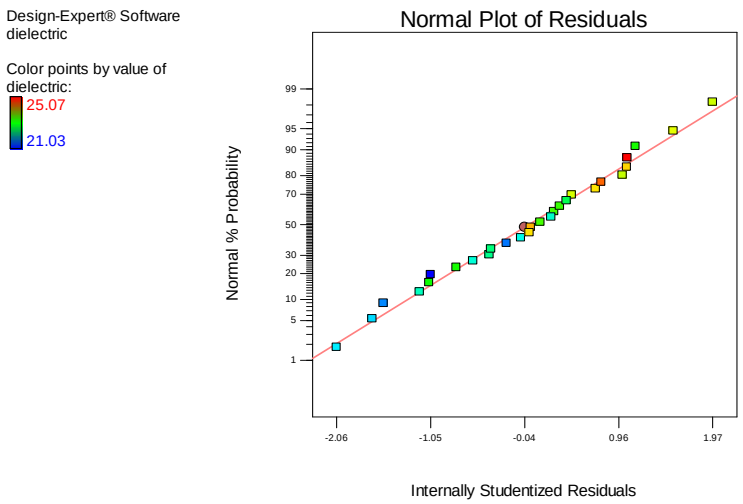

Figure 78. Scatter plot of residuals versus the normal percent probability of dielectric constant. To verify the normality assumption, this plot should show a close fit of the residuals to the red straight line. An indication of poor normality would be an "S" shape. This plot appears to verify the normality assumption.

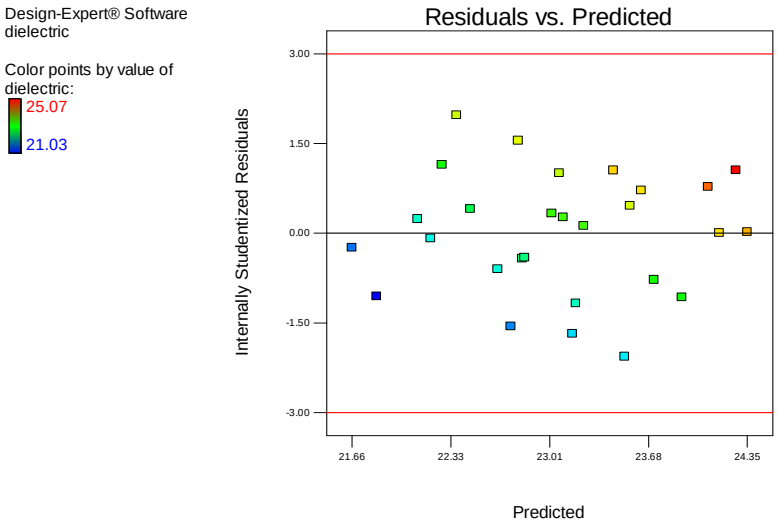

Figure 79. Scatter plot of internally studentized residuals versus the predicted dielectric constant. This plot should show random scatter, indicating that the variance is constant over the predicted range. There do not appear to be any trends in the residuals.

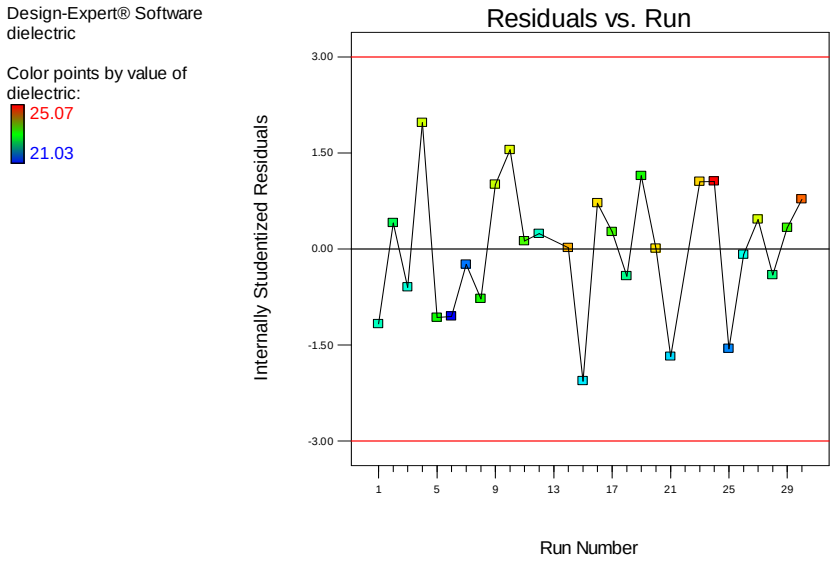

Figure 80. Scatter plot of internally studentized residuals versus run number. Residual values below ±3.00 indicate that the proposed model of dissolved is fairly good. Random scatter indicates that the variance is constant over all runs with no trends between residual and run number. All of the runs lie within the confidence interval, and there do not appear to be any trends in the residuals based on run order.

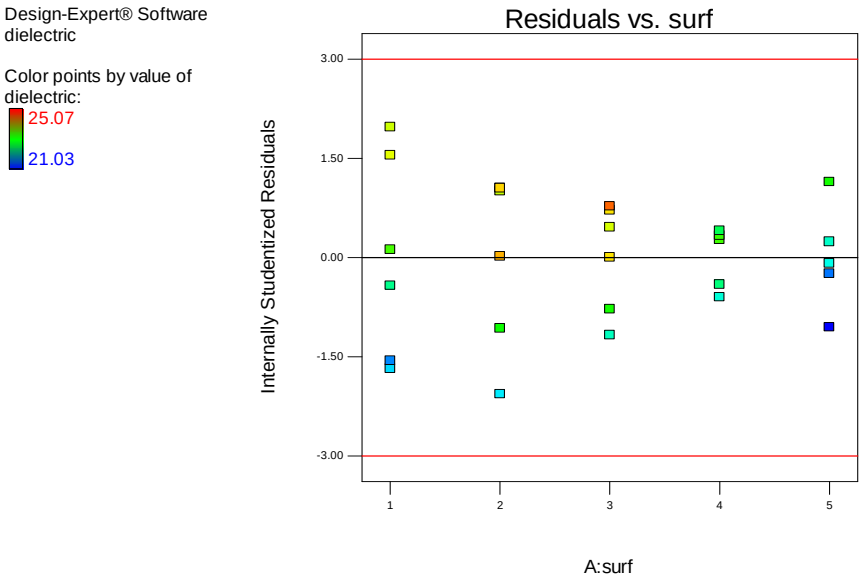

Figure 81. Plot of residuals by surfactant type and concentration. This plot should show fairly consistent range across the 5 surfactants. The overall fit is good, although the 5.0% Dowfax treatment has a much smaller range than the other surfactants.

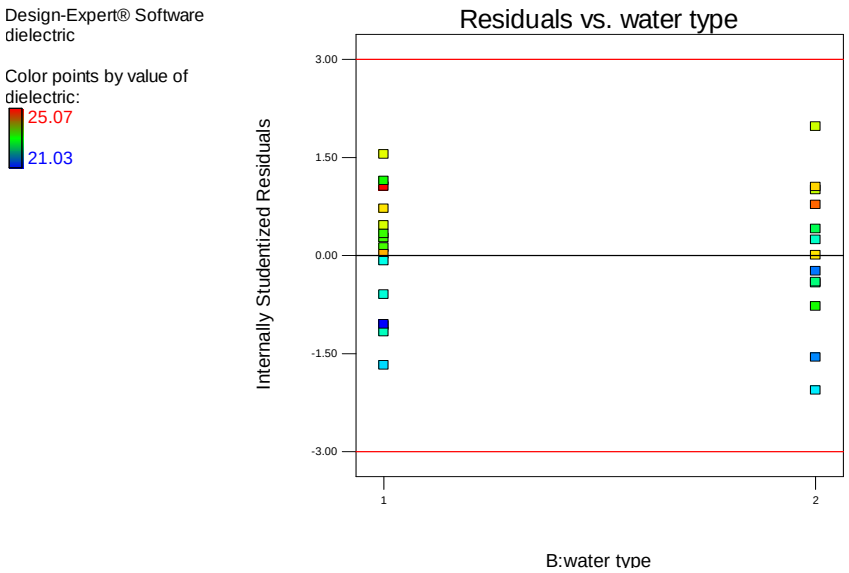

Figure 82. Plot of residuals by water type. This plot should show fairly consistent range in residuals between the two water types. Type 1 is DI; Type 2 is tap water. The overall fit of the data is good.

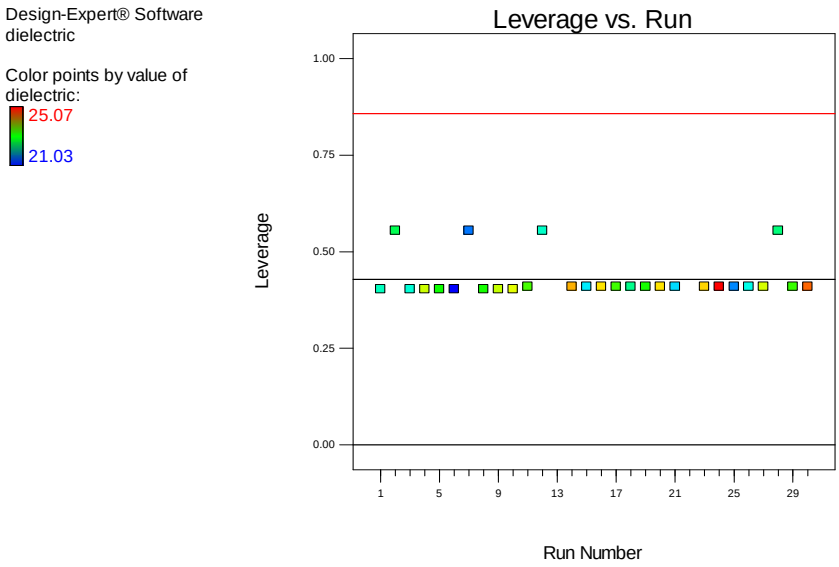

Figure 83. Leverage versus Run Number in Dielectric Constant. Leverage values at or above 2 times the leverage average may unduly influence at least one model parameter. The dielectric constant plot does not appear to show any points with exceptional leverage.

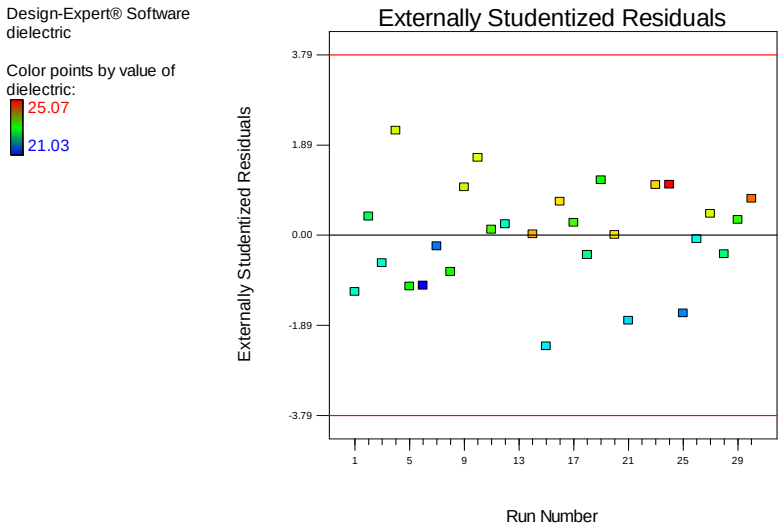

Figure 84. Externally Studentized Residuals versus Run Number in Dielectric Constant. This plot is used to indicate whether data falls inside of the 95% confidence interval (t-test). All data points lie within the confidence interval.

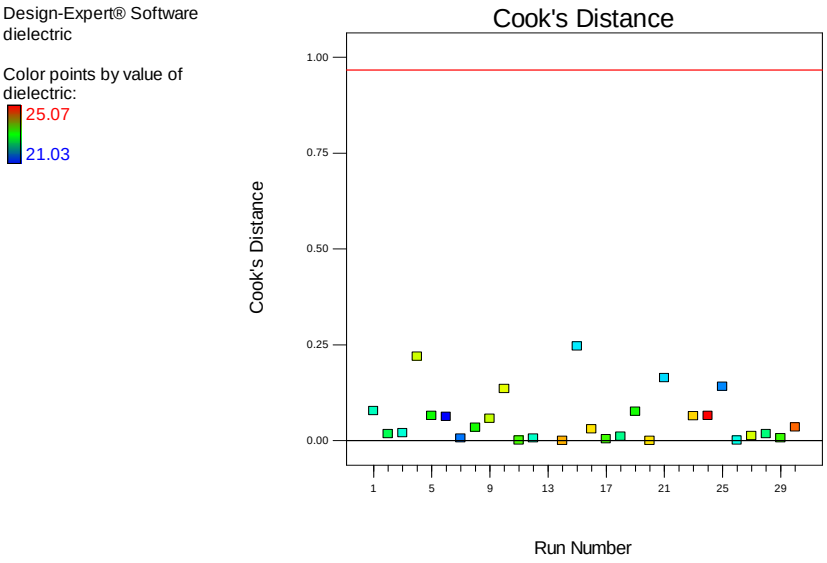

Figure 85. Cook's Distance of Dielectric Constant. It is a measure of how much the estimated parameter, in this case dielectric constant, would change if a particular run was omitted, and can be used to identify potential outliers. This plot does not appear to identify any potential outliers.

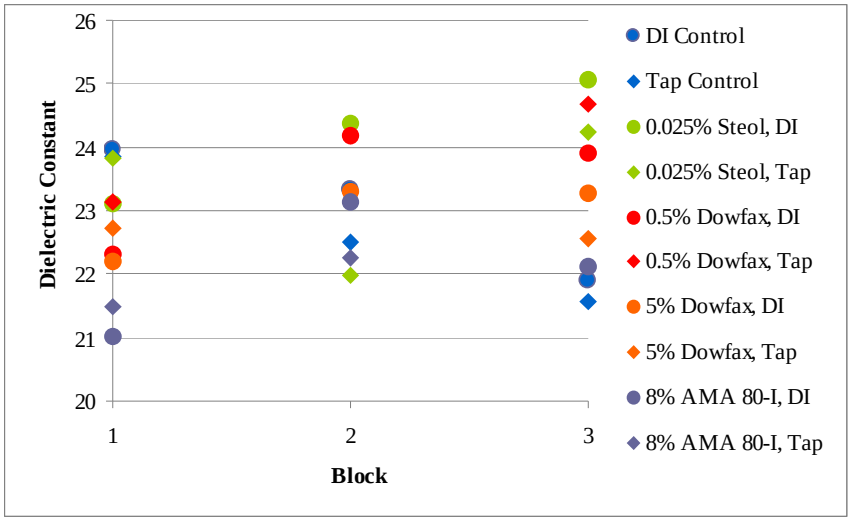

Figure 86. Plot of dielectric constant values by block and surfactant treatment. The plot indicates that dielectric constant value in an individual surfactant treatment is inconsistent across runs. There is also substantial overlap among all treatments.

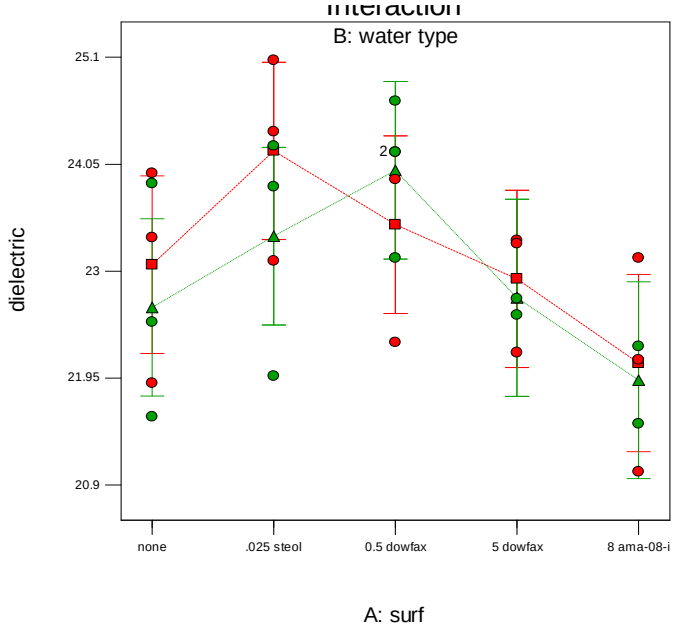

Figure 87. Plot of the modeled and measured dielectric constant. The green triangles and error bars connected with a dotted line represent the modeled dielectric constant in tap water solutions. The green circles represent the measured data. The red square and error bars connected with a dashed line represent the modeled dielectric constant in DI solutions. The red circles represent the measured data.

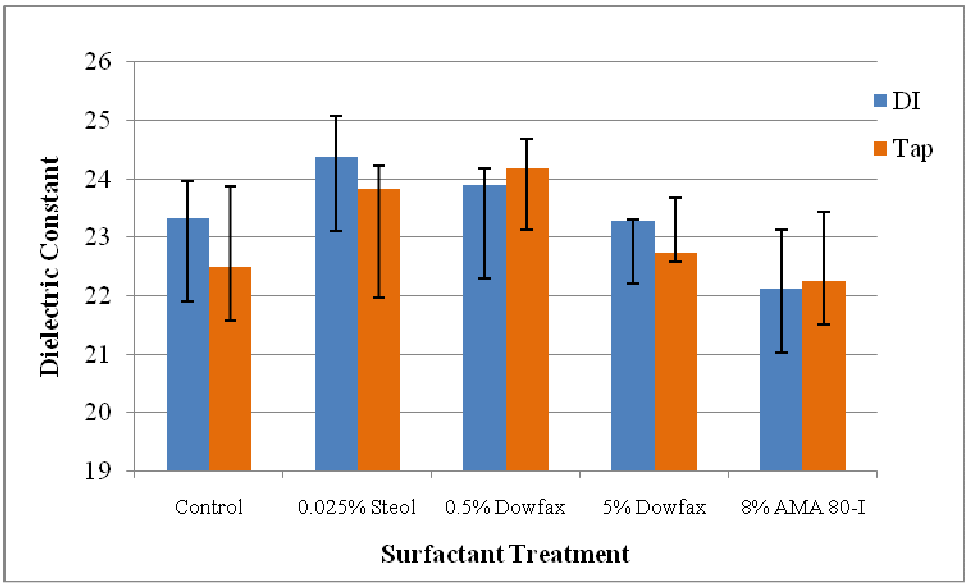

Figure 88. Bar graph of measured dielectric constant values. The bar represents the median value, while the upper error bar is the treatment's maximum, and the lower error bar is the minimum.

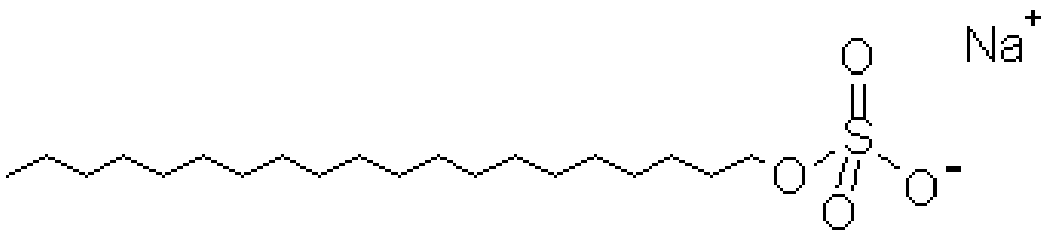

Figure 89. Molecular structure of Steol CS-330 (sodium laureth sulfate). Key Centre for Polymer Colloids, University of Sydney, Australia.

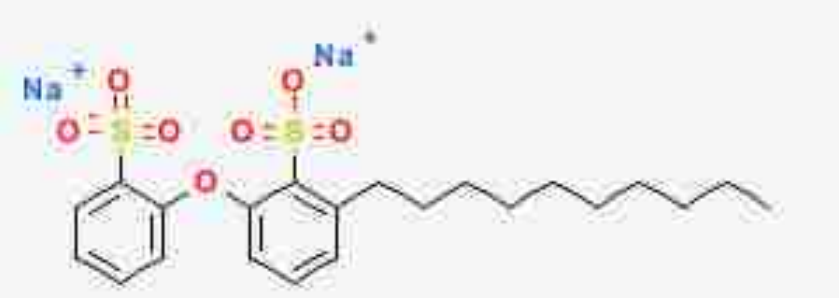

Figure 90. Molecular structure of Dowfax 8390. www.chemicalregister.com

Figure 91. Molecular structure of Aerosol MA 80-I. Key Centre for Polymer Colloids. University of Sydney, Australia.

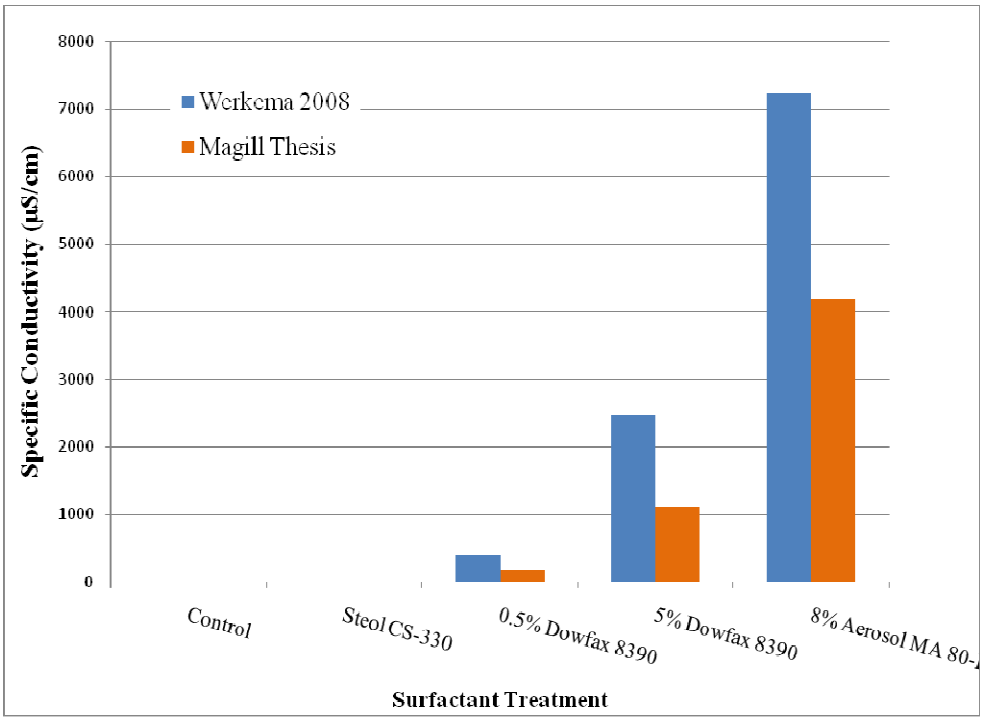

Figure 92. Comparison plot of specific conductivity results in Werkema 2008 and Magill thesis. This graph indicates that specific conductivity trend with respect to surfactant treatment is consistent in both investigations.

APPENDIX A

SYSTEMATIC ERROR RESULTS

Spectral Induced Polarization

Five randomly chosen 18 cm PVC columns were filled with 283.0 ±1.6 g (±0.5%) sand and saturated with 64.4 ±0.72 g (±1.1%) DI water. As eighteen columns were used to perform all of the SIP tests, 27.8% of the columns were tested for systematic error. Spectral induced polarization (SIP) measurements were made over 2 days. The data collected are located in Table 21. All measurements are in µS/cm. Three columns, numbers 9, 2, and 18, were tested on November 10, 2008 and have been examined together. The other two columns, numbers 3 and 16, were tested on November 11, 2008 and so have been examined separately from the first 3. This was done in order to limit error due to daily environmental (i.e. laboratory temperature fluctuations, etc.) changes and instrument drift.

Averages and standard deviations of the data are located in Table 22. Two separate averages were calculated to eliminate the daily variability. Columns 9, 2, and 18 were averaged together separately from columns 3 and 16. There is variation in both real and imaginary conductivity in the very high end of the frequency spectrum. The variability lessens at 187 Hz and lower frequencies. This is important as the range of interest is between 93.75 and 0.366 Hz. The real conductivity variation at 11.7 Hz, the frequency analyzed in this research, is ±5.1% from the average. This was determined by calculating the percent error of the measured real conductivity values of each column relative to the average real conductivity value (Eqn 17). This was done separately for each day's measurements.

$$PE = \frac{\sigma'_{avg} - \sigma'_{act}}{\sigma'_{avg}} * 100 \quad (17)$$

This equation describes the method for calculating the percent error. PE is the percent error, σ'_{avg} is the average real conductivity, and σ'_{act} is the actual real conductivity. In addition, this equation was modified to calculate the errors associated with imaginary conductivity, dielectric constant, and the water quality measurements.

The largest percent error was then chosen to represent the mean system error. In this case, the mean system error is defined as error attributable to physical differences between columns, packing, water to sand ratios, and instrument drift and error. The imaginary conductivity variation at the same frequency is ±4.6% from the average. The error for imaginary conductivity was calculated in the same manner as real conductivity.

Plotting the real conductivity by frequency for the columns separated per day (Figures 93, 94) shows that all columns have the same general trend, with stable values through the low and middle sections of the frequency range. All columns show a real conductivity drop between 750 and 1500 Hz and continue to fall through the highest frequencies. Similarly, the imaginary conductivity plotted by column number and separated by day (Figure 95, 96) appears to follow a similar trend which lies within the same value range regardless of column number. Columns 9, 2, and 18 show a slightly different shape through the frequency range than columns 3 and 16, but all columns' imaginary response over the measured frequency range are similar in shape to others tested on the same day. This analysis suggest the differences between columns due to the packing method and column preparation results in a mean system error of 5.1% for

real conductivity and 4.6% for imaginary conductivity. This systematic error has not been added to the measured data, but is included as a heading in tables.

The amount of sand and solution added to each column is located in Table 23. Also in this table is the sand to water ratio of each column. This ratio has been plotted against the average measured real conductivity (Figure 97) and imaginary conductivity (Figure 98) to identify any related trends. There do not appear to be any clear relationships between the measured real and imaginary conductivity values and the sand to water ratio within the range of ratios.

pH, Specific Conductivity, Dissolved Oxygen

Four randomly chosen 18cm PVC columns were filled with 283.0 ±1.6 g (±0.5%) sand and saturated with 64.4 ±0.72 g (±1.1%) tap water. In total, fifteen different columns were used for water quality measurements. As such, 26.7% of the columns were tested for systematic error. pH, specific conductivity, and dissolved oxygen measurements were made using the In-Situ, Inc.'s Troll 9500 multi-parameter water quality monitoring instrument. The data, collected over 3 days, are located in Table 24.

Over the measured time ranges, temperature, pH, conductivity, and saturated RDO (Rugged Dissolved Oxygen) were averaged within each different column to yield a percent change in each parameter. Each parameter's data range and the largest calculated percent change follow. Temperature overall ranges from 22.60 to 26.68ºC. Within each column, the largest percent difference in temperature was ±11.8%. pH measurements ranged between 7.53 and 8.13, with a maximum percent difference of ±0.37%. Specific conductivity measurements ranged between 128.4 and 534.6 µS/cm, with a maximum

percent difference of ±10.1%. DO measurements ranged from 6619 to 7794 µg/L, with a maximum percent difference of ±4.3%.

The combined calculations (Table 25), display differences among columns in the conductivity, DO, and saturated DO parameters. These differences are most likely due to laboratory temperature or other environmental differences in the laboratory as the experiments were run on 3 separate days. Columns 2 and 3 were run on the same day, followed by column 16 the next day, and column 18 the day after. Additional specific conductivity measurements were made using an Accumet 4-electrode specific conductivity probe as a quality check for the Troll 9500. The readings made with this instrument corroborated the differences in conductivity among the columns, suggesting that the specific conductivity value of the tap water was not consistent for the entirety of the systematic error tests.

Dielectric Constant

Systematic error tests were performed on the TDR apparatus and four columns. A sand mass of 8535 ±218 g (±2.5%) was loaded into each column. The column was saturated with 1863 ±100 mL (±5.4%) of DI water by gravity feed infiltration through the bottom of the column (Figure 12). Six dielectric constant measurements were made on each column in two groups of three. The first set was collected immediately upon saturation, with the second set following ten minutes later. All systematic error testing of time domain reflectometry was performed on November 8, 2009. In total, five columns were used in the TDR tests, resulting in systematic error testing of 80% of the columns.

The measured dielectric constant values are located in Table 25. The values are separated by column, and from there into readings. Overall, the first readings appear to be slightly higher than the second set of readings across all four columns, although there is overlap between the two sets. In addition, standard deviations of readings, both within a column and among the columns, are small.

The amount of sand and solution added to each column is located in Table 26. Also in this table is the sand to water ratio of each column. This ratio has been plotted against the average dielectric constant measured to identify any related trends (Figure 99). There do not appear to be any clear relationship between the measured dielectric constants and the sand to water ratio, although the ratio range measured is small.

Based on the dielectric constants measured during the systematic error tests, the physical differences between columns should not contribute substantially to the water quality responses. However, the percent error in the sand to water ratio is ±5.5%, while the maximum percent error of measured dielectric values is ±3.6%. It is possible that the ratio, related to packing error, could account for the majority of error in the dielectric constant measurements.

Table 21. Systematic error tests for SIP response. Data is reported in µS/cm.

Date of test	11/10/2009		11/10/2009		11/10/2009		11/11/2009		11/11/2009	
	Column #9		Column #2		Column #18		Column #16		Column #3	
Frequency (Hz)	**Real**	**Imaginary**	**Real**	**Imaginary**	**Real**	**Imaginary**	**Real**	**Imaginary**	**Real**	**Imaginary**
12000	3.82	3.820	13.35	3.405	1.21	4.367	-16.33	2.976	6.71	2.225
6000	14.46	1.905	15.75	1.731	-9.18	2.212	-8.46	1.459	-12.9	1.166
3000	-15.70	0.967	-16.72	0.896	-5.60	1.130	-13.20	0.791	-4.60	0.559
1500	-2.94	0.497	-0.57	0.470	-9.06	0.580	7.63	0.403	8.70	0.319
750	9.70	0.265	-1485.9	-3198.47	6.37	0.295	15.96	0.215	15.25	0.154
375	14.28	0.142	14.99	0.138	11.97	0.167	18.64	0.111	16.24	0.113
187.5	15.57	0.082	16.38	0.064	14.24	0.081	19.12	0.081	17.06	0.062
93.75	16.07	0.042	16.61	0.041	14.58	0.058	19.35	0.060	17.16	0.049
46.875	16.16	0.028	16.70	0.028	14.86	0.028	19.46	0.046	17.27	0.034
23.4375	16.18	0.021	16.73	0.019	14.91	0.019	19.50	0.040	17.28	0.031
11.71875	16.19	0.018	16.73	0.021	14.90	0.021	19.54	0.030	17.28	0.031
5.859375	16.20	0.015	16.75	0.015	14.93	0.016	19.55	0.028	17.30	0.025
2.929687	16.20	0.014	16.75	0.015	14.96	0.013	19.58	0.024	17.33	0.019
1.464844	16.20	0.013	16.78	0.012	15.01	0.012	19.62	0.019	17.33	0.019
0.732422	16.21	0.011	16.81	0.015	15.10	0.013	19.70	0.014	17.43	0.013
0.366211	16.22	0.012	16.88	0.013	15.26	0.011	19.82	0.013	17.52	0.009
0.183105	16.25	0.011	16.98	0.013	15.51	0.012	20.05	0.011	17.67	0.009
0.091553	16.30	0.014	17.15	0.013	15.85	0.015	20.42	0.008	17.95	0.006

Table 22. Averages and standard deviations of SIP systematic error tests. Calculations combine readings from the five columns. Readings from columns were initially averaged according to day of experiment, and then those averages were used to calculate an overall average.

	Real (µS/cm)		Imaginary (µS/cm)	
Frequency (Hz)	**Average (±5.1%)**	**Stdev**	**Average (±4.6%)**	**Stdev**
12000	5.26	33.23	10.076	2.448
6000	-0.21	41.89	5.084	1.207
3000	-33.49	17.08	2.607	0.638
1500	2.26	22.35	1.361	0.295
750	-863.20	2009.48	-1918.52	4291.510
375	45.66	7.39	0.403	0.070
187.5	49.42	5.44	0.222	0.030
93.75	50.26	5.23	0.150	0.026
46.875	50.67	5.07	0.099	0.023
23.4375	50.76	5.06	0.079	0.028
11.71875	50.78	5.13	0.072	0.017
5.859375	50.84	5.11	0.060	0.018
2.929687	50.89	5.11	0.051	0.014
1.464844	50.97	5.12	0.046	0.011
0.732422	51.15	5.14	0.040	0.005
0.366211	51.42	5.15	0.034	0.005
0.183105	51.87	5.22	0.034	0.004
0.091553	52.59	5.41	0.034	0.011

Table 23. Experimental conditions of SIP systematic error tests.

Column	Sand (g)	Water (mL)	Sand:Water	% Difference
9	282.7	63.7	4.44	-0.97
2	284.6	65.1	4.37	0.54
18	282.4	63.8	4.43	-0.70
16	282	64.2	4.39	0.07
3	283.1	65.1	4.35	1.06

Table 24. Systematic error tests for water quality responses. Percent difference column indicates the largest percent difference from the calculated average of each column. The column labeled "Accumet" refers to conductivity values measured with an Accumet 4-electrode specific conductivity probe.

		0min	15min	30min	45 min	60min	90min	Average	Std Dev	Accumet	% Difference
Column #2 11/16/2009	**T(°C)**	26.22	26.24			26.34	26.47	26.32	0.11		-0.58
	pH	8.00	8.03			8.04	8.03	8.03	0.02		0.31
	σ(µS/cm)	397.1	398.3			388.2	382.7	391.6	7.44	327.0	2.27
	RDO(µg/L)	7351	7347			7030	6998	7181.5	193.86		2.56
	sat RDO(%)	97.3	97.3			93.2	93.2	95.3	2.37		-2.15
Column #3 11/16/2009	**T**	26.57	22.60			26.66	26.68	25.63	1.75		11.81
	pH	8.06	8.05			8.10	8.07	8.07	0.02		-0.37
	σ	179.1	196.3			203.3	207.1	196.5	10.74	106.0	8.83
	RDO	7182	7064			6749	6619	6903.5	228.11		4.12
	sat RDO	95.7	94.2			90.0	88.4	92.1	2.98		3.99
Column #16 11/17/2009	**T**	25.31	25.39	25.47	25.50	25.64		25.46	0.11		-0.70
	pH	8.13	8.12	8.11	8.11	8.10		8.11	0.01		-0.20
	σ	128.4	144.1	147.4	142.1	152.4		142.9	8.04	78.0	10.13
	RDO	7364	7256	7145	7003	6814		7116.4	192.8		4.25
	sat RDO	95.4	94.2	92.9	91.1	88.9		92.5	2.30		3.89
Column #18 11/18/2009	**T**	24.29	24.35	24.37				24.34	0.04		0.19
	pH	7.53	7.56	7.56				7.55	0.02		0.26
	σ	532.9	534.59	531.63				533.0	1.48	479.0	0.26
	RDO	7794	7757	7751				7767.3	23.29		-0.34
	sat RDO	99.4	99.03	99.02				99.2	0.22		-0.25

Table 25. Measured dielectric constant values from TDR systematic error tests. All readings were made on November 8, 2008.

Column	1st Rdg	2nd Rdg	Average	Std Dev	Percent Error
1	24.3	23.7	23.9	0.30	-2.26
	24.1	23.6			
	24.1	23.6			
2	23.3	23.0	23.1	0.17	1.09
	23.0	22.9			
	23.3	23.2			
3	23.7	23.0	23.3	0.39	0.37
	23.5	22.9			
	23.7	22.9			
4	23.4	23.4	23.2	0.34	0.80
	23.4	22.8			
	23.4	22.7			
Average	23.6	23.1	23.4	0.30	
Std Dev	0.37	0.33	0.36	0.09	

Table 26. Experimental conditions of TDR systematic error tests.

Column	Sand (g)	Water (mL)	Sand:Water	Percent Error
1	8493	1960	4.33	5.41
2	8753.6	1820	4.81	-4.99
3	8447.6	1900	4.45	2.95
4	8334.8	1760	4.74	-3.37

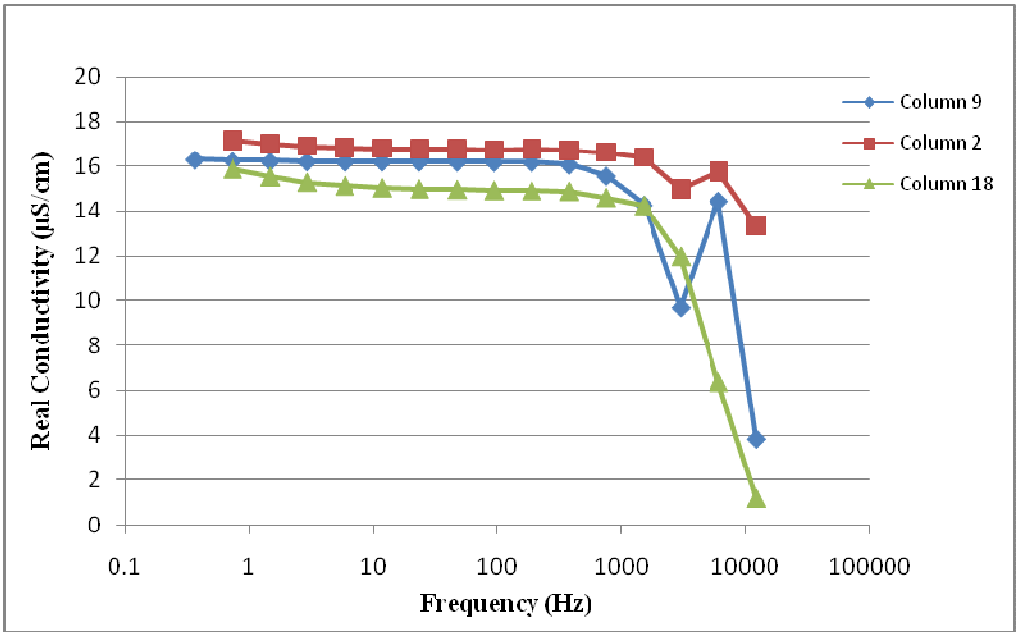

Figure 93. Plot of real conductivities measured during systematic error tests on columns 9, 2, and 18. The columns are listed in the order they were tested, and values show a stable real conductivity reading in the low and medium ranges of the frequency spectrum.

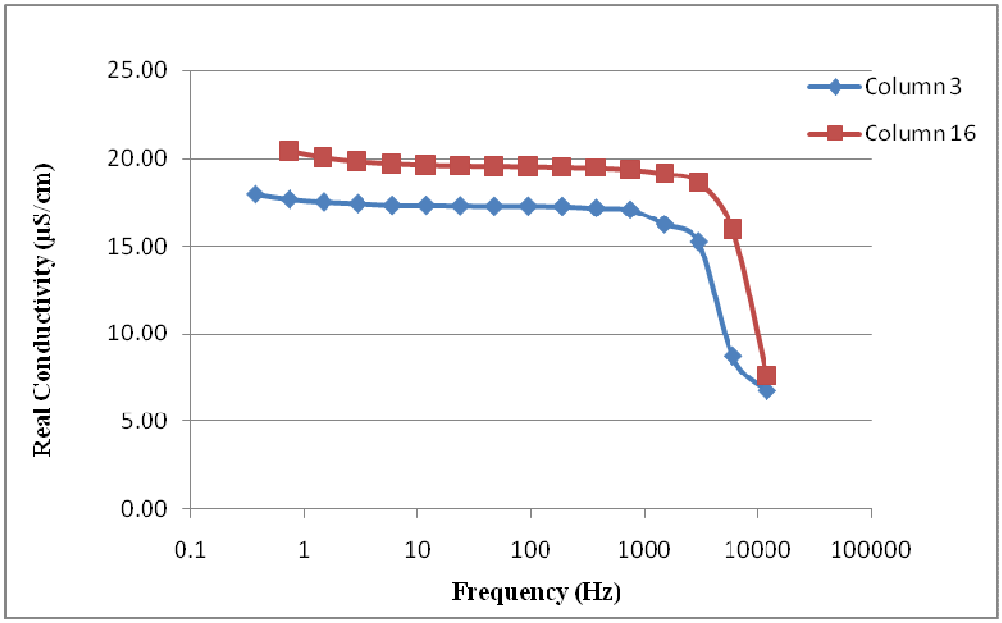

Figure 94. Plot of real conductivities measured during systematic error tests on columns 9, 2, and 18. The columns are listed in the order they were tested, and values show a stable real conductivity reading in the low and medium ranges of the frequency spectrum.

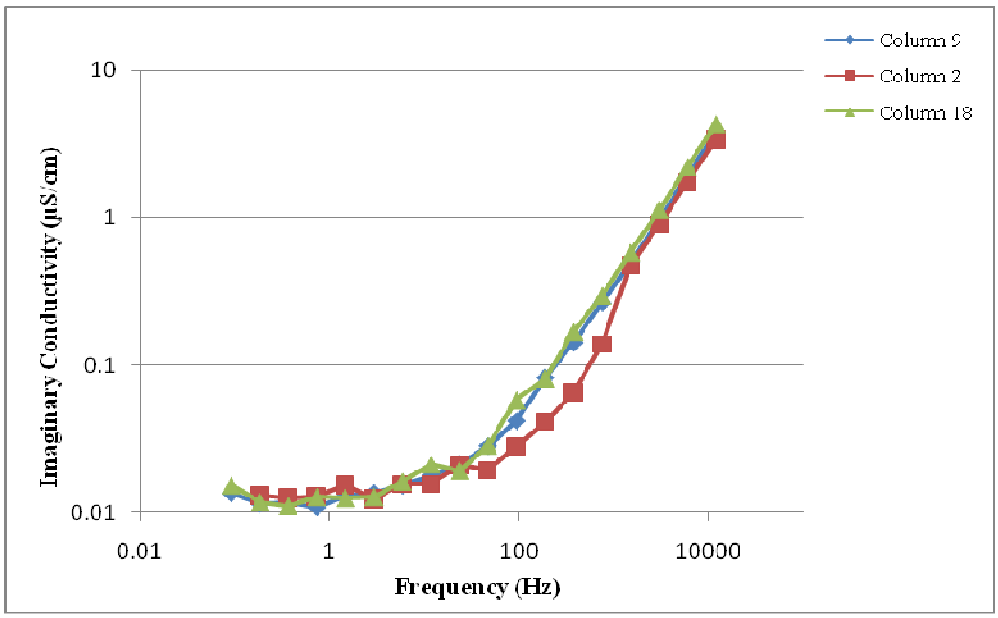

Figure 95. Plot of imaginary conductivities measured during systematic error tests of columns 9, 2, and 18. The columns are listed in the order they were tested. Overall, measurements show a similar trend and value range among different columns, with imaginary conductivity increasing with frequency.

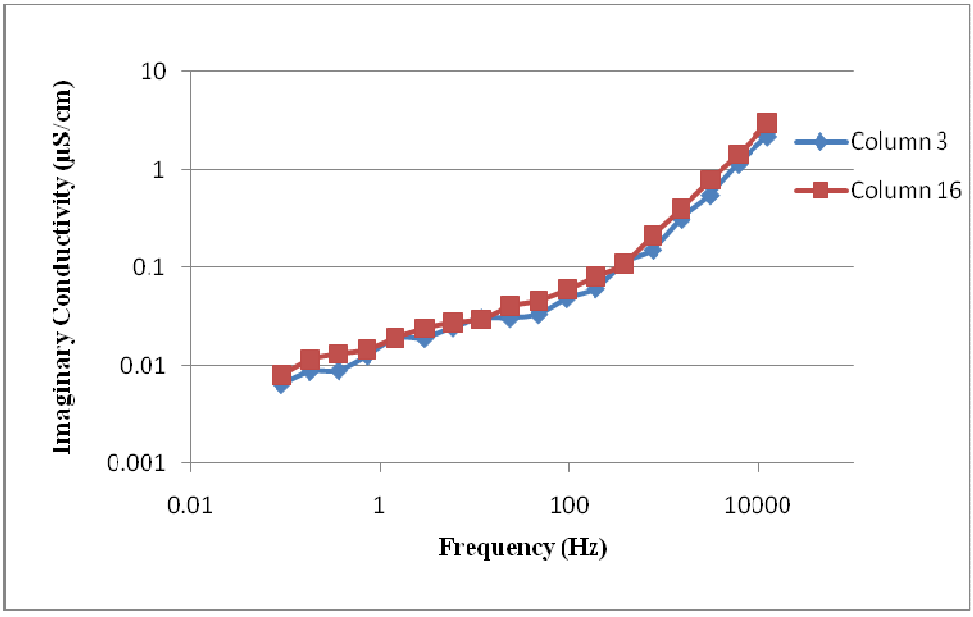

Figure 96. Plot of imaginary conductivities measured during systematic error tests of columns 3 and 16. The columns are listed in the order they were tested. Overall, measurements show a similar trend and value range among different columns, with imaginary conductivity increasing with frequency.

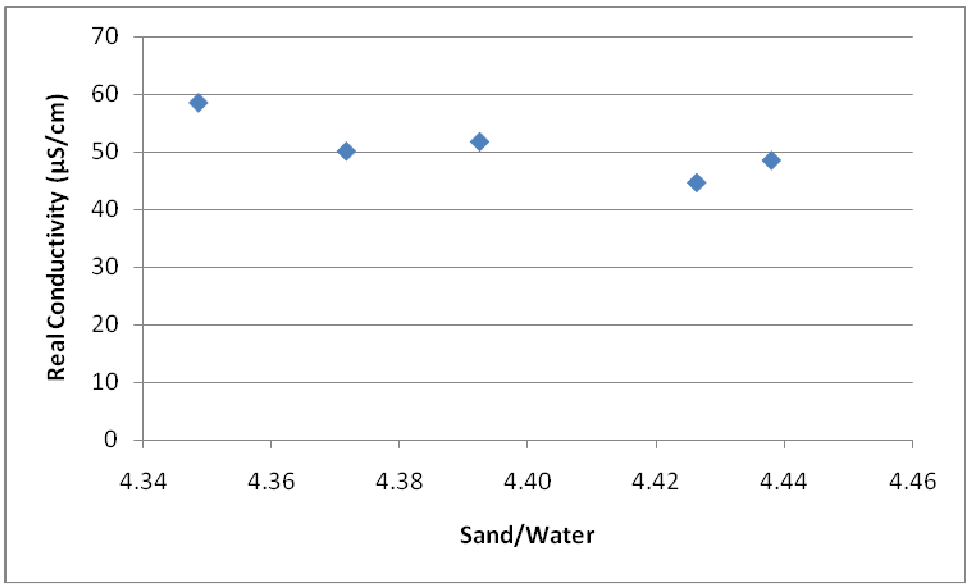

Figure 97. Plot of sand to water ratio and associated real conductivity values. There is a decrease in real conductivity relative with increasing sand. The largest percent difference in real conductivity values in these systematic error tests is 1.06, associated with a water to sand ratio of 4.35.

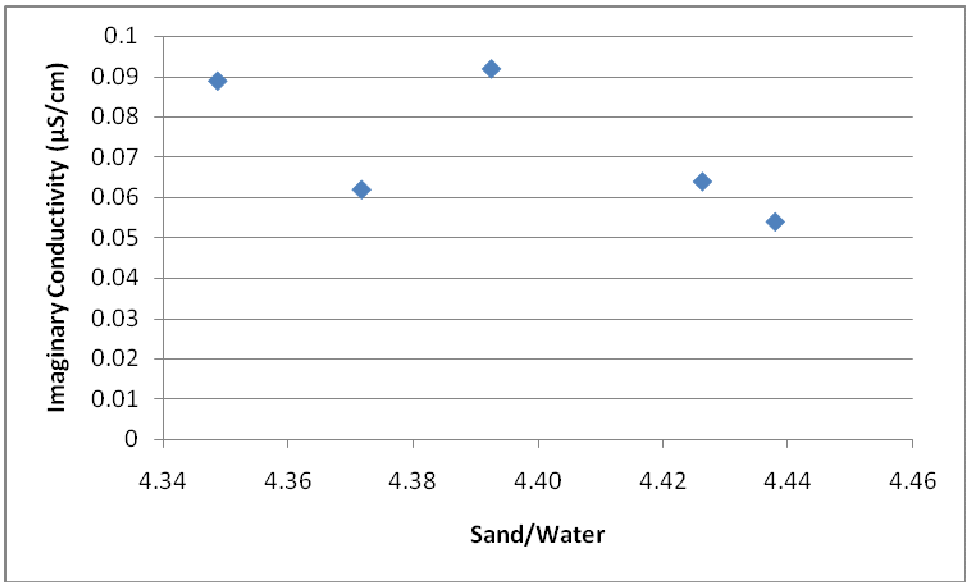

Figure 98. Plot of sand to water ratio and measured imaginary conductivity. There does not appear to be a systematic relationship of the sand to water ratio and imaginary conductivity within this ratio range.

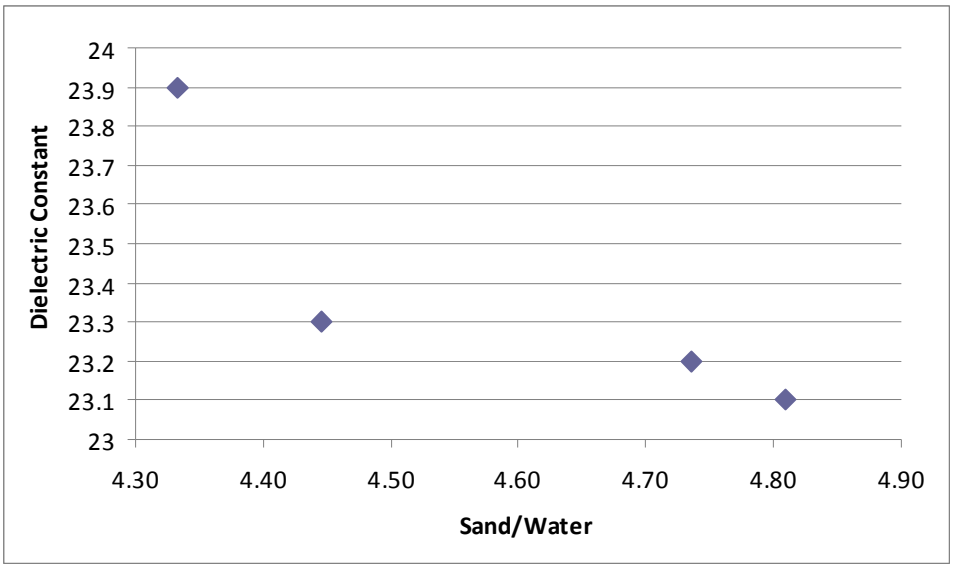

Figure 99. Plot of sand to water ratio and measured dielectric constant. There may be a systematic relationship of the sand to water ratio and dielectric constant within this ratio range. The plot shows a slightly higher dielectric constant response at higher sand to water ratios. It should be noted that the range of the response is only 0.8.

APPENDIX B

RAW DATA

This appendix contains the complete data sets used for each measured parameter. The first 10 tables outline the data from the SIP measurements. They are separated by experimental treatment, with the 5 DI solutions first, followed by the 5 tap solutions. The next tables are the raw data for pH, specific conductivity, dissolved oxygen, and dielectric constant.

Data that is missing from a table, either due to recording error or simple absence of data, is denoted by a hyphen (-). Data in parentheses, as seen in specific conductivity, denotes values measured using a 4-electrode conductivity probe. This data was used as a quality control check and was not included in analysis.

Complete SIP data set for DI control solutions.

No.	Run	Freq./Hz	Resistance (ohm)	Resistivity (ohm-m)	Phase (deg)	Phase (rad)	Phase (mrad)	Real Cond (µS/cm)	Imag Cond (µS/cm)
1	10	12000	49658.46	265.4281	-14.8008	-0.25832	258.3178	-7.7354	3.2081
	10	6000	48487.93	259.1715	-7.17718	-0.12526	125.2633	8.0552	1.6069
	10	3000	48344.26	258.4036	-3.667	-0.064	64.00006	-11.1598	0.8250
	10	1500	48304.24	258.1897	-2.00926	-0.03507	35.06753	-5.4810	0.4526
	10	750	48321.65	258.2827	-1.00801	-0.01759	17.59287	6.8858	0.2270
	10	375	48338.47	258.3726	-0.5668	-0.00989	9.892325	10.8838	0.1276
	10	187.5	48303.97	258.1882	-0.31384	-0.00548	5.477415	12.2799	0.0707
	10	93.75	48372.34	258.5536	-0.18872	-0.00329	3.293748	12.6633	0.0425
	10	46.875	48347.53	258.421	-0.13451	-0.00235	2.347516	12.7823	0.0303
	10	23.4375	48354.05	258.4559	-0.06641	-0.00116	1.159036	12.8687	0.0149
	10	11.71875	48366.52	258.5225	-0.07484	-0.00131	1.306183	12.8577	0.0168
	10	5.859375	48301.68	258.176	-0.06503	-0.00113	1.134899	12.8838	0.0147
	10	2.929687	48207.25	257.6712	-0.07879	-0.00138	1.375035	12.8963	0.0178
	10	1.464844	48022.24	256.6824	-0.06475	-0.00113	1.130064	12.9590	0.0147
	10	0.732422	47688.52	254.8986	-0.06274	-0.00109	1.094914	13.0514	0.0143
	10	0.366211	47146.3	252.0004	-0.06183	-0.00108	1.079084	13.2022	0.0143
	10	0.183105	46385.42	247.9334	-0.05489	-0.00096	0.95796	13.4242	0.0129
	10	0.091553	45461.08	242.9927	-0.06412	-0.00112	1.119104	13.6896	0.0154
2	11	12000	51352.95	274.4852	-21.3072	-0.37187	371.8737	-9.4122	4.4126
	11	6000	50950.16	272.3323	-10.62	-0.18535	185.3508	-4.4897	2.2557
	11	3000	50795.93	271.5079	-5.27639	-0.09209	92.08883	6.5630	1.1290
	11	1500	50733.07	271.1719	-2.66319	-0.04648	46.48067	-10.9123	0.5711
	11	750	50781.27	271.4296	-1.37071	-0.02392	23.92302	2.4408	0.2938

	11	375	50905.14	272.0916	-0.75728	-0.01322	13.21672	8.9028	0.1619
	11	187.5	50897.29	272.0497	-0.39078	-0.00682	6.820196	11.3290	0.0836
	11	93.75	50857.02	271.8344	-0.25405	-0.00443	4.433917	11.8688	0.0544
	11	46.875	50854.4	271.8204	-0.13973	-0.00244	2.43869	12.1435	0.0299
	11	23.4375	50906.4	272.0984	-0.09341	-0.00163	1.630267	12.1971	0.0200
	11	11.71875	50882.3	271.9696	-0.1084	-0.00189	1.891923	12.1843	0.0232
	11	5.859375	50840.03	271.7436	-0.07489	-0.00131	1.30702	12.2321	0.0160
	11	2.929687	50732.78	271.1704	-0.07138	-0.00125	1.245813	12.2611	0.0153
	11	1.464844	50552.96	270.2092	-0.07136	-0.00125	1.245359	12.3047	0.0154
	11	0.732422	50209.05	268.371	-0.06	-0.00105	1.047163	12.3983	0.0130
	11	0.366211	49659.02	265.431	-0.0678	-0.00118	1.183348	12.5293	0.0149
	11	0.183105	48843.39	261.0715	-0.06339	-0.00111	1.106363	12.7423	0.0141
	11	0.091553	47843.18	255.7252	-0.05432	-0.00095	0.947995	13.0156	0.0124
	21	12000	47493.33	253.8553	-17.2814	-0.30161	301.6125	0.0348	3.9007
	21	6000	-39382	-210.5	-9.05279	-0.158	157.9984	14.7523	-2.4916
	21	3000	46634.88	249.2668	-4.36289	-0.07615	76.14543	-4.5792	1.0173
	21	1500	46703.33	249.6327	-2.21759	-0.0387	38.70363	-8.0469	0.5167
	21	750	46696.76	249.5975	-1.21333	-0.02118	21.17616	4.6729	0.2828
	21	375	46732.95	249.791	-0.67331	-0.01175	11.75135	10.4322	0.1568
3	21	187.5	46731.63	249.7839	-0.44541	-0.00777	7.773723	12.0429	0.1037
	21	93.75	46662.72	249.4156	-0.2098	-0.00366	3.66157	13.0715	0.0489
	21	46.875	46686.72	249.5439	-0.15359	-0.00268	2.680589	13.2005	0.0358
	21	23.4375	46683.27	249.5254	-0.08943	-0.00156	1.560804	13.3053	0.0209
	21	11.71875	46702.68	249.6292	-0.10478	-0.00183	1.828673	13.2799	0.0244
	21	5.859375	46668.66	249.4474	-0.06852	-0.0012	1.195862	13.3315	0.0160
	21	2.929687	46593.88	249.0477	-0.0645	-0.00113	1.125736	13.3565	0.0151

	21	1.464844	46426.5	248.153	-0.06313	-0.0011	1.101825	13.4058	0.0148
	21	0.732422	46138.3	246.6125	-0.05835	-0.00102	1.018313	13.4935	0.0138
	21	0.366211	45678.17	244.1531	-0.04551	-0.00079	0.794216	13.6385	0.0108
	21	0.183105	45055.39	240.8243	-0.0714	-0.00125	1.246197	13.8061	0.0172
	21	0.091553	44198.46	236.2439	-0.04737	-0.00083	0.826714	14.0939	0.0117

Complete SIP data set for 0.025% Steol CS-330, DI solutions.

No.	Run	Freq./Hz	Resistance (ohm)	Resistivity (ohm-m)	Phase (deg)	Phase (rad)	Phase (mrad)	Real Cond (µS/cm)	Imag Cond (µS/cm)
1	5	12000	40025.37094	213.9384984	-14.409207	-0.2514839	251.4838898	-4.1865	3.8771
	5	6000	39512.46114	211.1969585	-7.155721	-0.1248888	124.8887986	10.1467	1.9660
	5	3000	39354.18901	210.3509825	-3.599902	-0.0628291	62.82908961	-14.2112	0.9950
	5	1500	39458.50659	210.9085675	-1.885441	-0.0329066	32.90660177	-4.8912	0.5200
	5	750	39490.49173	211.0795304	-0.97691	-0.01705	17.05001023	8.8369	0.2692
	5	375	39575.59904	211.5344351	-0.551163	-0.0096194	9.619447839	13.4244	0.1516
	5	187.5	39496.10156	211.1095153	-0.315311	-0.0055031	5.503122883	15.0112	0.0869
	5	93.75	39532.90441	211.3062292	-0.169556	-0.0029593	2.959260868	15.5487	0.0467
	5	46.875	39532.50879	211.3041146	-0.169891	-0.0029651	2.965107623	15.5479	0.0468
	5	23.4375	39551.81675	211.407317	-0.080707	-0.0014086	1.408579271	15.7160	0.0222
	5	11.71875	39553.76182	211.4177136	-0.081727	-0.0014264	1.426381331	15.7139	0.0225
	5	5.859375	39573.42152	211.5227961	-0.069368	-0.0012107	1.210679704	15.7208	0.0191
	5	2.929687	39578.70989	211.5510628	-0.05988	-0.0010451	1.04508564	15.7284	0.0165
	5	1.464844	39574.6653	211.5294442	-0.061555	-0.0010743	1.074319415	15.7284	0.0169
	5	0.732422	39544.60923	211.3687923	-0.060108	-0.0010491	1.049064924	15.7417	0.0165
	5	0.366211	39480.17793	211.0244024	-0.057148	-0.0009974	0.997404044	15.7702	0.0158
	5	0.183105	39350.22844	210.329813	-0.05586	-0.0009749	0.97492458	15.8234	0.0155
	5	0.091553	39134.41607	209.1762803	-0.049038	-0.0008559	0.855860214	15.9164	0.0136

2	14	12000	42295.96973	226.0750129	-13.963157	-0.243699	243.6989791	2.5527	3.5577
	14	6000	41390.1402	221.2332887	-6.926636	-0.1208906	120.8905781	12.0541	1.8170
	14	3000	41516.70495	221.9097864	-3.524894	-0.06152	61.51997498	-13.9311	0.9235
	14	1500	41558.15759	222.1313537	-1.875861	-0.0327394	32.73940203	-4.5072	0.4912
	14	750	41592.6629	222.3157871	-0.981581	-0.0171315	17.13153319	8.3321	0.2569
	14	375	41731.67887	223.0588375	-0.612613	-0.0106919	10.69193469	12.2262	0.1598
	14	187.5	41561.75053	222.1505582	-0.349233	-0.0060952	6.095163549	14.0991	0.0915
	14	93.75	41667.64944	222.7165956	-0.160879	-0.0028078	2.807821187	14.7734	0.0420
	14	46.875	41583.34325	222.2659729	-0.00865	-0.000151	0.15096845	14.9965	0.0023
	14	23.4375	41695.61893	222.8660945	-0.059276	-0.0010345	1.034544028	14.9304	0.0155
	14	11.71875	41692.22471	222.8479522	-0.058254	-0.0010167	1.016707062	14.9325	0.0152
	14	5.859375	41719.76719	222.9951687	-0.066144	-0.0011544	1.154411232	14.9153	0.0173
	14	2.929687	36085.70536	192.8807013	-64.758329	-1.1302271	1130.227116	-6.0180	15.6316
	14	1.464844	41723.47561	223.0149905	-0.052105	-0.0009094	0.909388565	14.9264	0.0136
	14	0.732422	41690.16248	222.8369294	-0.053594	-0.0009354	0.935376082	14.9371	0.0140
	14	0.366211	41613.50243	222.4271759	-0.048958	-0.0008545	0.854463974	14.9682	0.0128
	14	0.183105	41465.62819	221.6367774	-0.054085	-0.0009439	0.943945505	15.0176	0.0142
	14	0.091553	41207.46254	220.2568634	-0.050813	-0.0008868	0.886839289	15.1143	0.0134
3	24	12000	43380.31157	231.8708984	-17.651809	-0.308077	308.0770225	5.2394	4.3591
	24	6000	42837.22658	228.9680699	-8.743363	-0.1525979	152.5979144	-11.3070	2.2129
	24	3000	42660.03825	228.0209854	-4.318074	-0.0753633	75.36334552	-5.6161	1.1007
	24	1500	42655.70969	227.997849	-2.286889	-0.0399131	39.91307372	-9.5972	0.5834
	24	750	42741.99103	228.459029	-1.231307	-0.02149	21.49000107	4.8587	0.3135
	24	375	42661.89977	228.0309354	-0.594477	-0.0103754	10.37540708	12.1101	0.1517
	24	187.5	42530.78736	227.3301301	-0.250154	-0.0043659	4.365937762	14.2066	0.0640
	24	93.75	42664.53447	228.0450181	-0.171615	-0.0029952	2.995196595	14.4023	0.0438
	24	46.875	42699.97128	228.2344304	-0.139544	-0.0024355	2.435461432	14.4629	0.0356
	24	23.4375	42685.42096	228.1566579	-0.11106	-0.0019383	1.93833018	14.5198	0.0283

	24	11.71875	42660.5607	228.023778	-0.091541	-0.0015977	1.597665073	14.5572	0.0234
	24	5.859375	42616.60626	227.7888383	-0.080384	-0.0014029	1.402941952	14.5862	0.0205
	24	2.929687	42556.73658	227.4688306	-0.063954	-0.0011162	1.116189162	14.6241	0.0164
	24	1.464844	42393.9679	226.5988202	-0.066656	-0.0011633	1.163347168	14.6776	0.0171
	24	0.732422	42102.20038	225.0393017	-0.050355	-0.0008788	0.878845815	14.7935	0.0130
	24	0.366211	41644.54234	222.5930865	-0.060403	-0.0010542	1.054213559	14.9477	0.0158
	24	0.183105	40932.58287	218.7876117	-0.048342	-0.0008437	0.843712926	15.2177	0.0129
	24	0.091553	40052.03726	214.0810318	-0.053137	-0.0009274	0.927400061	15.5485	0.0144

Complete SIP data set for 0.5% Dowfax 8390, DI solutions.

No.	Run	Freq./Hz	Resistance (ohm)	Resistivity (ohm-m)	Phase (deg)	Phase (rad)	Phase (mrad)	Real Cond (µS/cm)	Imag Cond (µS/cm)
	1	12000	7639.887112	40.83574838	-2.527112	-0.0441057	44.10568574	-66.6959	3.5991
	1	6000	7598.780192	40.61602893	-1.270714	-0.0221778	22.17777144	24.2596	1.8200
	1	3000	7593.487768	40.58774054	-0.671071	-0.0117122	11.71220216	64.3180	0.9619
	1	1500	7595.313781	40.59750071	-0.358215	-0.0062519	6.251926395	76.8951	0.5133
	1	750	7594.166339	40.59136755	-0.186461	-0.0032543	3.254303833	80.6958	0.2672
	1	375	7600.310673	40.62420946	-0.110626	-0.0019308	1.930755578	81.5513	0.1584
	1	187.5	7597.242229	40.6078084	-0.066879	-0.0011672	1.167239187	81.9025	0.0958
1	1	93.75	7599.004791	40.61722942	-0.034494	-0.000602	0.602023782	82.0182	0.0494
	1	46.875	7599.92798	40.62216394	-0.022426	-0.0003914	0.391400978	82.0364	0.0321
	1	23.4375	7600.000953	40.62255398	-0.019469	-0.0003398	0.339792457	82.0407	0.0279
	1	11.71875	7600.716536	40.62637883	-0.007965	-0.000139	0.139013145	82.0459	0.0114
	1	5.859375	7600.154687	40.6233757	-0.006991	-0.000122	0.122013923	82.0526	0.0100
	1	2.929687	7599.057451	40.6175109	-0.006233	-0.0001088	0.108784549	82.0648	0.0089
	1	1.464844	7596.722834	40.6050322	-0.004038	-7.048E-05	0.070475214	82.0910	0.0058
	1	0.732422	7592.48449	40.58237795	-0.003875	-6.763E-05	0.067630375	82.1368	0.0056

	1	0.366211	7586.201407	40.54879441	-0.002846	-4.967E-05	0.049671238	82.2052	0.0041
	1	0.183105	7577.113796	40.50022048	-0.003186	-5.561E-05	0.055605258	82.3037	0.0046
	1	0.091553	7567.905627	40.45100215	-0.006446	-0.0001125	0.112502038	82.4025	0.0093
2	16	12000	7245.246363	38.72636508	-2.278996	-0.0397753	39.77531719	-55.9883	3.4227
	16	6000	7209.772325	38.53675378	-1.184086	-0.0206659	20.66585296	32.6220	1.7874
	16	3000	7191.698624	38.44014855	-0.596765	-0.0104153	10.41533955	71.7269	0.9031
	16	1500	7191.563219	38.4394248	-0.329726	-0.0057547	5.754707878	82.0452	0.4990
	16	750	7194.124106	38.45311292	-0.180955	-0.0031582	3.158207615	85.2703	0.2738
	16	375	7193.653104	38.45059538	-0.100113	-0.0017473	1.747272189	86.2573	0.1515
	16	187.5	7197.012059	38.46854924	-0.054896	-0.0009581	0.958099888	86.5203	0.0830
	16	93.75	7194.445609	38.45483138	-0.03382	-0.0005903	0.59026046	86.6322	0.0512
	16	46.875	7196.784047	38.4673305	-0.02244	-0.0003916	0.39164532	86.6318	0.0339
	16	23.4375	7195.538424	38.46067255	-0.01484	-0.000259	0.25900252	86.6591	0.0224
	16	11.71875	7196.041859	38.46336345	-0.012333	-0.0002152	0.215247849	86.6560	0.0187
	16	5.859375	7193.84383	38.45161483	-0.009917	-0.0001731	0.173081401	86.6848	0.0150
	16	2.929687	7191.110605	38.43700554	-0.00766	-0.0001337	0.13368998	86.7194	0.0116
	16	1.464844	7186.677331	38.41330937	-0.004866	-8.493E-05	0.084926298	86.7745	0.0074
	16	0.732422	7179.598933	38.37547482	-0.00539	-9.407E-05	0.09407167	86.8598	0.0082
	16	0.366211	7169.646107	38.32227625	-0.008459	-0.0001476	0.147634927	86.9785	0.0128
	16	0.183105	7158.790716	38.2642534	-0.007877	-0.0001375	0.137477281	87.1108	0.0120
	16	0.091553	7150.022028	38.21738413	-0.010649	-0.0001859	0.185856997	87.2154	0.0162
3	27	12000	7869.620204	42.06368835	-2.566074	-0.0447857	44.78568952	-66.4794	3.5479
	27	6000	7826.122546	41.83119023	-1.301528	-0.0227156	22.71556818	21.1984	1.8099
	27	3000	7819.781752	41.79729823	-0.676446	-0.011806	11.80601204	62.1892	0.9415
	27	1500	7822.816577	41.81351959	-0.37284	-0.0065072	6.50717652	74.2421	0.5187
	27	750	7823.031702	41.81466944	-0.197268	-0.0034429	3.442918404	78.1708	0.2745
	27	375	7822.077785	41.80957069	-0.105717	-0.0018451	1.845078801	79.2815	0.1471
	27	187.5	7824.95386	41.82494352	-0.065102	-0.0011362	1.136225206	79.5284	0.0906

	27	93.75	7825.974256	41.83039761	-0.038052	-0.0006641	0.664121556	79.6292	0.0529
	27	46.875	7825.474257	41.82772508	-0.023718	-0.000414	0.413950254	79.6695	0.0330
	27	23.4375	7824.235303	41.82110278	-0.022137	-0.0003864	0.386357061	79.6850	0.0308
	27	11.71875	7824.103166	41.8203965	-0.011444	-0.0001997	0.199732132	79.7007	0.0159
	27	5.859375	7822.016861	41.80924505	-0.008322	-0.0001452	0.145243866	79.7244	0.0116
	27	2.929687	7818.430979	41.79007825	-0.007962	-0.000139	0.138960786	79.7612	0.0111
	27	1.464844	7812.394718	41.757814	-0.006716	-0.0001172	0.117214348	79.8236	0.0094
	27	0.732422	7802.664996	41.70580793	-0.006869	-0.0001199	0.119884657	79.9230	0.0096
	27	0.366211	7788.470199	41.62993571	-0.006879	-0.0001201	0.120059187	80.0687	0.0096
	27	0.183105	7771.760949	41.54062357	-0.007214	-0.0001259	0.125905942	80.2406	0.0101
	27	0.091553	7755.67774	41.45465765	-0.008754	-0.0001528	0.152783562	80.4061	0.0123

Complete SIP data set for 5% Dowfax 8390, DI solutions

No.	Run	Freq./Hz	Resistance	Resistivity	Phase/deg	Phase (rad)	phase (mrad)	Real Cond	Imag Cond
1	3	12000	1277.216526	6.826814575	-0.37181	-0.0064892	6.48919993	454.9078	3.1685
	3	6000	1276.079507	6.820737126	-0.188641	-0.0032924	3.292351373	480.0361	1.6090
	3	3000	1275.840051	6.819457217	-0.100985	-0.0017625	1.762491205	486.3072	0.8615
	3	1500	1275.865237	6.819591838	-0.05376	-0.0009383	0.93827328	488.0816	0.4586
	3	750	1275.948316	6.820035901	-0.029763	-0.0005195	0.519453639	488.5395	0.2539
	3	375	1275.961355	6.820105595	-0.017509	-0.0003056	0.305584577	488.6761	0.1494
	3	187.5	1276.021566	6.820427427	-0.009775	-0.0001706	0.170603075	488.7046	0.0834
	3	93.75	1276.031672	6.820481445	-0.005805	-0.0001013	0.101314665	488.7158	0.0495
	3	46.875	1276.070468	6.820688812	-0.003601	-6.285E-05	0.062848253	488.7060	0.0307
	3	23.4375	1276.096632	6.820828661	-0.002955	-5.157E-05	0.051573615	488.6970	0.0252
	3	11.71875	1276.133174	6.82102398	-0.002203	-3.845E-05	0.038448959	488.6840	0.0188
	3	5.859375	1276.18041	6.82127646	-0.001704	-2.974E-05	0.029739912	488.6664	0.0145

	3	2.929687	1276.239026	6.821589767	-0.001117	-1.95E-05	0.019495001	488.6443	0.0095
	3	1.464844	1276.390924	6.822401673	-0.000751	-1.311E-05	0.013107203	488.5864	0.0064
	3	0.732422	1276.726925	6.824197622	-0.000838	-1.463E-05	0.014625614	488.4577	0.0071
	3	0.366211	1277.513063	6.828399587	-0.000295	-5.149E-06	0.005148635	488.1573	0.0025
	3	0.183105	1279.386551	6.838413515	-0.002368	-4.133E-05	0.041328704	487.4411	0.0201
	3	0.091553	1283.349346	6.859594941	-0.002114	-3.69E-05	0.036895642	485.9363	0.0179
2	17	12000	1324.042905	7.077104953	-0.409527	-0.0071475	7.147474731	432.0549	3.3664
	17	6000	1322.310958	7.067847571	-0.204056	-0.0035614	3.561389368	461.8345	1.6796
	17	3000	1321.891026	7.065603004	-0.107826	-0.0018819	1.881887178	469.0293	0.8878
	17	1500	1321.813652	7.065189434	-0.056207	-0.000981	0.980980771	471.0517	0.4628
	17	750	1321.778925	7.065003816	-0.02888	-0.000504	0.50404264	471.6124	0.2378
	17	375	1321.794604	7.065087621	-0.016698	-0.0002914	0.291430194	471.7378	0.1375
	17	187.5	1321.761812	7.064912346	-0.010321	-0.0001801	0.180132413	471.7901	0.0850
	17	93.75	1321.76937	7.064952744	-0.007146	-0.0001247	0.124719138	471.8005	0.0588
	17	46.875	1321.761412	7.064910208	-0.003631	-6.337E-05	0.063371843	471.8123	0.0299
	17	23.4375	1321.735364	7.064770979	-0.003116	-5.438E-05	0.054383548	471.8224	0.0257
	17	11.71875	1321.695825	7.06455964	-0.002983	-5.206E-05	0.052062299	471.8367	0.0246
	17	5.859375	1321.611924	7.064111184	-0.002563	-4.473E-05	0.044732039	471.8672	0.0211
	17	2.929687	1321.468147	7.063342685	-0.002518	-4.395E-05	0.043946654	471.9186	0.0207
	17	1.464844	1321.241795	7.062132817	-0.002374	-4.143E-05	0.041433422	471.9996	0.0196
	17	0.732422	1320.944588	7.060544224	-0.002664	-4.649E-05	0.046494792	472.1055	0.0220
	17	0.366211	1320.726802	7.059380143	-0.001338	-2.335E-05	0.023352114	472.1846	0.0110
	17	0.183105	1320.968624	7.060672699	-0.002482	-4.332E-05	0.043318346	472.0971	0.0205
	17	0.091553	1322.054488	7.06647672	-0.001139	-1.988E-05	0.019878967	471.7105	0.0094
3	29	12000	1226.394078	6.55516492	-0.352068	-0.0061446	6.144642804	477.3140	3.1246
	29	6000	1225.567459	6.550746582	-0.182915	-0.0031924	3.192415495	500.3591	1.6245
	29	3000	1225.377404	6.549730724	-0.095464	-0.0016661	1.666133192	506.6095	0.8479
	29	1500	1225.385083	6.549771769	-0.048506	-0.0008466	0.846575218	508.3250	0.4308

	29	750	1225.475288	6.550253921	-0.027441	-0.0004789	0.478927773	508.6945	0.2437
	29	375	1225.495706	6.550363057	-0.016857	-0.0002942	0.294205221	508.8053	0.1497
	29	187.5	1225.388675	6.549790968	-0.008845	-0.0001544	0.154371785	508.9022	0.0786
	29	93.75	1225.459014	6.550166935	-0.005694	-9.938E-05	0.099377382	508.8846	0.0506
	29	46.875	1225.409279	6.549901098	-0.00349	-6.091E-05	0.06091097	508.9104	0.0310
	29	23.4375	1225.40384	6.549872026	-0.003129	-5.461E-05	0.054610437	508.9133	0.0278
	29	11.71875	1225.354008	6.549605671	-0.001739	-3.035E-05	0.030350767	508.9357	0.0154
	29	5.859375	1225.265013	6.549129986	-0.000979	-1.709E-05	0.017086487	508.9732	0.0087
	29	2.929687	1225.117716	6.548342673	-0.000558	-9.739E-06	0.009738774	509.0346	0.0050
	29	1.464844	1224.896958	6.547162705	-0.000759	-1.325E-05	0.013246827	509.1262	0.0067
	29	0.732422	1224.542734	6.545269352	-0.000655	-1.143E-05	0.011431715	509.2736	0.0058
	29	0.366211	1224.160636	6.543227011	-0.001331	-2.323E-05	0.023229943	509.4322	0.0118
	29	0.183105	1224.050536	6.542638519	-0.001638	-2.859E-05	0.028588014	509.4778	0.0146
	29	0.091553	1224.520134	6.545148554	-0.001959	-3.419E-05	0.034190427	509.2821	0.0174

Complete SIP data for 8% Aerosol MA 80-I, DI solutions

No.	Run	Freq./Hz	Resistance (ohm)	Resistivity (ohm-m)	Phase (deg)	Phase (rad)	phase (mrad)	Real Cond (µS/cm)	Imag Cond (µS/cm)
1	6	12000	356.508799	1.905565279	-0.167806	-0.0029287	2.928718118	1724.6913	5.1231
	6	6000	355.780798	1.901674061	-0.071864	-0.0012542	1.254242392	1748.3173	2.1985
	6	3000	355.603374	1.900725716	-0.034661	-0.0006049	0.604938433	1752.6628	1.0609
	6	1500	355.564279	1.900516751	-0.01852	-0.0003232	0.32322956	1753.6082	0.5669
	6	750	355.557285	1.900479367	-0.009591	-0.0001674	0.167391723	1753.8628	0.2936
	6	375	355.559099	1.900489063	-0.00555	-9.686E-05	0.09686415	1753.9075	0.1699
	6	187.5	355.558811	1.900487524	-0.003594	-6.273E-05	0.062726082	1753.9246	0.1100
	6	93.75	355.566908	1.900530803	-0.002473	-4.316E-05	0.043161269	1753.8906	0.0757

	6	46.875	355.565387	1.900522673	-0.00189	-3.299E-05	0.03298617	1753.9003	0.0579
	6	23.4375	355.570177	1.900548276	-0.001404	-2.45E-05	0.024504012	1753.8781	0.0430
	6	11.71875	355.575713	1.900577866	-0.001117	-1.95E-05	0.019495001	1753.8515	0.0342
	6	5.859375	355.575713	1.900577866	-0.001117	-1.95E-05	0.019495001	1753.8515	0.0342
	6	2.929687	355.589228	1.900650105	-0.000401	-6.999E-06	0.006998653	1753.7857	0.0123
	6	1.464844	355.618273	1.900805353	0.000018	3.142E-07	-0.00031415	1753.6426	-0.0006
	6	0.732422	355.680751	1.901139302	-0.00013	-2.269E-06	0.00226889	1753.3346	0.0040
	6	0.366211	355.889993	1.902257716	0.000584	1.019E-05	-0.01019255	1752.3035	-0.0179
	6	0.183105	356.281362	1.904349611	-0.012766	-0.0002228	0.222804998	1750.2362	0.3900
	6	0.091553	357.108893	1.908772824	-0.00708	-0.0001236	0.12356724	1746.2789	0.2158
2	19	12000	353.163203	1.887682826	-0.054936	-0.0009588	0.958798008	1763.1694	1.6931
	19	6000	353.083449	1.887256535	-0.027639	-0.0004824	0.482383467	1765.5577	0.8520
	19	3000	353.070709	1.887188439	-0.015102	-0.0002636	0.263575206	1766.0946	0.4656
	19	1500	353.064384	1.887154632	-0.009142	-0.0001596	0.159555326	1766.2538	0.2818
	19	750	353.075299	1.887212973	-0.004937	-8.617E-05	0.086165461	1766.2515	0.1522
	19	375	353.063744	1.887151211	-0.001972	-3.442E-05	0.034417316	1766.3274	0.0608
	19	187.5	353.068926	1.887178909	-0.001784	-3.114E-05	0.031136152	1766.3021	0.0550
	19	93.75	353.061247	1.887137864	-0.000685	-1.196E-05	0.011955305	1766.3429	0.0211
	19	46.875	353.057169	1.887116067	-0.000718	-1.253E-05	0.012531254	1766.3633	0.0221
	19	23.4375	353.052882	1.887093153	-0.000687	-1.199E-05	0.011990211	1766.3847	0.0212
	19	11.71875	353.05356	1.887096777	-0.000468	-8.168E-06	0.008168004	1766.3816	0.0144
	19	5.859375	353.040662	1.887027836	-0.000381	-6.65E-06	0.006649593	1766.4462	0.0117
	19	2.929687	353.033696	1.886990602	0.000462	8.063E-06	-0.00806329	1766.4810	-0.0142
	19	1.464844	353.013131	1.886880681	-0.000576	-1.005E-05	0.010052928	1766.5838	0.0178
	19	0.732422	353.01351	1.886882706	-0.000619	-1.08E-05	0.010803407	1766.5818	0.0191
	19	0.366211	353.053517	1.887096547	-0.001398	-2.44E-05	0.024399294	1766.3803	0.0431
	19	0.183105	353.198671	1.887872405	-0.006567	-0.0001146	0.114613851	1765.6180	0.2024
	19	0.091553	353.969055	1.891990163	-0.00061	-1.065E-05	0.01064633	1761.8129	0.0188

3	26	12000	336.064882	1.796291066	-0.155709	-0.0027176	2.717589177	1833.2252	5.0430
	26	6000	335.398887	1.792731274	-0.066851	-0.0011668	1.166750503	1855.2070	2.1694
	26	3000	335.246355	1.79191598	-0.032872	-0.0005737	0.573715016	1859.2013	1.0672
	26	1500	335.204659	1.791693112	-0.017879	-0.000312	0.312042187	1860.1403	0.5805
	26	750	335.186377	1.791595393	-0.009525	-0.0001662	0.166239825	1860.4547	0.3093
	26	375	335.187803	1.791603015	-0.005592	-9.76E-05	0.097597176	1860.5021	0.1816
	26	187.5	335.18681	1.791597707	-0.002949	-5.147E-05	0.051468897	1860.5286	0.0958
	26	93.75	335.180092	1.791561799	-0.002192	-3.826E-05	0.038256976	1860.5695	0.0712
	26	46.875	335.176803	1.791544219	-0.001317	-2.299E-05	0.022985601	1860.5907	0.0428
	26	23.4375	335.17256	1.79152154	-0.001278	-2.23E-05	0.022304934	1860.6143	0.0415
	26	11.71875	335.17256	1.79152154	-0.001278	-2.23E-05	0.022304934	1860.6143	0.0415
	26	5.859375	335.114413	1.79121074	-0.000774	-1.351E-05	0.013508622	1860.9381	0.0251
	26	2.929687	335.101705	1.791142815	-0.000333	-5.812E-06	0.005811849	1861.0091	0.0108
	26	1.464844	335.092477	1.791093491	0.000431	7.522E-06	-0.00752224	1861.0603	-0.0140
	26	0.732422	335.105188	1.791161432	0.000211	3.683E-06	-0.00368258	1860.9899	-0.0069
	26	0.366211	335.14925	1.791396946	-0.000689	-1.203E-05	0.012025117	1860.7448	0.0224
	26	0.183105	335.411573	1.792799082	0.008598	0.0001501	-0.15006089	1859.2212	-0.2790
	26	0.091553	335.943615	1.795642885	-0.001571	-2.742E-05	0.027418663	1856.3431	0.0509

Complete SIP data set for Tap control solutions

No.	Run	Freq./Hz	Resistance (ohm)	Resistivity (ohm-m)	Phase (deg)	Phase (rad)	Phase (mrad)	Real Cond (µS/cm)	Imag Cond (µS/cm)
	4	12000	2891.281478	15.45410831	-0.787551	-0.013745128	13.7451276	152.1888	2.9646
	4	6000	2885.834894	15.42499593	-0.401679	-0.007010504	7.010503587	198.8992	1.5150
	4	3000	2884.380968	15.41722459	-0.203781	-0.00355659	3.556589793	211.7347	0.7690
	4	1500	2884.05171	15.41546468	-0.105947	-0.001849093	1.849092991	215.0206	0.3998
	4	750	2884.023099	15.41531175	-0.0565	-0.000986095	0.9860945	215.8902	0.2132

1	4	375	2884.504822	15.4178866	-0.030651	-0.000534952	0.534951903	216.0976	0.1157
	4	187.5	2883.744756	15.41382399	-0.022232	-0.000388015	0.388015096	216.2027	0.0839
	4	93.75	2884.046601	15.41543737	-0.011616	-0.000202734	0.202734048	216.2189	0.0438
	4	46.875	2883.790764	15.41406991	-0.008437	-0.000147251	0.147250961	216.2449	0.0318
	4	23.4375	2883.789697	15.4140642	-0.007327	-0.000127878	0.127878131	216.2469	0.0277
	4	11.71875	2883.632612	15.41322457	-0.004509	-7.86956E-05	0.078695577	216.2623	0.0170
	4	5.859375	2883.211367	15.41097299	-0.003882	-6.77525E-05	0.067752546	216.2945	0.0147
	4	2.929687	2882.491212	15.40712371	-0.003141	-5.48199E-05	0.054819873	216.3491	0.0119
	4	1.464844	2881.162912	15.40002385	-0.003028	-5.28477E-05	0.052847684	216.4489	0.0114
	4	0.732422	2879.089924	15.38894358	-0.002608	-4.55174E-05	0.045517424	216.6050	0.0099
	4	0.366211	2876.121659	15.37307799	-0.002523	-4.40339E-05	0.044033919	216.8286	0.0095
	4	0.183105	2872.665056	15.35460219	-0.004328	-7.55366E-05	0.075536584	217.0881	0.0164
	4	0.091553	2869.805054	15.33931528	-0.00365	-6.37035E-05	0.06370345	217.3051	0.0138
2	18	12000	2818.497459	15.06507248	-1.028465	-0.0179498	17.94979965	114.2011	3.9714
	18	6000	2805.843888	14.99743823	-0.491952	-0.008586038	8.586038256	195.9029	1.9083
	18	3000	2803.577778	14.9853257	-0.253529	-0.004424842	4.424841637	215.3292	0.9843
	18	1500	2803.011664	14.98229978	-0.131879	-0.002301684	2.301684187	220.5528	0.5121
	18	750	2802.941067	14.98192244	-0.066046	-0.001152701	1.152700838	222.0053	0.2565
	18	375	2803.151233	14.98304579	-0.038469	-0.000671399	0.671399457	222.3091	0.1494
	18	187.5	2803.106071	14.9828044	-0.02119	-0.000369829	0.36982907	222.4273	0.0823
	18	93.75	2803.018155	14.98233448	-0.012266	-0.000214078	0.214078498	222.4675	0.0476
	18	46.875	2803.023205	14.98236147	-0.008167	-0.000142539	0.142538651	222.4764	0.0317
	18	23.4375	2802.894605	14.9816741	-0.006075	-0.000106027	0.106026975	222.4899	0.0236
	18	11.71875	2802.633687	14.98027947	-0.003939	-6.87474E-05	0.068747367	222.5130	0.0153
	18	5.859375	2802.218497	14.97806025	-0.003464	-6.04572E-05	0.060457192	222.5464	0.0135
	18	2.929687	2801.514931	14.97429964	-0.003023	-5.27604E-05	0.052760419	222.6026	0.0117
	18	1.464844	2800.248378	14.96752982	-0.001947	-3.3981E-05	0.033980991	222.7039	0.0076
	18	0.732422	2798.312344	14.95718158	-0.001918	-3.34749E-05	0.033474854	222.8580	0.0075
	18	0.366211	2795.533743	14.94232976	-0.002733	-4.7699E-05	0.047699049	223.0791	0.0106
	18	0.183105	2792.2921	14.92500294	-0.002457	-4.2882E-05	0.042882021	223.3382	0.0096
	18	0.091553	2789.013481	14.90747848	-0.002646	-4.61806E-05	0.046180638	223.6006	0.0103
	25	12000	2817.90434	15.06190221	-0.792374	-0.013829303	13.82930342	155.3936	3.0605
	25	6000	2811.736926	15.02893694	-0.400048	-0.006982038	6.982037744	204.2820	1.5486

3	25	3000	2811.060373	15.02532071	-0.204634	-0.003571477	3.571477202	217.2190	0.7923
	25	1500	2810.275908	15.02112769	-0.110657	-0.001931297	1.931296621	220.5524	0.4286
	25	750	2810.564929	15.02267253	-0.060171	-0.001050164	1.050164463	221.4853	0.2330
	25	375	2810.472113	15.02217642	-0.031918	-0.000557065	0.557064854	221.7811	0.1236
	25	187.5	2810.46535	15.02214027	-0.021971	-0.00038346	0.383459863	221.8411	0.0851
	25	93.75	2810.416105	15.02187706	-0.01302	-0.000227238	0.22723806	221.8798	0.0504
	25	46.875	2810.382048	15.02169502	-0.008581	-0.000149764	0.149764193	221.8931	0.0332
	25	23.4375	2810.176915	15.02059857	-0.004566	-7.96904E-05	0.079690398	221.9152	0.0177
	25	11.71875	2810.011646	15.01971519	-0.005489	-9.57995E-05	0.095799517	221.9272	0.0213
	25	5.859375	2809.716769	15.01813905	-0.006486	-0.0001132	0.113200158	221.9492	0.0251
	25	2.929687	2808.899291	15.01376958	-0.002566	-4.47844E-05	0.044784398	222.0177	0.0099
	25	1.464844	2807.754771	15.00765203	-0.002266	-3.95485E-05	0.039548498	222.1083	0.0088
	25	0.732422	2805.704289	14.99669206	-0.00241	-4.20617E-05	0.04206173	222.2706	0.0093
	25	0.366211	2802.553308	14.97984984	-0.00265	-4.62505E-05	0.04625045	222.5204	0.0103
	25	0.183105	2740.032874	14.6456736	-1.119485	-0.019538372	19.53837171	99.2662	4.4466
	25	0.091553	2751.038291	14.70449835	-1.623632	-0.028337249	28.3372493	-11.9716	6.4229

Complete SIP data set for 0.025% Steol CS-330, tap solutions

No.	Run	Freq./Hz	Resistance (ohm)	Resistivity (ohm-m)	Phase (deg)	Phase (rad)	Phase (mrad)	Real Cond (µS/cm)	Imag Cond (µS/cm)
1	9	12000	2707.81901	14.47348817	-0.721084	-0.012585079	12.58507905	172.9808	2.8983
	9	6000	2702.46101	14.44484928	-0.360809	-0.006297199	6.297199477	215.9043	1.4531
	9	3000	2701.330853	14.43880851	-0.183392	-0.003200741	3.200740576	226.9880	0.7389
	9	1500	2701.042567	14.4372676	-0.099261	-0.001732402	1.732402233	229.7475	0.4000
	9	750	2701.06799	14.43740348	-0.053679	-0.00093686	0.936859587	230.5492	0.2163
	9	375	2701.526808	14.4398559	-0.033797	-0.000589859	0.589859041	230.7107	0.1362
	9	187.5	2701.300037	14.43864379	-0.018388	-0.000320926	0.320925764	230.8229	0.0741
	9	93.75	2701.480769	14.43960982	-0.014119	-0.000246419	0.246418907	230.8235	0.0569
	9	46.875	2701.581336	14.44014736	-0.007543	-0.000131648	0.131647979	230.8313	0.0304
	9	23.4375	2701.436865	14.43937515	-0.005174	-9.03018E-05	0.090301822	230.8472	0.0208
	9	11.71875	2701.319492	14.43874778	-0.004747	-8.28494E-05	0.082849391	230.8577	0.0191

	9	5.859375	2701.225297	14.4382443	-0.00384	-6.70195E-05	0.06701952	230.8666	0.0155
	9	2.929687	2700.872543	14.43635881	-0.002986	-5.21147E-05	0.052114658	230.8975	0.0120
	9	1.464844	2700.22942	14.43292127	-0.002478	-4.32485E-05	0.043248534	230.9528	0.0100
	9	0.732422	2699.284581	14.42787103	-0.002884	-5.03345E-05	0.050334452	231.0334	0.0116
	9	0.366211	2698.036805	14.42120158	-0.002811	-4.90604E-05	0.049060383	231.1403	0.0113
	9	0.183105	2697.145899	14.41643962	-0.002769	-4.83274E-05	0.048327357	231.2166	0.0112
	9	0.091553	2697.051287	14.41593392	-0.004225	-7.37389E-05	0.073738925	231.2236	0.0171
2	15	12000	2655.757132	14.19521368	-1.061747	-0.01853067	18.53067039	114.4394	4.3511
	15	6000	2649.169457	14.16000208	-0.533681	-0.009314334	9.314334493	202.6695	2.1926
	15	3000	2647.893262	14.15318072	-0.277776	-0.004848025	4.848024528	226.4904	1.1418
	15	1500	2647.894767	14.15318877	-0.142543	-0.002487803	2.487802979	233.1295	0.5859
	15	750	2647.952273	14.15349614	-0.079725	-0.00139144	1.391440425	234.7650	0.3277
	15	375	2648.253775	14.15510769	-0.040642	-0.000709325	0.709324826	235.2918	0.1670
	15	187.5	2648.364879	14.15570155	-0.026692	-0.000465855	0.465855476	235.3925	0.1097
	15	93.75	2648.359396	14.15567224	-0.014737	-0.000257205	0.257204861	235.4513	0.0606
	15	46.875	2648.325511	14.15549112	-0.009547	-0.000166624	0.166623791	235.4691	0.0392
	15	23.4375	2648.449935	14.15615618	-0.006196	-0.000108139	0.108138788	235.4643	0.0255
	15	11.71875	2648.359349	14.15567199	-0.005397	-9.41938E-05	0.094193841	235.4734	0.0222
	15	5.859375	2648.294999	14.15532804	-0.00373	-6.50997E-05	0.06509969	235.4810	0.0153
	15	2.929687	2648.12426	14.15441542	-0.003142	-5.48373E-05	0.054837326	235.4966	0.0129
	15	1.464844	2647.780794	14.15257957	-0.003224	-5.62685E-05	0.056268472	235.5271	0.0133
	15	0.732422	2647.249059	14.14973741	-0.002729	-4.76292E-05	0.047629237	235.5748	0.0112
	15	0.366211	2646.748944	14.14706426	-0.002523	-4.40339E-05	0.044033919	235.6194	0.0104
	15	0.183105	2646.826171	14.14747704	-0.002844	-4.96363E-05	0.049636332	235.6123	0.0117
	15	0.091553	2646.902987	14.14788763	-0.003917	-6.83634E-05	0.068363401	235.6046	0.0161
3	23	12000	2646.393966	14.14516688	-0.735095	-0.012829613	12.82961304	174.7987	3.0232
	23	6000	2641.412361	14.11853984	-0.368904	-0.006438482	6.438481512	220.2124	1.5201
	23	3000	2640.578114	14.11408073	-0.192964	-0.003367801	3.367800692	231.7875	0.7954
	23	1500	2640.222692	14.11218097	-0.098531	-0.001719662	1.719661543	235.0569	0.4062
	23	750	2640.669596	14.11456971	-0.052189	-0.000910855	0.910854617	235.8410	0.2151
	23	375	2640.654591	14.1144895	-0.030935	-0.000539909	0.539908555	236.0509	0.1275
	23	187.5	2640.572238	14.11404932	-0.017424	-0.000304101	0.304101072	236.1354	0.0718
	23	93.75	2640.673949	14.11459297	-0.010406	-0.000181616	0.181615918	236.1494	0.0429

	23	46.875	2640.782717	14.11517435	-0.006744	-0.000117703	0.117703032	236.1471	0.0278
	23	23.4375	2640.66881	14.1145655	-0.005838	-0.000101891	0.101890614	236.1586	0.0241
	23	11.71875	2640.619819	14.11430364	-0.004513	-7.87654E-05	0.078765389	236.1646	0.0186
	23	5.859375	2640.457919	14.11343828	-0.00625	-0.000109081	0.10908125	236.1769	0.0258
	23	2.929687	2639.945213	14.11069783	-0.003205	-5.59369E-05	0.055936865	236.2262	0.0132
	23	1.464844	2639.37898	14.10767127	-0.002837	-4.95142E-05	0.049514161	236.2771	0.0117
	23	0.732422	2638.289344	14.10184709	-0.002914	-5.0858E-05	0.050858042	236.3747	0.0120
	23	0.366211	2636.721286	14.0934657	-0.002723	-4.75245E-05	0.047524519	236.5154	0.0112
	23	0.183105	2634.909724	14.08378277	-0.003334	-5.81883E-05	0.058188302	236.6775	0.0138
	23	0.091553	2634.234099	14.08017151	-0.003196	-5.57798E-05	0.055779788	236.7383	0.0132

Complete SIP data set for 0.5% Dowfax 8390, tap solutions.

No.	Run	Freq./Hz	Resistance (ohm)	Resistivity (ohm-m)	Phase (deg)	Phase (rad)	Phase (mrad)	Real Cond (µS/cm)	Imag Cond (µS/cm)
1	8	12000	2288.109024	12.23010799	-0.61825	-0.010790317	10.79031725	222.1005	2.9409
	8	6000	2283.839048	12.20728466	-0.307929	-0.005374285	5.374284837	260.2171	1.4675
	8	3000	2282.923435	12.20239064	-0.159419	-0.00278234	2.782339807	269.7066	0.7601
	8	1500	2282.764563	12.20154146	-0.085565	-0.001493366	1.493365945	272.1901	0.4080
	8	750	2282.872488	12.20211832	-0.046714	-0.000815299	0.815299442	272.8786	0.2227
	8	375	2282.844626	12.2019694	-0.028063	-0.000489784	0.489783539	273.0724	0.1338
	8	187.5	2283.279462	12.20429363	-0.018576	-0.000324207	0.324206928	273.0808	0.0885
	8	93.75	2282.979311	12.2026893	-0.013407	-0.000233992	0.233992371	273.1393	0.0639
	8	46.875	2283.002303	12.20281219	-0.010092	-0.000176136	0.176135676	273.1472	0.0481
	8	23.4375	2282.92974	12.20242434	-0.006328	-0.000110443	0.110442584	273.1643	0.0302
	8	11.71875	2282.900985	12.20227064	-0.005797	-0.000101175	0.101175041	273.1686	0.0276
	8	5.859375	2282.669838	12.20103514	-0.004564	-7.96555E-05	0.079655492	273.1980	0.0218
	8	2.929687	2282.256214	12.19882429	-0.00426	-7.43498E-05	0.07434978	273.2479	0.0203
	8	1.464844	2281.584145	12.19523204	-0.003803	-6.63738E-05	0.066373759	273.3289	0.0181
	8	0.732422	2280.528035	12.18958705	-0.00324	-5.65477E-05	0.05654772	273.4560	0.0155
	8	0.366211	2279.247644	12.18274327	-0.003983	-6.95153E-05	0.069515299	273.6089	0.0190

	8	0.183105	2278.077859	12.17649068	-0.003387	-5.91133E-05	0.059113311	273.7500	0.0162
	8	0.091553	2277.409157	12.17291642	-0.004529	-7.90446E-05	0.079044637	273.8291	0.0216
	20	12000	2208.603473	11.80514507	-0.797573	-0.013920042	13.92004157	197.2150	3.9304
	20	6000	2200.850397	11.76370432	-0.387546	-0.00676384	6.763840338	262.3435	1.9166
	20	3000	2199.100764	11.75435241	-0.19974	-0.003486062	3.48606222	277.9448	0.9886
	20	1500	2198.918238	11.75337679	-0.104334	-0.001820941	1.820941302	282.0642	0.5164
	20	750	2198.964501	11.75362407	-0.060261	-0.001051735	1.051735233	283.0857	0.2983
	20	375	2198.888307	11.75321681	-0.032399	-0.00056546	0.565459747	283.4615	0.1604
	20	187.5	2198.891691	11.7532349	-0.013453	-0.000234795	0.234795209	283.5842	0.0666
	20	93.75	2198.500586	11.75114441	-0.012383	-0.00021612	0.216120499	283.6386	0.0613
2	20	46.875	2198.50436	11.75116459	-0.009992	-0.00017439	0.174390376	283.6457	0.0495
	20	23.4375	2198.50436	11.75116459	-0.009992	-0.00017439	0.174390376	283.6457	0.0495
	20	11.71875	2198.1726	11.7493913	-0.005966	-0.000104125	0.104124598	283.6976	0.0295
	20	5.859375	2197.994528	11.7484395	-0.004897	-8.54673E-05	0.085467341	283.7222	0.0242
	20	2.929687	2197.644709	11.74656969	-0.00319	-5.56751E-05	0.05567507	283.7693	0.0158
	20	1.464844	2197.049261	11.74338698	-0.002726	-4.75769E-05	0.047576878	283.8466	0.0135
	20	0.732422	2196.081768	11.73821566	-0.002364	-4.12589E-05	0.041258892	283.9720	0.0117
	20	0.366211	2194.826954	11.73150858	-0.002506	-4.37372E-05	0.043737218	284.1342	0.0124
	20	0.183105	2193.683774	11.7253982	-0.002159	-3.7681E-05	0.037681027	284.2825	0.0107
	20	0.091553	2193.153974	11.72256639	-0.003116	-5.43835E-05	0.054383548	284.3505	0.0155
	30	12000	2355.153735	12.58846681	-0.896254	-0.015642321	15.64232106	165.3736	4.1418
	30	6000	2344.158689	12.52969749	-0.417608	-0.007288512	7.288512424	243.1721	1.9390
	30	3000	2341.849507	12.51735475	-0.223838	-0.003906645	3.906644614	259.6536	1.0403
	30	1500	2341.240184	12.51409787	-0.113847	-0.001986972	1.986971691	264.6419	0.5293
	30	750	2341.221238	12.51399661	-0.065411	-0.001141618	1.141618183	265.7988	0.3041
	30	375	2341.022135	12.51293239	-0.037593	-0.000656111	0.656110629	266.2028	0.1748
3	30	187.5	2341.330199	12.51457901	-0.020492	-0.000357647	0.357646876	266.3001	0.0953
	30	93.75	2341.338245	12.51462202	-0.013532	-0.000236174	0.236173996	266.3307	0.0629
	30	46.875	2341.441172	12.51517217	-0.009529	-0.00016631	0.166309637	266.3313	0.0443
	30	23.4375	2341.369549	12.51478934	-0.008022	-0.000140008	0.140007966	266.3430	0.0373
	30	11.71875	2341.218622	12.51398262	-0.006832	-0.000119239	0.119238896	266.3625	0.0318
	30	5.859375	2340.976232	12.51268703	-0.005023	-8.76664E-05	0.087666419	266.3929	0.0234
	30	2.929687	2340.546657	12.51039092	-0.004605	-8.03711E-05	0.080371065	266.4424	0.0214

	30	1.464844	2339.750192	12.50613376	-0.004436	-7.74215E-05	0.077421508	266.5333	0.0206
	30	0.732422	2338.51748	12.49954482	-0.003895	-6.79794E-05	0.067979435	266.6744	0.0181
	30	0.366211	2336.995981	12.4914123	-0.003699	-6.45586E-05	0.064558647	266.8482	0.0172
	30	0.183105	2335.330437	12.48250985	-0.003848	-6.71591E-05	0.067159144	267.0383	0.0179
	30	0.091553	2334.268836	12.47683551	-0.004677	-8.16277E-05	0.081627681	267.1588	0.0218

Complete SIP data set for 5% Dowfax 8390, tap solutions

No.	Run	Freq./Hz	Resistance (ohm)	Resistivity (ohm-m)	Phase (deg)	Phase (rad)	Phase (mrad)	Real Cond (µS/cm)	Imag Cond (µS/cm)
1	2	12000	1010.731534	5.402433047	-0.266096	-0.004644173	4.644173488	595.2903	2.8655
	2	6000	1010.043436	5.398755113	-0.136782	-0.002387256	2.387256246	611.6595	1.4740
	2	3000	1009.982497	5.39842939	-0.07003	-0.001222234	1.22223359	615.9501	0.7547
	2	1500	1009.971475	5.398370476	-0.036974	-0.000645307	0.645307222	617.0483	0.3985
	2	750	1010.006952	5.398560103	-0.021631	-0.000377526	0.377525843	617.3041	0.2331
	2	375	1010.068268	5.398887842	-0.012308	-0.000214812	0.214811524	617.3643	0.1326
	2	187.5	1010.123316	5.399182077	-0.007118	-0.00012423	0.124230454	617.3618	0.0767
	2	93.75	1010.155394	5.399353537	-0.00497	-8.67414E-05	0.08674141	617.3502	0.0536
	2	46.875	1010.20196	5.399602435	-0.003485	-6.08237E-05	0.060823705	617.3257	0.0375
	2	23.4375	1010.221606	5.399707445	-0.00289	-5.04392E-05	0.05043917	617.3148	0.0311
	2	11.71875	1010.250517	5.399861976	-0.002233	-3.89725E-05	0.038972549	617.2982	0.0241
	2	5.859375	1010.251601	5.39986777	-0.002076	-3.62324E-05	0.036232428	617.2977	0.0224
	2	2.929687	1010.480961	5.401093716	-0.001077	-1.87969E-05	0.018796881	617.1586	0.0116
	2	1.464844	1010.588776	5.401669995	-0.000491	-8.56942E-06	0.008569423	617.0930	0.0053
	2	0.732422	1010.798373	5.402790306	-0.000543	-9.47698E-06	0.009476979	616.9651	0.0058
	2	0.366211	1011.19174	5.404892881	-0.00045	-7.85385E-06	0.00785385	616.7251	0.0048
	2	0.183105	1011.951025	5.408951314	-0.000681	-1.18855E-05	0.011885493	616.2623	0.0073
	2	0.091553	1013.324247	5.416291285	-0.001514	-2.64238E-05	0.026423842	615.4266	0.0163
2	13	12000	847.906832	4.532123255	-1.158082	-0.020212005	20.21200515	295.0032	14.8647
	13	6000	848.678372	4.536247192	-1.466204	-0.025589658	25.58965841	76.7167	18.8018
	13	3000	859.208573	4.592531877	-0.385242	-0.006723629	6.723628626	672.6192	4.8801

	13	1500	854.993265	4.570000751	-0.754454	-0.013167486	13.16748566	531.4701	9.6040
	13	750	848.716173	4.536449241	-2.005046	-0.034994068	34.99406784	-309.1477	25.7080
	13	375	814.434123	4.353209208	2.610395	0.045559224	-45.5592239	-660.2034	-34.8735
	13	187.5	744.837845	3.981212075	0.695197	0.012133273	-12.1332732	642.9596	-10.1585
	13	93.75	745.908489	3.986934745	1.989428	0.034721487	-34.7214869	-339.8690	-29.0236
	13	46.875	810.125976	4.330181851	-0.252703	-0.004410425	4.410425459	745.3422	3.3951
	13	23.4375	889.755071	4.755805115	0.213954	0.003734139	-3.73413916	684.9166	-2.6172
	13	11.71875	905.137531	4.838025474	0.00336	5.86421E-05	-0.05864208	688.9824	-0.0404
	13	5.859375	890.956806	4.762228475	-0.837165	-0.014611041	14.61104075	468.6680	10.2267
	13	2.929687	890.958611	4.762238123	-0.837253	-0.014612577	14.61257661	468.6213	10.2277
	13	1.464844	905.070065	4.837664864	-0.005247	-9.15759E-05	0.091575891	689.0282	0.0631
	13	0.732422	905.233193	4.838536795	0.000316	5.51515E-06	-0.00551515	688.9135	-0.0038
	13	0.366211	905.390979	4.839380172	-0.001024	-1.78719E-05	0.017871872	688.7931	0.0123
	13	0.183105	906.363791	4.844579923	-0.001215	-2.12054E-05	0.021205395	688.0536	0.0146
	13	0.091553	908.22894	4.854549279	-0.001602	-2.79597E-05	0.027959706	686.6403	0.0192
3	28	12000	954.822343	5.103594383	-0.419528	-0.007322022	7.322022184	596.4955	4.7822
	28	6000	952.426943	5.090790797	-0.200917	-0.003506604	3.506604401	641.6056	2.2960
	28	3000	951.881634	5.087876081	-0.101099	-0.001764481	1.764480847	651.8069	1.1560
	28	1500	951.774205	5.087301865	-0.052562	-0.000917365	0.917364586	654.3213	0.6011
	28	750	951.734478	5.087089521	-0.028894	-0.000504287	0.504286982	654.9800	0.3304
	28	375	951.755359	5.087201132	-0.016062	-0.00028033	0.280330086	655.1546	0.1837
	28	187.5	951.792652	5.087400466	-0.008986	-0.000156833	0.156832658	655.1870	0.1028
	28	93.75	951.780014	5.087332914	-0.005175	-9.03193E-05	0.090319275	655.2134	0.0592
	28	46.875	951.76583	5.0872571	-0.00418	-7.29535E-05	0.07295354	655.2262	0.0478
	28	23.4375	951.778371	5.087324133	-0.002439	-4.25679E-05	0.042567867	655.2214	0.0279
	28	11.71875	951.765044	5.087252899	-0.001968	-3.43475E-05	0.034347504	655.2312	0.0225
	28	5.859375	951.725468	5.087041362	-0.001682	-2.93559E-05	0.029355946	655.2588	0.0192
	28	2.929687	951.666697	5.086727227	-0.001509	-2.63366E-05	0.026336577	655.2994	0.0173
	28	1.464844	951.572923	5.086225998	-0.001198	-2.09087E-05	0.020908694	655.3643	0.0137
	28	0.732422	951.572923	5.086225998	-0.001198	-2.09087E-05	0.020908694	655.3643	0.0137
	28	0.366211	951.302329	5.084779654	-0.001524	-2.65984E-05	0.026598372	655.5504	0.0174
	28	0.183105	951.351303	5.085041423	-0.001313	-2.29158E-05	0.022915789	655.5169	0.0150
	28	0.091553	951.659994	5.086691399	-0.001549	-2.70347E-05	0.027034697	655.3040	0.0177

Complete SIP data set for 8% Aerosol MA 80-I, tap solutions

No.	Run	Freq./Hz	Resistance (ohm)	Resistivity (ohm-m)	Phase (deg)	Phase (rad)	phase (mrad)	Real Cond (µS/cm)	Imag Cond (µS/cm)
1	7	12000	327.641146	1.751265588	-0.154046	-0.002688565	2.688564838	1880.8462	5.1174
	7	6000	326.833375	1.746947994	-0.05824	-0.001016463	1.01646272	1904.8545	1.9395
	7	3000	326.610433	1.745756353	-0.02415	-0.00042149	0.42148995	1908.8353	0.8048
	7	1500	326.539153	1.745375356	-0.010891	-0.000190081	0.190080623	1909.6956	0.3630
	7	750	326.518751	1.745266306	-0.005897	-0.00010292	0.102920341	1909.8950	0.1966
	7	375	326.500552	1.745169031	-0.002601	-4.53953E-05	0.045395253	1910.0282	0.0867
	7	187.5	326.497825	1.745154455	-0.001434	-2.50276E-05	0.025027602	1910.0486	0.0478
	7	93.75	326.486789	1.745095467	-0.001352	-2.35965E-05	0.023596456	1910.1134	0.0451
	7	46.875	326.476696	1.745041519	-0.000644	-1.12397E-05	0.011239732	1910.1738	0.0215
	7	23.4375	326.467827	1.744994114	-0.000449	-7.8364E-06	0.007836397	1910.2259	0.0150
	7	11.71875	326.456297	1.744932485	-0.000429	-7.48734E-06	0.007487337	1910.2934	0.0143
	7	5.859375	326.435853	1.74482321	-0.000143	-2.49578E-06	0.002495779	1910.4132	0.0048
	7	2.929687	326.410148	1.744685815	-0.000371	-6.47506E-06	0.006475063	1910.5635	0.0124
	7	1.464844	326.376522	1.744506082	-0.000528	-9.21518E-06	0.009215184	1910.7602	0.0176
	7	0.732422	326.370189	1.744472231	-0.000491	-8.56942E-06	0.008569423	1910.7974	0.0164
	7	0.366211	326.534219	1.745348984	-0.000716	-1.24963E-05	0.012496348	1909.8372	0.0239
	7	0.183105	326.942719	1.747532446	-0.004079	-7.11908E-05	0.071190787	1907.4356	0.1358
	7	0.091553	327.854288	1.752404848	-0.002557	-4.46273E-05	0.044627321	1902.1418	0.0849
2	12	12000	323.157207	1.727298611	-0.112277	-0.00195957	1.959570481	1917.6448	3.7816
	12	6000	323.056564	1.726760666	-0.060753	-0.001060322	1.060322109	1926.8355	2.0468
	12	3000	323.055944	1.726757352	-0.036004	-0.000628378	0.628377812	1929.1495	1.2130
	12	1500	323.059096	1.7267742	-0.021473	-0.000374768	0.374768269	1929.9367	0.7234
	12	750	323.080108	1.726886511	-0.010882	-0.000189924	0.189923546	1930.1419	0.3666
	12	375	323.095828	1.726970535	-0.006426	-0.000112153	0.112152978	1930.1224	0.2165
	12	187.5	323.091306	1.726946365	-0.002957	-5.16085E-05	0.051608521	1930.1808	0.0996
	12	93.75	323.095363	1.72696805	-0.002083	-3.63546E-05	0.036354599	1930.1608	0.0702
	12	46.875	323.097468	1.726979301	-0.002051	-3.57961E-05	0.035796103	1930.1484	0.0691
	12	23.4375	323.100741	1.726996796	-0.001069	-1.86573E-05	0.018657257	1930.1318	0.0360

	12	11.71875	323.100501	1.726995513	-0.000626	-1.09256E-05	0.010925578	1930.1340	0.0211
	12	5.859375	323.102179	1.727004482	-0.000147	-2.56559E-06	0.002565591	1930.1243	0.0050
	12	2.929687	323.110338	1.727048092	-0.000273	-4.76467E-06	0.004764669	1930.0755	0.0092
	12	1.464844	323.139292	1.727202854	-0.000159	-2.77503E-06	0.002775027	1929.9026	0.0054
	12	0.732422	323.216797	1.727617123	0.000023	4.01419E-07	-0.00040142	1929.4399	-0.0008
	12	0.366211	323.422531	1.728716786	-0.000288	-5.02646E-06	0.005026464	1928.2124	0.0097
	12	0.183105	323.911373	1.731329682	0.000854	1.49049E-05	-0.01490486	1925.3018	-0.0287
	12	0.091553	325.038169	1.737352488	0.00023	4.01419E-06	-0.00401419	1918.6281	-0.0077
	22	12000	336.904658	1.800779729	-0.184324	-0.003217007	3.217006772	1819.6939	5.9548
	22	6000	336.239917	1.79722664	-0.081832	-0.001428214	1.428213896	1848.5030	2.6489
	22	3000	-269.849307	-1.44236404	10.33924	0.180450773	-180.450773	1410.2220	414.7659
	22	1500	335.949257	1.795673042	-0.0208	-0.000363022	0.3630224	1855.9126	0.6739
	22	750	335.938166	1.795613759	-0.011497	-0.000200657	0.200657141	1856.2528	0.3725
	22	375	335.929037	1.795564964	-0.006282	-0.00010964	0.109639746	1856.3893	0.2035
	22	187.5	334.872923	1.789919959	0.106859	0.00186501	-1.86501013	1851.6582	-3.4732
	22	93.75	335.48912	1.793213576	0.039618	0.000691453	-0.69145295	1857.4016	-1.2853
3	22	46.875	335.641672	1.794028978	0.017438	0.000304345	-0.30434541	1857.7328	-0.5655
	22	23.4375	335.676273	1.794213922	0.006201	0.000108226	-0.10822605	1857.7881	-0.2011
	22	11.71875	335.683262	1.794251279	0.002453	4.28122E-05	-0.04281221	1857.7795	-0.0795
	22	5.859375	335.674033	1.79420195	0.001702	2.9705E-05	-0.02970501	1857.8335	-0.0552
	22	2.929687	335.652439	1.794086528	0.000397	6.92884E-06	-0.00692884	1857.9556	-0.0129
	22	1.464844	335.628219	1.79395707	0.000852	1.487E-05	-0.01486996	1858.0891	-0.0276
	22	0.732422	335.612495	1.793873024	0.000176	3.07173E-06	-0.00307173	1858.1768	-0.0057
	22	0.366211	335.680806	1.794238152	0.000467	8.15055E-06	-0.00815055	1857.7985	-0.0151
	22	0.183105	335.93873	1.795616774	-0.000306	-5.34062E-06	0.005340618	1856.3723	0.0099
	22	0.091553	336.483848	1.798530469	-0.001663	-2.90243E-05	0.029024339	1853.3624	0.0538

Complete pH data set

	DI			Tap		
	1st	*2nd*	*3rd*	*1st*	*2nd*	*3rd*
Control	9.33	9.23	9.27	7.67	7.61	7.61
	9.34	9.11	9.26	7.66	7.62	7.59
	9.34	9.08	9.25	7.64	7.63	7.60
0.025% Steol	9.41	9.17	9.33	7.72	7.32	7.38
	9.40	9.20	9.29	7.70	7.32	7.37
	9.37	9.13	9.27	7.71	7.32	7.37
0.5% Dowfax	9.46	8.93	9.28	7.85	8.09	8.08
	9.44	9.15	9.22	7.85	8.05	8.07
	9.43	9.12	9.16	7.85	8.00	8.07
5% Dowfax	9.13	8.89	8.67	8.39	8.26	8.37
	9.12	8.78	8.61	8.37	8.24	8.39
	-	8.77	8.61	8.36	8.23	8.37
8% AMA 80-I	6.75	6.73	6.32	7.76	7.78	7.89
	6.40	6.32	6.14	7.76	7.81	7.88
	6.32	6.34	6.17	7.76	7.79	7.88

Complete specific conductivity data set. Data in parenthesis was measured using the Accumet 4-electrode conductivity probe.

	DI			Tap		
	1st	*2nd*	*3rd*	*1st*	*2nd*	*3rd*
Control	23.87	19.56	16.54	1020.93	1047.64	1075.56
	24.52	18.99	34.29	1019.96	1048.29	1075.52
	24.43	17.76	34.91	1019.93	1049.25	1076.5
	(13.1)	(17.6)	(37.6)	(1010)	(1040)	(1020)
0.025% Steol	32.37	29.15	31.54	1049.96	1068.69	1073.62
	33.34	35.2	31.67	1051.87	1068.96	1079.28
	32.5	36.13	33.25	1055.42	1069.23	1080.26
	(25.7)	(27.8)	(26.2)	(1030)	(1040)	(1050)
0.5% Dowfax	355.15	366.4	362.79	1250.13	1250.73	1278.9
	382.62	364.52	363.21	1252.17	1254	1279.3
	388.18	364.44	364.57	1256.55	1255.71	1280.55
	(364)	(362)	(331)	(1220)	(1240)	(1210)
5% Dowfax	2215.57	2241	2264.86	3043.41	3133.12	3117.85
	2223	2248	2270.3	3047.08	3135.45	3127.09
	-	2253	2274.63	3049.79	3137.72	3132.16
	(2150)	(2280)	(2170)	(2780)	(2830)	(2820)
8% AMA 80-I	8355.21	8365.47	8364.3	8948.88	8906.66	9012.64
	8349.7	8366.57	8367.92	8957.92	8914.17	9029.82
	8354.65	8371.75	8376.07	8969.32	8953.22	9047.16
	(6050)	(7830)	(6340)	(6010)	(6060)	(6220)

Complete dissolved oxygen data set

	DI			Tap		
	1st	*2nd*	*3rd*	*1st*	*2nd*	*3rd*
Control	7231	7725	7468	8564	8139	8706
	7149	7679	7558	8486	8082	8675
	7168	7673	7563	8527	8080	8613
0.025% Steol	7518	7681	7518	7672	4091	5205
	7417	7677	7468	7658	4357	5036
	7348	7417	7417	7641	4394	5323
0.5% Dowfax	7485	7269	7354	7798	7777	7533
	7453	7175	7220	7793	7591	7473
	7388	7108	7160	7842	7520	7377
5% Dowfax	7526	7426	7400	7939	7689	7586
	7453	7307	7391	7887	7650	7543
	-	7280	7426	7831	7643	7463
8% AMA 80-I	7537	7574	7421	7414	7641	7626
	7430	7496	7358	7340	7588	7585
	7382	7445	7338	7286	7542	7550

Complete dielectric constant data set

	DI			Tap		
	1st	*2nd*	*3rd*	*1st*	*2nd*	*3rd*
Control	23.8	25.5	21.9	23.7	23.4	22.4
	23.9	23.6	21.9	23.5	23.4	22.4
	24.0	23.6	22.1	23.6	23.4	22.4
	24.0	23.4	21.9	23.8	23.3	21.5
	23.9	23.3	21.9	23.9	23.4	21.6
	24.0	23.3	21.9	23.9	22.8	21.6
0.025% Steol	23.6	24.5	25.2	24.1	22.1	25.3
	23.5	25.1	25.2	24.0	22.1	25.4
	23.4	25.0	25.2	24.0	22.0	25.3
	23.2	24.4	25.1	23.9	22.1	24.2
	23.2	24.4	25.1	23.8	22.1	24.3
	22.9	24.3	25.0	23.8	21.7	24.2
0.5% Dowfax	22.8	24.8	25.1	25.1	24.1	25.1
	22.8	24.5	25.1	25.1	24.2	25.0
	22.8	24.4	25.2	25.2	24.2	24.9
	22.6	24.1	23.9	23.9	24.2	24.9
	22.4	24.1	23.9	23.9	24.1	24.9
	22.4	24.3	23.9	23.9	24.2	24.2
5% Dowfax	22.3	23.7	24.7	24.7	23.5	23.4
	22.4	23.7	24.7	24.7	23.5	23.4
	22.4	23.7	23.4	23.4	23.4	23.3
	22.4	23.4	23.2	23.2	23.6	22.6
	22.2	23.3	23.4	23.4	23.8	22.5
	22.0	23.2	23.2	23.2	23.6	22.6
8% AMA 80-I	21.4	24.1	24.0	21.8	22.4	24.0
	21.3	24.1	24.2	21.8	22.5	23.7
	21.5	24.0	22.8	21.7	22.7	24.0
	21.1	23.5	22.2	21.6	22.5	23.4
	21.1	23.2	22.2	21.4	22.3	23.5
	20.9	23.0	22.0	21.5	22.0	23.4

REFERENCES CITED

Aal, G.Z.A., Atekwana, E.A., Slater, L.D., and Atekwana, E.A., 2004, Effects of microbial processes on electrolytic and interfacial electrical properties of unconsolidated sediments: Geophysical Research Letters, v. 31.

Adamson, A.W. and Gast, A.P., 1997, Physical Chemistry of Surfaces: New York, Wiley.

Adepelumi, A.A., Solanke, A.A., Sanusi, O.B., and Shallangwa, A.M., 2006, Model tank electrical resistivity characterization of LNAPL migration in a clayey-sand formation: Environmental Geology, v. 50, p. 1221-1233.

Ajo-Franklin, J.B., Geller, J.T., and Harris, J.M., 2006, A survey of the geophysical properties of chlorinated DNAPLs: Journal of Applied Geophysics, v. 59, p. 177-189.

Anderson, M.J. and Whitcomb, P.J., 2000, DOE Simplified: Practical tools for effective experimentation: Portland, Productivity, Inc..

Archie, G.E., 1942, The electrical resistivity log as an aid in determining some reservoir characteristics: Transactions of the American Institute of Mining and Metallurgical Engineers, v. 146, p. 54-61.

Atekwana, E.A., Atakwana, E.A., Rowe, R.S., Werkema, D.D., and Legall, F.D., 2004, The relationship of total dissolved solids measurements to bulk electrical conductivity in an aquifer contaminated with hydrocarbon: Journal of Applied Geophysics, v. 56, p. 281-294.

Barranco, F.T. and Dawson, H.E., 1999, Influence of aqueous pH on the interfacial properties of coal tar: Environmental Science & Technology, v. 33, p. 1598-1603.

Battelle and Duke Engineering Services, 2002, Surfactant-enhanced aquifer remediation (SEAR) design manual, Naval Facilities Engineering Command, p. 1-110.

Black, B., Johnson, L., Cepeda, M., and Rocky Mountain Oilfield Testing Center, 2007, Geophysical imaging technology provides insight on EOR practices, p. 133-135.

Borden, R.C., Gomez, C.A., and Becker, M.T., 1995, Geochemical indicators of intrinsic bioremediation: Groundwater, v. 33, p. 180-189.

Box, G.E.P. and Cox, D.R., 1964, An Analysis of Transformations: Journal of the Royal Statistical Society Series B-Statistical Methodology, v. 26, p. 211-252.

Bradford, S.A., Abriola, L.M., and Rathfelder, K.M., 1998, Flow and entrapment of dense nonaqueous phase liquids in physically and chemically heterogeneous aquifer formations: Advances in Water Resources, v. 22, p. 117-132.

Bramwell, D.P. and Laha, S., 2000, Effects of surfactant addition on the biomineralization and microbial toxicity of phenanthrene: Biodegradation, v. 11, p. 263-277.

Brewster, M.L. and Annan, A.P., 1994, Ground-penetrating radar monitoring of a controlled DNAPL release: 200 MHz radar: Geophysics, v. 59, p. 1211-1221.

Brewster, M.L., Annan, A.P., Greenhouse, J.P., Kueper, B.H., Olhoeft, G.R., Redman, J.D., and Sander, K.A., 1995, Observed migration of a controlled DNAPL release by geophysical methods: Groundwater, v. 33, p. 977-987.

Brown, C.L., Delshad, M., Dwarakanath, V., Jackson, R.E., Londergan, J.T., Meinardus, H.W., McKinney, T., Oolman, T., Pope, G.A., and Wade, W.H., 1999, Demonstration of surfactant flooding of an alluvial aquifer contaminated with DNAPL, Proceedings Field Testing of Innovative Subsurface Remediation Technologies: Washington, D.C., American Chemical Society, p. 64-85.

Chambers, J.E., Loke, M.H., Ogilvy, R.D., and Meldrum, P.I., 2004, Noninvasive monitoring of DNAPL migration through a saturated porous medium using electrical impedance tomography: Journal of Contaminant Hydrology, v. 68, p. 1-22.

Conrad, S.H., Glass, R.J., and Peplinski, W.J., 2002, Bench-scale visualization of DNAPL remediation processes in analog heterogeneous aquifers: surfactant floods and in-situ oxidation using permanganate: Journal of Contaminant Hydrology, v. 58, p. 15-49.

Cook, R.D., 1977, Detection of influential observation in linear regression: Technometrics, v. 19, p. 15-18.

Cytec Industries, I., 1994, Aerosol MA 80-I Data Sheet.

Dalton, F.N., Herkelrath, W.N., Rawlins, D.S., and Rhoades, J.D., 1984, Time-domain reflectometry: Simultaneous measurement of soil water content and electrical conductivity with a single probe: Science, v. 224, p. 989-990.

Dow Chemical Company, 2009, Dowfax 8390 Technical Data Sheet.

Dwarakanath, V., Kostarelos, K., Pope, G.A., Shotts, D., and Wade, W.H., 1999, Anionic surfactant remediation of soil columns contaminated by light nonaqueous phase liquids: Journal of Contaminant Hydrology, v. 38, p. 465-488.

Endres, A.L. and Knight, R.J., 1993, A model for incorporating surface phenomena into the dielectric response of a heterogeneous medium: Journal of Colloid and Interface Science, v. 157, p. 418-425.

Fountain, J.C., Starr, R.C., Middleton, T., Beikirch, M., Taylor, C., and Hodge, D., 1996, A controlled field test of surfactant-enhanced aquifer remediation: Groundwater, v. 34, p. 910-916.

Grimm, R.E., Olhoeft, G.R., McKinley, K., Rossabi, J., and Riha, B., 2005a, Nonlinear complex-resistivity survey for DNAPL at the Savannah River Site A-014 Outfall: Journal of Environmental and Engineering Geophysics, v. 10, p. 351-364.

Harwell, J.H., 1992, Factors Affecting Surfactant Performance in Groundwater Remediation Applications, *in* Sabatini, D.A. and Knox, R.C., eds., Transport and remediation of subsurface contaminants: Colloidal, interfacial, and surfactant phenomena: Washington, D.C., American Chemical Society, p. 124-132.

Howarth, D.J. and Sondheimer, E.H., 1953, The Theory of Electronic Conduction in Polar Semi-Conductors: Proceedings of the Royal Society of London Series A-Mathematical and Physical Sciences, v. 219, p. 53-74.

Hoyle, B.L., 1989, Ground-water quality variations in a silty alluvial soil aquifer, Oklahoma: Groundwater, v. 27, p. 540-549.

Hwang, Y.K., Endres, A.L., Piggott, S.D., and Parker, B.L., 2008, Long-term ground penetrating radar monitoring of a small volume DNAPL release in a natural groundwater flow field: Journal of Contaminant Hydrology, v. 97, p. 1-12.

IDEX Corporation, 2007, Ismatec IP Peristaltic Pump Operating Manual.

In-Situ, I., 2008, Multi-parameter TROLL 9500, WQP-100 Operator's Manual.

Jawitz, J.W., Annable, M.D., Rao, P.S.C., and Rhue, R.D., 1998, Field Implementation of a Winsor Type I Surfactant/Alcohol Mixture for in Situ Solubilization of a Complex LNAPL as a Single-Phase Microemulsion: Environmental Science & Technology, v. 32, p. 523-530.

Karapanagioti, H.K., Sabatini, D.A., and Bowman, R.S., 2005, Partitioning of hydrophobic organic chemicals (HOC) into anionic and cationic surfactant-modified sorbents: Water Research, v. 39, p. 699-709.

Kehew, A.E. and Passero, R.N., 1990, Ph and Redox Buffering Mechanisms in A Glacial Drift Aquifer Contaminated by Landfill Leachate: Ground Water, v. 28, p. 728-737.

Kelleners, T.J., Robinson, D.A., Shouse, P.J., Ayars, J.E., and Skaggs, T.H., 2005, Frequency dependence of the complex permittivity and its impact on dielectric sensor calibration in soils: Soil Science Society of America Journal, v. 69, p. 67-76.

Kirsch, R., 2006, Petrophysical properties of permeable and low-permeable rocks, *in* Kirsch, R., ed., Groundwater Geophysics: A Tool for Hydrogeology: New York, Springer, p. 1-22.

Kleinbaum, D.G., Kupper, L.L., Muller, K.E., and Nizam, A., 1998, Applied Regression Analysis and Other Multivariable Methods: Pacific Grove, California, Duxbury Press.

Kueper, B.H. and McWhorter, D.B., 1991, The behavior of dense, nonaqueous phase liquids in fractured clay and rock: Groundwater, v. 29, p. 716-728.

Kueper, B.H., Redman, J.D., Starr, R.C., Reitsma, S., and Mah, M., 1993, A field experiment to study the behavior of tetrachloroethylene below the water table: Spatial distribution of residual and pooled DNAPL: Groundwater, v. 31, p. 756-766.

Lesmes, D.P. and Frye, K.M., 2001, Influence of pore fluid chemistry on the complex conductivity and induced polarization responses of Berea sandstone: Journal of Geophysical Research, v. 106, p. 4079-4090.

Londergan, J.T., Meinardus, H.W., Mariner, P.E., Jackson, R.E., Brown, C.L., Dwarakanath, V., Pope, G.A., Ginn, J.S., and Taffinder, S., 2001, DNAPL removal by a heterogeneous alluvial aquifer by surfactant-enhanced aquifer remediation: Groundwater Monitoring and Remediation, v. 21, p. 57-67.

Longino, B.L. and Kueper, B.H., 1995, The use of upward gradients to arrest downward dense, nonaqueous phase liquid (DNAPL) migration in the presence of solubilizing surfactants: Canadian Geotechnical Journal, v. 32, p. 296-308.

Lowe, D.F., Oubre, C.L., and Ward, C.H., 1999, Surfactants and cosolvents for NAPL remediation: A technology practices manual: New York, Lewis Publishers.

Lowrie, W., 2003, Fundamentals of Geophysics: New York City, Cambridge University Press.

Mackay, D.M. and Cherry, J.A., 1989, Groundwater Contamination - Pump-And-Treat Remediation .2: Environmental Science & Technology, v. 23, p. 630-636.

Marshall, D.J. and Madden, T.R., 1959, Induced polarization, a study of its causes: Geophysics, v. 24, p. 790-816.

Martel, R., Gölinas, P.J., and Saumure, L., 1998, Aquifer washing by micellar solutions:: 3 Field test at the Thouin Sand Pit (L'Assomption, Quebec, Canada): Journal of Contaminant Hydrology, v. 30, p. 33-48.

Martinez, A. and Byrnes, A.P., 2001, Modeling dielectric constant values of geologic materials: An aid to ground-penetrating radar data collection and interpretation: Current Research in Earth Sciences, v. 247.

Mercer, J.W. and Cohen, R.M., 1990, A review of immiscible fluids in the subsurface: Properties, models, characterization and remediation: Journal of Contaminant Hydrology, v. 6, p. 107-163.

Montgomery, D.C., 1997, Design and Analysis of Experiments: New York, John Wiley & Sons.

National Research Council of the National Academies, 2005, Contaminants in the subsurface: Source zone assessment and remediation: Washington, D.C., National Academies Press.

Nicholson, R.V., Cherry, J.A., and Reardon, E.J., 1983, Migration of Contaminants in Groundwater at A Landfill - A Case-Study .6. Hydrogeochemistry: Journal of Hydrology, v. 63, p. 131-176.

Olhoeft, G.R., 1985, Low-frequency electrical properties: Geophysics, v. 50, p. 2492-2503.

Pope, G.A. and Wade, W.H., 1995, Lessons from Enhanced Oil Recovery Research for Surfactant-Enhanced Aquifer Remediation
Surfactant-Enhanced Subsurface Remediation, Surfactant-enhanced Subsurface Remediation: Washington, DC, American Chemical Society, p. 142-160.

Prego, M., Cabeza, O., Carballo, E., Franjo, C.F., and Jimenez, E., 2000, Measurement and interpretation of the electrical conductivity of 1-alcohols from 273K to 333K: Journal of Molecular Liquids, v. 89, p. 233-238.

Qin, X.S., Guang, G.H., Chakma, A., Chen, B., and Zeng, G.M., 2007, Simulatin-based process optimization for the surfactant-enhanced aquifer remediation at heterogeneous DNAPL-contaminated sites: Science of the Total Environment, v. 381, p. 17-37.

Radic Research, 2007, SIPLab II Operating Manual.

Ramsburg, C.A. and Pennell, K.D., 2001, Experimental and economic assessment of 2 surfactant formulations for source zone remediation at a former dry cleaning facility: Groundwater Monitoring and Remediation, v. 21, p. 68-82.

Revil, A. and Glover, P.W.J., 1998, Nature of surface electrical conductivity in natural sands, sandstones, and clays: Geophysical Research Letters, v. 25, p. 691-694.

Reynolds, D.A. and Kueper, B.H., 2000, DNAPL flow through fractured porous media, *in* Wickramanayake, G.B., Gavaskar, A.R., and Gupta, N., eds., Treating dense nonaqueous-phase liquids (DNAPLs): Remediation of chlorinated and recalcitrant sompounds: Columbus, Battelle Press, p. 165-172.

Robert, T., Martel, R., Conrad, S.H., Lefebvre, R., and Gabriel, U., 2006, Visualization of TCE recovery mechanisms using surfactant-polymer solutions in a two-dimensional heterogeneous sand model: Journal of Contaminant Hydrology, v. 86, p. 3-31.

Rosen, M.J., 2004, Surfactants and interfacial phenomena: Hoboken, NJ, Wiley-Interscience, p. 1-444.

Rothmel, R.K., Peters, R.W., St.Martin, E., and Deflaun, M.F., 1998, Surfactant foam/bioaugmentation technology for in situ treatment of TCE-DNAPLs: Environmental Science Technology, v. 32, p. 1667-1675.

Sabatini, D.A. and Knox, R.C., 1992, Transport and remediation of subsurface contaminants : colloidal, interfacial, and surfactant phenomena : Washington, D.C., American Chemical Society.

Sauck, W.A., 2000, A model for the resistivity structure of LNAPL plumes and their environs in sandy sediments: Journal of Applied Geophysics, v. 44, p. 151-165.

Schoen, J.H., 1996, Physical properties of rocks: Fundamentals and principles of petrophysics: Tarrytown, NY, Pergamon, p. 1-583.

Schwarz, G., 1962, A theory of the low-frequency dielectric dispersion of colloidal particles in electrolyte solution: Journal of Physical Chemistry, v. 66, p. 2636-2642.

Slater, L.D. and Glaser, D.R., 2003, Controls on induced polarization in sandy unconsolidated sediments and application to aquifer characterization: Geophysics, v. 68, p. 1547-1558.

Slater, L.D. and Lesmes, D., 2002, IP interpretation in environmental investigations: Geophysics, v. 67, p. 77-88.

Sogade, J.A., Scira-Scappuzzo, F., Vichabian, Y., Weiqun Shi, Rodi, W., Lesmes, D.P., and Morgan, F.D., 2006a, Induced-polarization detection and mapping of contaminant plumes: Geophysics, v. 71, p. B75-B84.

Soilmoisture Equipment Corporation, 2005, MiniTrase 6050X3K1 Operating Instructions.

Stat-Ease, I., 2007, Design Expert 7.1.1, Design Expert.

Stepan Company, 2005, Steol CS-330 Material Safety Data Sheet.

Telford, W.M., Geldard, L.P., and Sheriff, R.E., 1990, Applied Geophysics: New York, Cambridge University Press.

Topp, G.C., Davis, J.L., and Annan, A.P., 1980, Electromagnetic determination of soil water content: Measurements in coaxial transmission lines: Water Resources Research, v. 16, p. 574-582.

U.S.EPA, 1991, Dense nonaqueous phase liquids: A workshop summary: U.S. EPA Report EPA/600/R-92/030, 81p.

U.S.EPA, 1996, Surfactant-enhanced DNAPL remediation: Surfactant selection, hydraulic efficiency, and economic factors: U.S. EPA Report EPA 600/S-96/002, 15p.

U.S.Silica Company, 1997, ASTM 20/30 unground silica product data sheet.

Vanhala, H., 1997, Mapping oil-contaminated sand and till with the spectral induced polarization (SIP) method: Geophysical Prospecting, v. 45, p. 303-326.

Vanhala, H. and Soininen, H., 1995, Laboratory technique for measurement of spectral induced polarization response of soil samples: Geophysical Prospecting, v. 43, p. 655-676.

Vinegar, H.J. and Waxman, M.H., 1984, Induced polarization of shaly sands: Geophysics, v. 49, p. 1267-1287.

Waxman, M.H. and Smits, L.J.M., 1968, Electrical conductivities in oil-bearing shaley sands: Society of Petroleum Engineering, v. 8, p. 107-122.

Werkema, D.D., 2008, Report on the geoelectrical detection of surfactant enhanced aquifer remediation of PCE: Property changes in aqueous solutions due to surfactant treatment of perchloroethylene: Implications to geophysical measurements: U.S. EPA Report EPA/600/R-08/031, 77p.

West, C.C. and Harwell, J.H., 1992, Surfactants and subsurface remediation: Environmental Science Technology, v. 26, p. 2324-2330.

Williams, J.H., Lapham, W.W., and Barringer, T.H., 1993, Application of Electromagnetic Logging to Contamination Investigations in Glacial Sand-And-Gravel Aquifers: Ground Water Monitoring and Remediation, v. 13, p. 129-138.

Willumsen, P.A., Karlson, U., and Pritchard, P.H., 1998, Response of fluoranthene-degrading bacteria to surfactants: Applied Microbiology and Biotechnology, v. 50, p. 475-483.

Zhong, L., Mayer, A., and Glass, R.J., 2001, Visualization of surfactant-enhanced nonaqueous phase liquid mobilization and solubilization in a two-dimensional micromodel: Water Resources Research, v. 37, p. 523-537.

Zonge, K., Wynn, J., and Urquhart, S., 2005, Resistivity, induced polarization, and complex resistivity, *in* Butler, D.K., ed., Near-surface geophysics: Tulsa, Society of Exploration Geophysicists, p. 219-263.

VITA

Graduate College
University of Nevada, Las Vegas

Meghan Therese Magill

Degrees:

Bachelor of Science, Geology, 2006
University of Oklahoma

Thesis Title: Geoelectrical Response of Surfactant Solutions in a Quartzitic Sand Analog Aquifer

Thesis Examination Committee:

Chairperson, Dave Kreamer, Ph. D.
Committee Member, Dale Werkema, Ph. D.
Committee Member, Michael Nicholl, Ph. D.
Graduate Faculty Representative, Barbara Luke, Ph. D.